A COMPARATIVE STUDY OF SURFACE ROUGHNESS, TENSILE STRENGTH, MICROSTRUCTURE, AND POROSITY OF THE UN-DRIED AND PRE-DRIED PETG/TPU FDM FILAMENTS

This report is submitted in accordance with the requirement of the University Teknikal Malaysia Melaka (UTeM) for Bachelor of Manufacturing Engineering (Hons)

by

SITI AISHAH BINTI BAKRULAZI

FACULTY OF MANUFACTURING ENGINEERING

2022

DECLARATION

I hereby, declared this report entitled “A Comparative Study of Surface Roughness, Tensile Strength, Microstructure, And Porosity of The Un-Dried and Pre-Dried PETG/TPU FDM Filaments” is the result of my own research except as cited in references.

Signature : ……

Author’s Name : SITI AISHAH BINTI BAKRULAZI

Date : 30/6/2022

APPROVAL

This report is submitted to the Faculty of Manufacturing Engineering of Universiti Teknikal Malaysia Melaka as a partial fulfilment of the requirement for the degree of Bachelor of Manufacturing Engineering (Hons.). The members of the supervisory committee are as follow:

……

(DR RAHIMAH BINTI ABD HAMID)

ABSTRAK

PETG dan filamen TPU adalah higroskopik, menyebabkan buih dan kualiti cetakan yang lemah dalam bahagian cetakan 3D. Mengeringkan filamen sebelum mencetak boleh menghilangkan lembapan dan meningkatkan kualiti permukaan, memulihkan prestasi asalnya dan menghalang liang-liang. Kesan kelembapan terhadap kualiti cetakan 3D printing kurang di terokai. Kelembapan boleh mengubah kekuatan tegangan dan topografi permukaan dengan menyebabkan kekasaran dan keliangan bahagian bercetak 3D. Kajian ini menggunakan ANOVA untuk menganalisis kekasaran permukaan bahagian PETG dan TPU cetakan 3D. Sampel pra-kering mempunyai permukaan yang lebih licin daripada sampel yang belum kering. TPU lebih kasar daripada PETG kerana ia mempunyai kekasaran permukaan yang lebih tinggi. Kajian ini mengukur kekuatan tegangan bahagian PETG dan TPU cetakan 3D pra-kering menggunakan Mesin Pengujian Universal dan mendapati ia lebih kuat daripada sampel yang tidak kering. Kekuatan tegangan meningkat dengan pengeringan. Kajian ini menilai struktur mikro keratan rentas bahagian cetakan 3D yang patah menggunakan SEM. Sampel yang tidak kering mempunyai jurang antara lapisan yang lebih besar, liang manik, dan corak resapan yang tidak lengkap disebabkan oleh kelembapan. Sampel pra-kering mempunyai lebih sedikit liang manik dan jurang antara lapisan. PETG mempunyai jurang interlayer kurang daripada TPU. Kajian ini juga menggunakan Prinsip Archimedes untuk mengukur keliangan kepingan PETG dan TPU cetakan 3D. Sampel yang belum kering lebih berliang daripada sampel pra-kering kerana perbezaan ketumpatan antara PETG dan TPU. Sampel yang belum kering berliang dan kurang tumpat. TPU telap dan ia Kurang tumpat daripada PETG. Untuk berbuat demikian, tiga tetapan bersyarat telah diwujudkan; (i) gulungan PETG dan TPU baharu bertindak sebagai rujukan, (ii) gulungan PETG dan TPU terpakai disimpan dalam beg vakum dengan gel silika untuk 50 gram, dan (iii) gulungan PETG dan TPU terpakai disimpan dalam persekitaran terbuka, terdedah dengan pelembap selama 48 jam, 96 jam dan 150 jam. Kertas kerja ini membentangkan penyiasatan komprehensif pertama tentang penilaian kekasaran permukaan, kekuatan tegangan, struktur mikro, dan keliangan filamen PETG/TPU FDM lembap pra-pengeringan. Akibatnya, kaedah pengeringan meningkatkan kekuatan tegangan, kekasaran permukaan dan topografi permukaan, serta mengurangkan keliangan bahagian cetakan 3D. Kajian lanjut diperlukan mengenai analisis FTIR, yang boleh menganalisis komposisi kimia zarah mikro dan nano, dan ujian mampat, yang boleh mengenal pasti modulus keanjalan, had berkadar, titik hasil mampatan, kekuatan hasil mampatan, dan kekuatan mampatan.

ABSTRACT

PETG and TPU filament are hygroscopic, causing bubbles and poor printing quality in 3D printed parts. Drying the filament before printing may remove moisture and improve surface quality, restoring its original performance and preventing pores. The effect of humidity on the quality of 3D printing is less explored. Moisture can alter the tensile strength and surface topography by causing roughness and porosity of 3D printed parts. This study used ANOVA to analyse the surface roughness of 3D printed PETG and TPU parts. Pre-dried samples have a smoother surface than un-dried samples. TPU is rougher than PETG because has higher surface roughness. This study measured the tensile strength of pre-dried 3D printed PETG and TPU parts using a Universal Testing Machine and found they are stronger than un-dried samples. Tensile strength increased with drying. This study evaluates the cross-sectional microstructure of fractured 3D printed parts using SEM. Un-dried samples have larger interlayer gaps, inter-bead pores, and an incomplete diffusion pattern due to dampness. Pre-dried sample had fewer inter-bead pores and interlayer gaps. PETG has less interlayer gaps than TPU. This study also used the Archimedes Principle to measure the porosity of 3D printed PETG and TPU pieces. Un-dried samples are more porous than pre-dried samples due to the density difference between PETG and TPU. Un-dried samples are porous and less dense. TPU is permeable and it is less dense than PETG. In order to do so, three conditional settings were established; (i) a new PETG and TPU roll acts as the reference, (ii) used PETG and TPU roll stored in the vacuum bag with silica gel for 50 grams, and (iii) used PETG and TPU roll stored in an open environment, exposed with the humidifier for 48 hours, 96 hours and 150 hours. This paper presents the first comprehensive investigation on evaluation of surface roughness, tensile strength, microstructure, and porosity of the pre-drying humidified PETG/TPU FDM filament. As a result, the drying method is improving the tensile strength, surface roughness and surface topography, as well as reduce the porosity of the 3D printed parts. Further research is needed on FTIR analysis, which can analyse the chemical composition of micro and nanoscale particles, and compress tests, which can identify the modulus of elasticity, proportional limit, compressive yield point, compressive yield strength, and compressive strength.

DEDICATION

Only

my beloved father, Bakrulazi bin Osman

my true loved mother, Rasidah binti Mohd Said

my siblings, Nurhidayah binti Bakrulazi and Siti Hawa binti Bakrulazi

for giving me moral support, money, cooperation, encouragement, and also understandings

Thank You So Much and Love You All Forever

ACKNOWLEDGEMENT

All praise and thanks to Allah s.w.t, the Almighty, for showering me with His mercy, grace, and blessing. He gave me the strength and the willpower I needed to finish my final year project without any problems.

In this opportunity, I would like to express my sincere thanks and gratitude towards Dr Rahimah binti Abdul Hamid, who has given their full effort in guiding me to achieve my goals, guidance, understanding, patience, and endless support to complete this project. It has been a pleasure to have her as my supervisor.

I would like to thank Encik Nor Akramin bin Mohamad, Chairman of JK PSM Committee, for his valuable guidance and training. His excitement for this undertaking motivated me greatly, and it helped me succeed. He also provides materials that are used as a key reference for this study as well as for addressing and clearing all doubts while doing the project.

Last but not least, my appreciation is also to my parents, siblings, fellow friends and individuals who are directly or indirectly involved giving supports and advises throughout the completion this project. I lack valuable words to thank everyone, but my heart is still full of gratitude. Thank you very much.

TABLE OF CONTENT

LIST OF TABLES

LIST OF FIGURES

LIST OF ABBREVIATIONS

2D	-	Two Dimensional
3D	-	Three Dimensional
ABS	-	Acrylonitrile Butadiene Styrene
AC	-	Alternating Current
AM	-	Additive Manufacturing
ANOVA	-	Analysis of Variance
ASTM	-	American Society for Testing and Materials
Au	-	Gold
CAD	-	Computer Aided Design
CAM	-	Computer Aided Manufacturing
CNF	-	Cellulose Nanofiber
CO2	-	Carbon Dioxide
FDM	-	Fused Deposition Modelling
FKP	-	Fakulti Kejuruteraan Pembuatan
H2O	-	Hydrogen
LCD	-	Liquid Crystal Display
Pd	-	Palladium
Pt	-	Platinum
PET	-	Polyethylene Terephthalate
PETG	-	Polyethylene Terephthalate Glycol
PLA	-	Polylactic Acid
PSM	-	Projek Sarjana Muda
RH	-	Relative Humidity
SEM	-	Scanning Electron Microscope
STL	-	Stereolithography
Tg	-	Glass Transition Temperature
TPU	-	Thermoplastic Polyurethane
ULTEM	-	Polyetherimide
UTeM	-	Universiti Teknikal Malaysia Melaka
UTS	-	Ultimate Tensile Strength

LIST OF SYMBOLS

°C	-	Degree Celsius
°F	-	Degree Fahrenheit
°	-	Degree
%	-	Percent
g	-	Gram
g/cm^3	-	Gram per Centimetre Cubic
kg	-	Kilogram
kN	-	Kilo Newton
lbs	-	Pounds
m	-	Metre
mm	-	Millimetre
mm/min	-	Millimetre per Minute
mm/s	-	Millimetre per Second
MPa	-	Megapascals
N	-	Newton
N/mm^2	-	Newton per Square Millimeter
nm	-	Nanometre
ρ_W	-	Density of distilled water
Ra	-	Arithmetic Average
rpm	-	Revolution per Minute
W	-	Watt
W_a	-	Weight in air
W_w	-	Weight in water
Zi	-	Standard Deviation
µm	-	Micrometre

CHAPTER 1
INTRODUCTION

This chapter describes the introduction of this work, including the background, problem statement, objective, and scope of the study. An investigation of the effect of humidity on the surface roughness, tensile strength, microstructure and density of the pre-dried 3D printed PETG and TPU filament is carried out in this report.

1.1 Background

3D printing, also known as Additive Manufacturing (AM) is a technique of creating three-dimensional (3D) solid items from a computer-aided design (CAD) file. Objects are built in the additive process by laying successive layers of material until the object is finished. When compared to traditional production methods, 3D printing allows the creation of complex shapes with less material. According to Kwon et al. (2020), Fused Deposition Modelling (FDM) is one of the most widely used AM techniques because of its versatility and inexpensive cost. The FDM process creates 3D structures by layering thermoplastic polymers materials using the heated nozzle of an FDM 3D printer at pre-determined process parameters. The filament is heated and deposited in layers to create a three-dimensional component based on a CAD file.

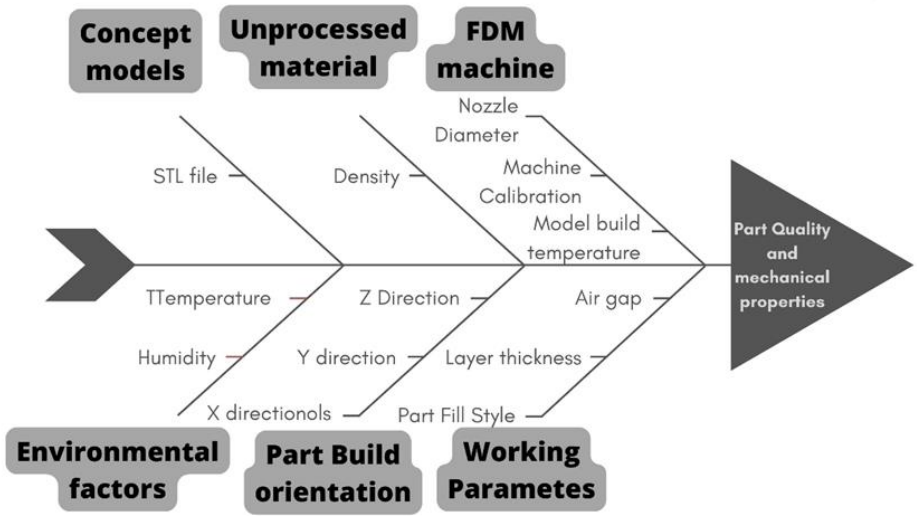

Figure 1.1: Cause and Effect Diagram of FDM Process Parameters

Figure 1.1. shows the cause and effects diagram for FDM that influencing the part quality and its mechanical properties, including environmental factors, build orientation, working parameters, concept models, raw materials, and the machine. Humidity is one of the causes, categorized under environmental factors that could influence the final output of the 3D printed parts. However, a research work investigating on humidity is still lacking as their studies are focusing on other factors, especially process parameters. Thermoplastic filament is sensitive to humidity unless the procedures are standardized and the place where the filament is created has a significant impact on the results (Valerga et al. 2018). Thermoplastic filaments like Polylactic Acid (PLA), Acrylonitrile Butadiene Styrene (ABS), Polyethylene Terephthalate Glycol (PETG), and Thermoplastic Polyurethane (TPU) are hygroscopic and tend to absorb moisture when expose to a humid environment which simultaneously affects the quality of the printed parts. PETG is an amorphous plastic resin manufactured by injection moulding or sheet extrusion and is used as a filament material for specimen manufacturing. PETG offers excellent strength, low shrinkage, and strong chemical printing capabilities (R. Srinivasan, 2020).

Drying the filament before printing has a tendency to reduce or eliminate the absorbed moisture, and improve the printing process. The popping or cracking sounds that might occur during extrusion can be avoided by drying the filament. Other than that, the drying process helps to improve the quality of the surface roughness, the tensile strength, and the microstructure of the fractured sample. It also helps to reduce the porosity, which is that will be discussed in more detail in this study. The term "pre-dried" refers to the filament after it

has been dried. For the purposes of this investigation, the dehydrator known as a SUNLU Dryer was utilised in order to achieve a pre-dried filament.

In this study, the influence of humidity on the surface topography, which includes the surface roughness, porosity and microstructure of PETG and TPU printed parts initially exposed to various humidity conditions and subsequently un-dried using a dehydrator before printing, was investigated. A comparison between the un-drying and pre-drying filaments was also executed to study the effectiveness of drying.

1.2 Problem Statement

Humidity refers to the amount of water that permeates a body or vapour in the atmosphere. Humidity or moisture of 3D printed filaments was the main problem throughout this study, as it affected the quality of 3D printing. Kwon et al. (2020) highlighted that humidity changes the properties of the filament and lowers the quality of 3D-printed things. For this reason, it is important to keep the filament supply at the same humidity level. It also happens because the thermoplastic filament absorbs moisture quickly once the seal is broken. Furthermore, moisture is the biggest enemy when using a 3D printer. It can ruin the filament by causing a rough or grainy surface on finished prints and filament popping, cracking, or hissing sound while printing (Asesar, 2015). Because of the moisture in the environment, the surface roughness of pre-dried filaments differs. Likewise, drying the filament before printing can help prevent printing bubbles and nozzle blockage (Dwamena, 2020). According to Valerga et al. (2018) the appearance of bubbles will have an impact on the findings of both surface quality and tensile strength as a result of the increase in relative humidity. When performing 3D printing, the filament should be stored in a dry environment, such as a dry cabinet, or the used filament should be sealed in a vacuum bag.

Besides that, porosity is caused by water breaking the polymeric chemical chain, causing the polymer composition to be amorphous, with a more porous structure. Wet filaments have less strength than dry ones and break more easily as H_2O molecules break polymer bonds and diminish resistance, causing their impact resistance to drop. Thermoplastic material with a double bond in the chemical structure tends to combine with water, as water molecules have one oxygen atom covalently bound to two hydrogen atoms. Polymers with hydrogen-bonding groups will soak up water. Moreover, the more water the filament is exposed to, the porous it becomes. Leite (2016) stated that the increase in porosity would decrease the material's mechanical properties. PETG is more hygroscopic than ABS and PLA, which means it collects more moisture from the environment and deteriorates faster if left out in the open environment. Besides, TPU is the least hygroscopic of the other polymers and is also the most sensitive to improper storage. To preserve filament in good condition, it is recommended to store the used filament in appropriate storage such as a dehydrator and drying cabinet. Humidity problems will reduce part printing quality; therefore, drying the filament may help to reduce moisture and hence enhance printing part quality. Thus, in this study, a hypothesis is that drying the filament before printing can eliminate water and increase the printed surface topography of parts. The assumption made will be proven and discussed as the findings of this work.

1.3 Objective of Study

The objectives of this study are as stated below:

a) To analyze the surface roughness (R_a) of the pre-dried 3D printed PETG and TPU parts using ANOVA.

b) To measure the tensile strength of the pre-dried 3D printed PETG and TPU parts using a Universal Testing Machine.

c) To evaluate the cross-sectional microstructure of the fractured tensile specimen of the pre-dried 3D printed parts using the SEM machine.

d) To examine the porosity of the pre-dried 3D printed PETG and TPU parts using the Archimedes Principle.

1.4 Scope of Study

The scopes of this study are:

a) In this study, a 1.75mm diameter of the PETG and TPU filament was used for all conditions.

b) The humidity level was decided through three conditions as follows:

   i. New PETG and TPU filament roll, which acts as the reference.

   ii. Used PETG and TPU filament roll stored in an open environment, exposed to a humidifier for 48, 96, and 150 hours.

   iii. Used PETG and TPU filament roll stored in the vacuum bag, with the silica gels for 50 g.

c) The PETG and TPU are exposed to the humidifier in an open environment for a few hours and then dry by using the SUNLU FilaDryer S1 dehydrator.

d) The FDM machine, Ender 3 V2, was used to print the samples.

e) Shimadzu Universal Testing Machine is used for the tensile test with a 20kN load and testing speed of 5 mm/min.

f) Mitutoyo SJ-301 surface roughness tester is used in this study, and the variation of data is analysed using Analysis of Variance (ANOVA).

g) The porosity of printed part 3D printing is examined using densimeter, which adopted the Archimedes principle due to the limitation of the porosity equipment at the laboratory.

h) The analysis of the surface topography is divided in two ways, which uses a contact method (profilometer) to measure the surface roughness, and a non-contact method (SEM) to observe the surface microstructure.

i) The samples used for SEM analysis were cut into 10 mm and then sputter-coated with 10nm thick of gold-palladium using SC 7620 Mini Sputter Coater machine.

j) Carls Zeiss Evo 50 is used to observe the cross-sectional of tensile specimen with 5kV acceleration and 30x and 150x magnification power.

CHAPTER 2
LITERATURE REVIEW

This chapter explains the content, steps, and every point related to the study. The data gathered from articles, journals, published literature, books, magazines, etc., focus on the 3D printing technology of the FDM process. Furthermore, this chapter reviews about the PETG and TPU materials. Humidity and its influence on 3D printing parts are also enclosed in this chapter. Besides, this chapter discusses the surface roughness analysis using ANOVA, tensile test, porosity analysis using Archimedes concept, and SEM analysis.

2.1 Overview of 3D printing

Three-dimensional (3D) printing is an additive manufacturing (AM) process used to create a variety of complex structures and geometries using three-dimensional (3D) model data. Printing successive layers of material generated on top of each other forms a process. It is a new technology used in various industries, including research, automotive, aerospace, healthcare, medical, architecture and construction, fashion, and food (Liu et al. 2017). Hossain et al. (2020) review that 3D printing is an automated method that creates complex shape geometries layer by layer, through a succession of cross-sectional slices, from a 3D computer-aided design (CAD) model. It can eliminate waste, lower labour costs, and increase production speed.

According to Tuan (2018), 3D printing, which uses a variety of procedures, materials, and equipment, has grown through time and can alter manufacturing and logistical operations. Additive manufacturing has found widespread application in various sectors, including building, prototyping, and biomechanics. Despite the benefits of reduced waste, design flexibility, and automation, the adoption of 3D printing in the construction sector has

been gradual and restricted. To fulfil the need for printing complicated structures at high resolutions, additive manufacturing (AM) methods have been created. Rapid prototyping, the capacity to print massive designs, minimising printing errors, and improving mechanical qualities are primary elements driving AM technology development.

Because of concerns like flexibility and design benefits for high-value-added items, additive manufacturing (AM) is increasing. These advantages are depended on a high level of material, geometry, and surface finish quality, all of which present significant issues (Valerga et al. 2018). On the other hand, 3D printing may be unfavourable in countries where the building is a significant employer and labour is less expensive. Furthermore, 3D structure printing will necessitate individuals with specialised knowledge of this new technology.

2.2 Fused Deposition Modelling (FDM) 3D printer

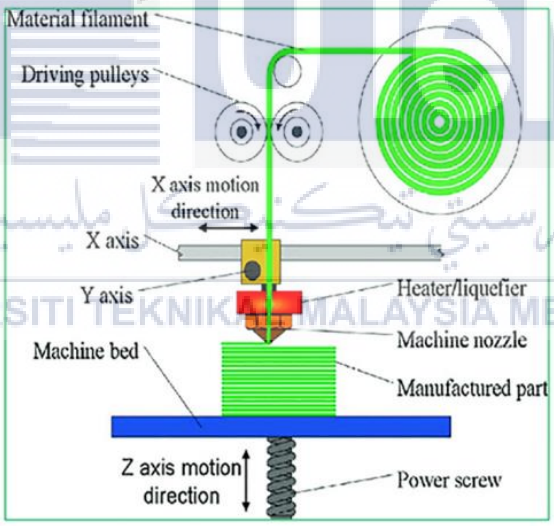

Figure 2.1: Schematic View of Fused Deposition Modelling Method (K. Durgashym, 2019)

One of the most common 3D printing technologies is fused deposition modelling (FDM), a layer-by-layer technique using CAD and computer-aided manufacturing (CAM). The main advantages of FDM are the ease of manufacturing complex shapes (i.e., parts with hollow cavities and parts within parts) and the ability to include various materials into a single piece (i.e., materials with different colours and mechanical properties) (Algarni, 2021). The filament is heated and deposited in layers to create a three-dimensional component based on a computer-aided design (CAD) file (Zaldivar et al. 2018).

Hsueh et al. (2021) stated that, FDM is the first choice of AM technology for polymer and composite materials due to its flexibility, higher printing speed, low cost, high strength and toughness, non-toxicity, and diversity of materials compared with other AM technologies. In filaments, a spool of thermoplastic material is most commonly used in FDM technology to produce the 3D parts.

Wang et al. (2020) highlighted that fused deposition modelling (FDM) had been utilised effectively to create short fibre reinforced polymer composite components. However, because of matrix polymers' intrinsic mechanical characteristics, there is vital to produce fibre-reinforced high-performance thermoplastic composites for FDM-3D printing to broaden engineering applications.

2.3 Polyethylene Terephthalate Glycol (PETG)

Figure 2.2: 2-Dimensional (2D) Chemical Structure Image of PETG (Instinct, 2019)

Figure 2.2 shows the 2D chemical structure image of PETG. The carbon atoms in the chemical structure of PETG are supposed to be placed at the corner(s), and hydrogen atoms coupled to carbon atoms are not mentioned - each carbon atom is considered to be associated with enough hydrogen atoms to give the carbon atom with four bonds. CO2 is implied to be present at the corners of PETG's chemical structure.

In this study, PETG thermoplastic filament has been used to analyse the surface topography of the effect of pre died 3D printed parts. Tyson (2019) stated that compared to other PET co-polyesters, the glycol in PETG provides increased printability and toughness, making it the most appropriate option for 3D printing. It is rare to find pure PET filaments

for printing due to the advantages and widespread use of PETG. Compared to PLA, PETG exhibits superior mechanical and thermal qualities while retaining outstanding printability and durability. However, while PETG is not a straight replacement for ABS, it is a fantastic solution for users who have problems printing ABS due to warping or cracking and require superior mechanical characteristics to PLA while maintaining good dimensional stability. When exposed to chemicals, PETG has a low chemical resistance and a moderate thermal resistance, melting at 80°C (Glass Transition and Vicat temperature). Arceo (2020) discovered PETG filament is hygroscopic, so it must be stored properly. Although it does absorb moisture, it does so at a far slower rate than other filament kinds, but still, moisture exposure should be avoided at all times.

In the 3D printing community, PETG (Polyethylene Terephthalate Glycol) is a polymer that has been steadily gaining in popularity because it combines the dependability of PLA (polylactic acid) in terms of overall easy printability with the durability of ABS (Acrylonitrile Butadiene Styrene) in terms of mechanical resilience properties. Consequently, when it comes to prototyping mechanical parts, this polymer is an excellent choice. Another point to notice is that PETG deforms significantly more than ABS before breaking, making it a better choice for structural applications requiring high strength. However, even if there are advantages, there are some complications in the material's use of the finished printed parts, even though there are advantages.

The fact that manufacturers have not widely standardised 3D printing makes it impossible to predict the final properties of the parts with confidence. Numerous parameters influence the printing portion of the process, such as the printing temperature and rate, the geometry and infill percentage, the printing surface’s temperature, and the nozzle width. Another issue is that the finished FDM portion becomes anisotropic due to the process, making structural computational simulations much more difficult (Ribeiro et al. 2019).

2.4 Thermoplastic Polyurethane (TPU)

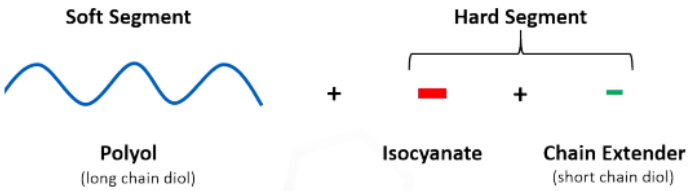

Figure 2.3: Hard and Soft Segment Diagram of TPU(Lubrizol Life Sciences, 2017)

Temperature-sensitive polyurethanes (TPU) are highly flexible elastomers with unique features that provide higher performance and greater processing flexibility. Specifically, Figure 2.3 shows TPU is a block copolymer composed of alternating sequences of hard and soft segment domains polymerised together. Achieving flexibility requires the presence of both hard and soft segments in a chemical structure, which TPU possesses. Changing the ratio of hard to delicate components allows for a wide range of durometers to be achieved. For example, a higher proportion of hard segments than soft segments will result in a more rigid thermoplastic.

TPU elastomers are hygroscopic by nature and tend to absorb moisture when exposed to high humidity levels in the environment. When heated at temperatures ranging from 180°C (355°F) to 200°C (392°F), aromatic polyurethanes conduct a polymerisation/depolymerisation reaction at a rate consistent with equilibrium. Temperatures in the range of 180°C (355°F) are required for typical extrusion conditions. If any water or moisture is present during the extrusion process, the reaction indicated in Figure 2.4 will occur. As a result, polymer chains are broken down, amines are released, and carbon dioxide is released into the atmosphere. Failure to remove moisture from polyurethanes can result in polymer rearrangement, molecular weight reduction, and a severe loss of physical characteristics, among other consequences. Furthermore, excessive moisture in TPU resins can result in voids and other flaws in extruded and moulded parts during the extrusion or moulding process, depending on the type of resin used (Lubrizol Life Sciences, 2017).

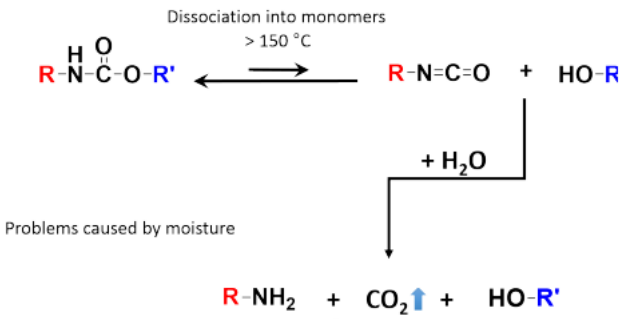

Figure 2.4: Result of Moisture in TPU Processing (Lubrizol Life Sciences, 2017)

2.5 Humidity Effects on 3D Printing

Lubrizol Life Sciences (2017) stated that thermoplastic polyurethane (TPU) elastomers are naturally hygroscopic and absorb moisture when exposed to high humidity levels. TPUs must decrease their moisture content to a bare minimum before processing (thermally or with a solvent).

This is necessary to prevent:

- Decreased the molecular weight
- Change in viscosity
- Loss of mechanical properties
- Defects in the finished product
- Rough surfaces
- Poor melt strength
- Pressure fluctuation during the manufacturing process

The majority of 3D printing plastics absorb moisture from the air, which might harm the quality of 3D printing. Hygroscopic polymers are those that can drink water. Moisture absorbed in the plastic will rapidly expand, boil, and break as the filament is extruded, generating bubbles in the extruded plastic. The surface quality, layer adhesion, and mechanical performance of your 3D printed parts can all be affected by these bubbles (Tyson, 2018).

Although drying polymeric filaments before printing is a good practice, the level of acceptable dryness is expected to be highly dependent on several factors such as the type of polymer used, the extrusion processing temperature, the filament glass transition temperature (Tg), and several other contributing factors, as a result of the absorption of moisture into polymers, the tensile strength and modulus of the material are reduced, as is the glass transition temperature. The failure strain is also increased as a result of the participation effect. In contrast, several research studies have discovered evidence of mechanical performance loss for neat thin-film polyetherimides when exposed to high humidity levels. According to Zaldivar et al. (2018) the effect is due to an anti-plasticization effect, in which stiffness increases, the strain-to-failure rate decreases, and creep are reduced. H_2O absorbed by the polymer chain forms bonds between the virgin material bond.

With the help of spectroscopic and theoretical models, Nicola (2017) demonstrated that these absorbed water molecules preferentially form bridges with two carbonyls of the same polyetherimide repeating unit (intra-chain) as well as through inter-chain interactions, resulting in "pseudo-crosslinking" of the polymer. Additional studies have shown that increases in filament moisture content can affect the flow characteristics of the polymer extrudate and that increases in porosity during high-temperature extrusion processing have been observed for a variety of other neat and filled FDM processed materials. Even though the chemistry and processing for the ULTEM 9085 used in FDM may differ, they are sufficiently similar to warrant further investigation to determine the acceptable filament moisture content before printing to produce high-quality parts in the first place.

2.6 Drying Methods

This subtopic discusses the drying method used to dry the filament before being produced into a specimen during the printing process. Even though no previous research has looked into the effects of filament drying, some information is available on the internet. The following are the key benefits of using a dryer that can improve fixing an unreeling and tangling filament spool reduces the likelihood of these problems. Apart from that, because it has two spool slots, it is particularly well suited for use with 3D printers that have the capability of printing with two different types of filaments. Also included are two threaded filament holes, which allow to print directly from the dryer without stopping and unwinding

the filament. This possibility is especially relevant in the case of nylon. Furthermore, because the dryer is small and lightweight, it is easy to store and move. In addition, a powerful heater of 250W makes it possible to maintain a consistent target temperature while also drying the air efficiently and effectively.

2.6.1 Oven

Figure 2.5: Filament Drying in Oven (Eureka, 2021)

Figure 2.5 shows the oven that has been used to dry the filament. The temperature at which filaments should be cured in an oven does not have a predetermined range that should be followed as a reference. It is possible to adjust the qualities of the thermoplastic filaments used to manufacture them because they are constructed using thermoplastic filaments, which may be heated from any source. Similarly, if the drying process is not adequately controlled, the filament being dried may become brittle as a result.

2.6.2 Silica gel desiccants

It is primarily essential to keep the filament enclosed in a dry, watertight environment most of the time. A tightly-sealed bag will suffice for storing filament for a period of up to a few days. If this is the case, silica gel or desiccants may be used to eliminate both oxygen and moisture from the environment. If the bag is not well sealed, water will be able to enter. Silica gel desiccants can absorb only a certain amount of moisture before being replaced, and they can initially create an arid environment. If not regularly monitored, silica desiccants can help to keep water inside the bag while the filament is in place.

Silica gel is a traditional desiccant that is available in porous, granular, and amorphous forms. It is produced by a chemical reaction between sulfuric acid and sodium silicate. Internally, Silica Gel is formed of a vast network of tiny pores that collect and hold water, alcohol, hydrocarbons, and other substances through the processes of physical adsorption and capillary condensation. Except for the blue gel containing cobalt chloride, the white silica gel can be considered a food-grade product, except for the blue gel. It is commonly used in various products, including auto/spare parts, electrical appliances, electronics, food packaging, furniture, footwear, pharmaceutical, and nutraceutical products.

Compound	SiO_2	Fe_2O_3	Al_2O_3	TiO_2	CaO	ZrO_2	Na_2O	Lg.Loss
Content (%)	99.71	0.03	0.10	0.09	0.01	0.02	0.02	0.02

Relative Humidity	**Absorbing Ability**
20%	15%
50%	25%
90%	35%

Figure 2.6: Chemical Data of Silica Gel (Pac, 2021)

Melting Point °F>2900	Solubility In Water
Melting Point °C>190	Percent Vaporizes by Weight <10% at 175°F
Appearance	Blue and Semi-transparent bead
Solubility In Water	Insoluble

Figure 2.7: Physical Data of Silica Gel (Pac, 2021)

2.6.3 Dry box or dehydrator

Figure 2.8: Dry Box (Bekathwia, 2017)

Figure 2.9: Dehydrator (Source: Amazon)

When not in use, a dry box is an excellent storage solution since it will physically separate the filament from the rest of the environment, preventing contamination. Long and short-term storage can be accomplished using this method, provided that there is some watertight barrier at the aperture to prevent moisture from entering. Essentially, these are solid plastic containers that allow users to safely store their filament without worrying about it becoming contaminated with moisture. The lid of these containers contains a vacuum valve. When activated with the aid of a manual pump (which is included with the containers), it allows for the extraction of air from the inside of the container, resulting in dust and moisture-free storage of the items stored within. As a result, even when the coil has been out of its original manufacturing seal for several months, the filament's correct state can be ensured in this manner (Carolo, 2021).

2.6.4 Storage Cabinet

Humidity control that operates on an automated basis dry cabinet is an easy and convenient solution to store filament without the inconvenience of keeping it in a liquid environment. It is only needed to set the necessary humidity level and keep the filaments, and our dehumidifier dry unit will take care of the rest. The filament will remain entirely dry, easily accessible, precisely recognized (i.e., there will be no need to open every box to discover the exact type of filament you are looking for), and ready to be used whenever they are required for a print project (Corporation, 2019).

- **<10% ±5% RH:** Optimal for all filament materials
- **Convenient:** No consumable parts
- **Low Energy Consumption:** 13W Avg. / 100W Max.
- **4 Filament Feed Ports:** Prints while in dry storage

Figure 2.10: Storage Cabinet (Corporation, 2019)

2.7 Surface Roughness Analysis

Figure 2.11: Surface Roughness Tester (R. Srinivasan, 2020)

As reported by R. Srinivasan (2020), an investigation was carried out to determine the effect of infill density on the surface roughness of an FDM component manufactured of Polyethylene Terephthalate Glycol (PET) while maintaining all other parameters constant. This study discovered that the individual process parameters had a significant impact on the surface roughness of PETG FDM-produced parts. Surface roughness is a measurable characteristic that is determined by the differences in roughness. The surface roughness gauge RUGOSURF 20 shown in Figure 2.11 is used to measure this parameter.

Kovan V et al. (2018) investigated all samples produced in the same printing orientation (upright position). The influence of alternative printing orientations (flatwise and edgewise) on surface roughness, on the other hand, will be immensely beneficial for technical applications. A profilometer (MahrSurf PS-10, MAHR) was used to quantify surface roughness. Ra, Rz, and Rsm have measured metrics for surface roughness evaluation. The results of the measurements were shown on an LCD screen and saved to a computer.

2.7.1 Analysis of variance (ANOVA)

Larson (2008) stated analysis of variance (ANOVA) is a statistical method used to analyse how a response variable (continuous random variable) changes when it is measured in a way that is defined by a set of discrete factors (classification variables, often with nominal levels). Often, the use of ANOVA to make sure that several means are the same by comparing the variance between groups and the variance inside groups (random error). While conducting an investigation into the relationship between variables, it can compare the means of two groups on the dependent variable by using the t-test or the ANOVA procedure. T-test and ANOVA are fundamentally different in that a t-test can only be used to compare two groups, whereas an ANOVA can be used to compare two or more groups (Sow, 2014).

2.8 Tensile Test

The rough part has a significant impact on the subsequent application of the FDM component, it is essential to consider its uniformity before proceeding with further application. Following the identification of the problem with mechanical properties, it must be conducted to assess the effect of the FDM portion of the process parameter's mechanical properties on the mechanical properties of the process parameter. Tensile testing must be completed in this project in order to obtain the tensile test results for both the PETG and TPU specimens that have been printed in this project. According to Jo et al. (2018), the head travel speed for the tensile test was set up at 5mm/min from the tensile test that had been completed previously. The initial grip was used to measure the stress elongation curves. In order to assess the tensile strength, the data received was converted into a stress elongation curve. Figure 2.12 depicts the part of the tensile test setup on the Shimadzu.

Figure 2.12: Tensile Test on UTM (K. Durgashym, 2019)

2.9 Porosity Test

The size of the reinforcement has a direct correlation to the rise in porosity content in AM processed composites. Another benefit of printing materials containing higher levels of design features is that reduce shrinkage and distortion, even if it causes porosity. In most structural applications, AM techniques are unable to produce parts with acceptable surface roughness and mechanical characteristics. Porous defects can be addressed by heating the material to improve its surface roughness and other morphological characteristics (Al-Maharma et al. 2020).

According to Liao et al. (2019), the porosity and crystallinity of the printed parts are two characteristics that can influence the mechanical properties of the printed parts. As a result, because the annealing was performed at 120°C and the melting point of the filament is approximately 150°C, there was no sign of porosity change.

2.10 Sputter-coating

Sputter-coating is an application technique that uses high-intensity lasers to deposit a skinny layer of material on a surface. It is possible to investigate the nanostructure properties of materials using a scanning electron microscope (SEM), which can be employed in many different applications. Some samples may be more difficult to scan than others, depending on their size and complexity. To put it differently, the procedure must be subjected to the sputter-coating process to obtain a high-resolution image. A variety of materials, both conductive and non-conductive, can be used to create sputter-coated surfaces. Sputter coating is typically performed in a vacuum chamber filled with either a chemically inert gas or a reactive gas, with the substrate positioned to face the target of the coating material. During the SEM method, a platinum (Pt) coating with an 8-nm thick layer is applied to the fracture component to maintain a clear scanning image throughout (Jo et al. 2018).

2.11 Surface Topography using Scanning Electron Microscope (SEM)

The scanning electron microscope (SEM) is a technique for examining the microstructure of a sample surface by generating a high-resolution image with an electron focus beam. According to Goldstein (2012), scanning electron microscopy (SEM) is the most extensively used microstructure scanning. SEM produces an image that can identify the meaning of a substance's surface composition and topography. The scanning of a fracture component is a technique used to analyse the mechanical qualities of 3D printed products.

Ghasemi *et al*. (2017) studied filament properties of drying temperature. Figure 2.13 shows SEM micrographs of the filaments after they have been dried at various drying temperatures. The morphological characteristics of the filaments were investigated using this micrograph, which was used to determine the effect of drying under different temperature and grinding on the CNF. In the experiments depicted in Figure 2.1(a–d), the drying temperature did not appear to affect filament structure. Additionally, scanning electron micrographs (SEM) were taken from cross-sections of the filaments-dried under different temperatures to determine the effect of the drying rate on the filament structure. These micrographs were taken for each of the other three forms of CNF suspensions using four different drying temperatures. Because the general morphology of the CNF suspensions was

comparable across the board, SEM micrographs of the 100G CNF formulation are provided in Figure 2.13 for the sake of conciseness. Even though very dilute suspensions were spun, as shown in Figure 2.13(e–h), the cross-sections of the filaments were almost identical, resulting in a pretty acceptable degree of circularity.

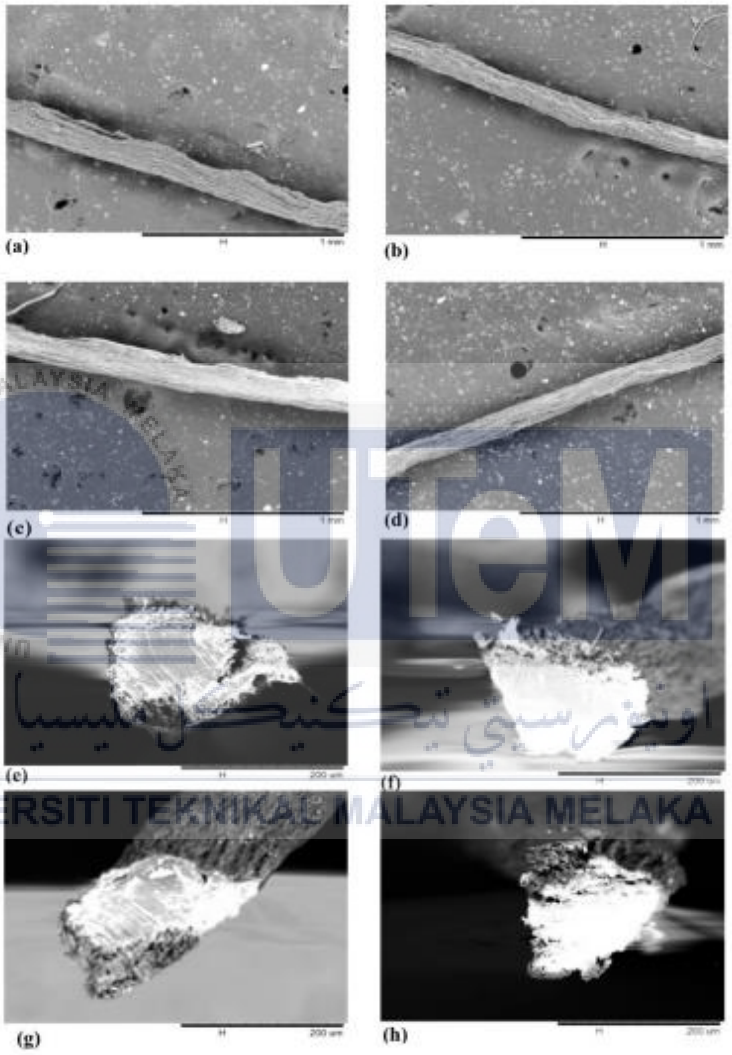

Figure 2.13: SEM image on the surface of dried filament under different temperatures: (a) CNF 100G air-dried; (b) CNF 100G 210°C; (c) CNF 100G 320 °C; (d) CNF 100G 430 °C. SEM image of cross-sections of filaments-dried under different temperatures: (e) CNF 100G air-dried; (f) CNF 100G 210 °C; (g) CNF 100G 320 °C; (h) CNF 100G 430 °C. (Ghasemi *et al.*, 2017).

CHAPTER 3
METHODOLOGY

This chapter describes the procedures adopted to accomplish this study's stated objectives. It is necessary to provide a thorough description of the mode of analysis employed and the data gathering process. The described methods are made according to the objectives of this study which are to analyze the surface roughness, to measure the tensile strength to evaluate the cross-sectional microstructure and to examine the porosity of the pre-dried 3D printed PETG and TPU filament.

3.1 General Process Planning

There are two parts of this study which are PSM 1 and PSM 2. The first three chapters of PSM consist of an introduction, a literature review, and a methodology section. PSM 2 is a compilation of all chapters: the Introduction, Literature Review, Methodology, Result and Discussion, and finally, the Conclusion and Recommendation.

3.2 Relationship between Objective and Methodology

There are four objectives set for this study, constructed based on the pre-identified research questions, as discussed in Chapter 1. Humidity is one of the factors influencing the final quality of the FDM 3D printed part, which users have almost neglected. This is a matter of the fact that many affordable FDM 3D printers are available today and owned by many hobbyists who are not capable of having a dry cabinet to store the used filaments properly, opening the opportunity for the humidity to affect the filament. Without a proper seal and with no de-humidifying agents, our humid environment tends to provide unwanted water, easily absorbed by thermoplastic materials, like PETG and TPU. As a result, the water will

alter the chemical chain of the polymer and cause porosity, which in the end affects the printing quality. Therefore, in this study, pre-drying the filament before using it for printing is proposed to eliminate the moisture and probably resolve the problems. Table 3.1 indicates the relationship between the objectives of this study to the methods used to achieve them.

Table 3.1: Relationship between objective and methodology

Objective	Method
To analyze the surface roughness (R_a) of the pre-dried 3D printed PETG and TPU parts using ANOVA	• Mitutoyo Surftest SJ-301 profilometer • ANOVA method
To measure the tensile strength of the pre-dried 3D printed PETG and TPU parts using a Universal Testing Machine.	• Tensile Test
To evaluate the cross-sectional microstructure of the fractured tensile specimen of the pre-dried 3D printed parts using the SEM machine.	• Tensile test • Sputter Coating • Microstructure Analysis (SEM machine)
To examine the porosity of the pre-dried 3D printed PETG and TPU parts using the Archimedes Principle.	• Densimeter • Principle Archimedes

3.3 Flow Chart of Methodology

Figure 3.1 shows the detailed procedures used to achieve all four objectives in this study. The procedure starts with preparing a 3D design for the samples, followed by the conversion of the design in the STL file format, which is the only format the 3D printing software could read. In this study, Ultimaker Cura software is used to generate the G-code according to the wanted process parameters. However, the PETG and TPU filaments are prepared according to three conditions before printing the samples. The first condition is set for reference in this study.

In contrast, the second condition is created to observe the effect of exposing the filament to different exposure times and pre-drying the exposed filament with a dehydrator to eliminate the moisture. In this study, the author would like to observe the effect of pre-drying the filament compared to un-dried. Also, the third condition is established to compare the filament in condition 2 with the un-dried filament in condition 3, which is stored in the vacuum bag with the addition of the dehumidifying agent. Then, all the tests according to the stated objectives are carried out, and the analysis of the results would be made. Finally, the conclusion of this study is drawn, which will be further elaborated in Chapter 5.

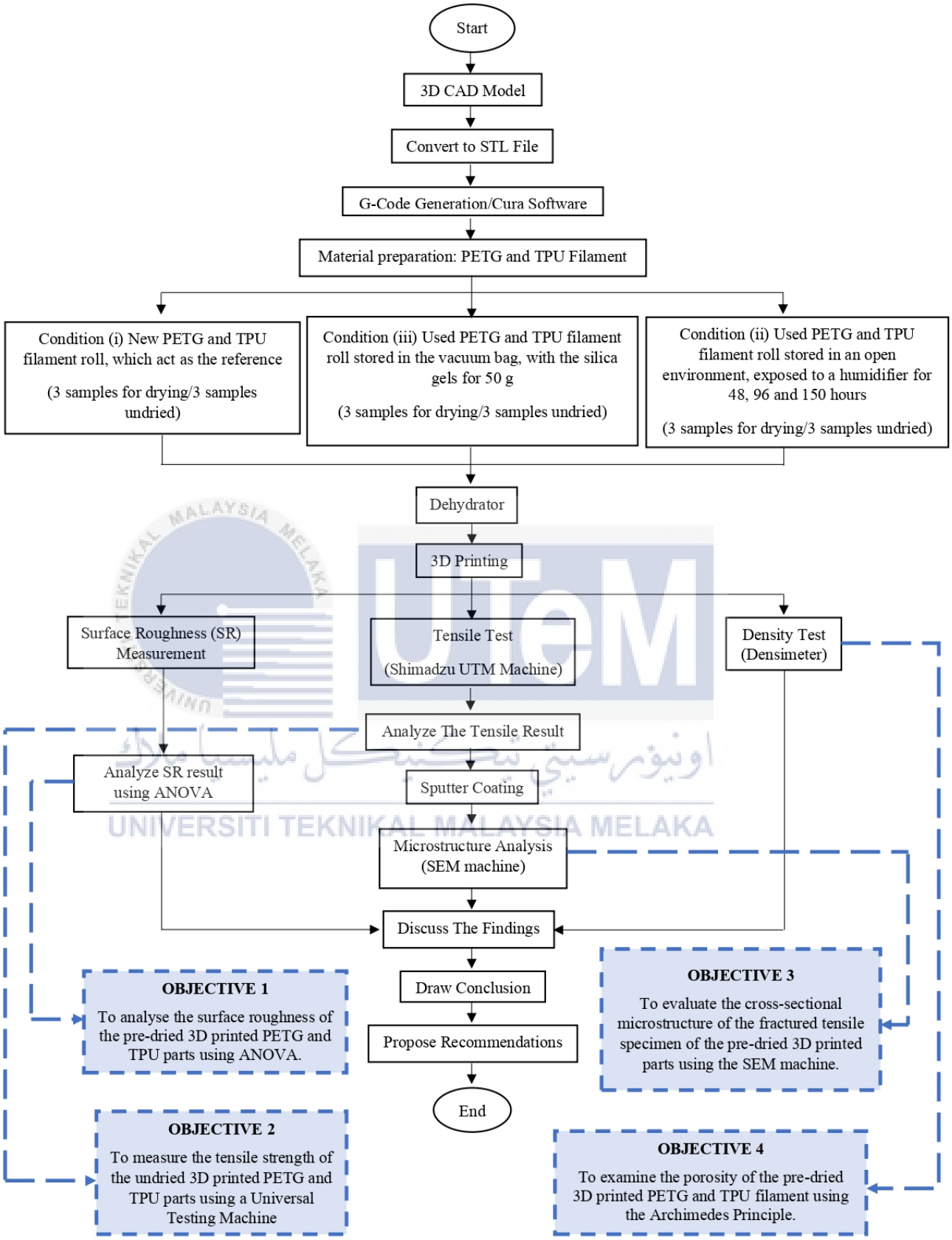

Figure 3.1: Flow chart of study.

3.4 CAD Model

Computer-aided Design (CAD) model is a type of software used to produce precision drawings or technical illustrations. This software is used to create a 2D drawing and a 3D drawing from a CAD model. There are several different types of 3D CAD software, including Fusion 360, CATIA, SolidWorks, AutoCAD, and etc. The CAD model is essential to the 3D printing process. A CAD model is set up for this study to perform the 3D printing process using Fusion 360. Figure 3.2-3.3 depicts a 3D specimen with millimeters (mm) dimensions that conform to the ASTM D638 Type IV standard. Type IV is chosen to reduce material waste, as this study uses many materials.

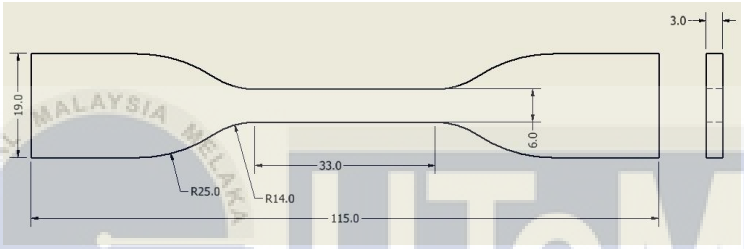

Figure 3.2: 2D dimension of Type IV specimen.

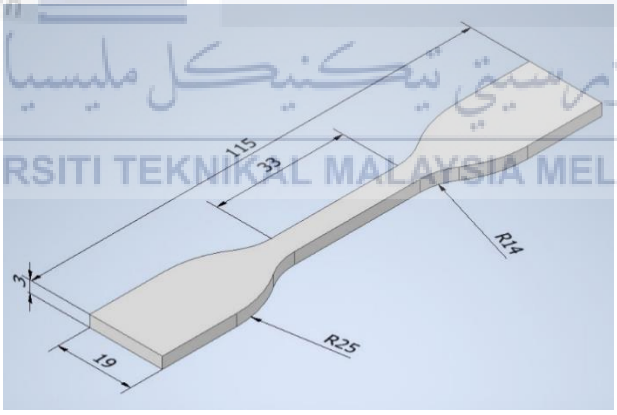

Figure 3.3: 3D CAD drawing of Type IV.

After the CAD model design has been completed with all dimensions by ASTM D638, the CAD model is converted to STL files (stereolithography format) to proceed with the 3D printing process. It is necessary to save the file in the STL file so that it can subsequently be used in CURA to generate G-code, which serves as the native language of the 3D printer. The G-code is then sent to the 3D printer, fabricating the finished sample. Alternatively, the file could have been saved to the cloud and then sent to the printer.

3.5 Preparation of PETG and TPU Filaments

In this study, PETG and TPU filaments were employed. It was chosen to study the influence of moisture on pre-dried filaments by utilizing a dehydrator in several conditions and then will be dried. The filament will be exposed in three conditions; (i) the new PETG and TPU filament roll, which acts as the reference; (ii) used PETG and TPU filament roll stored in an open environment, exposed to a humidifier for 48, 96, and 150 hours; (iii) used PETG and TPU filament roll stored in the vacuum bag, with the silica gels for 50 g. The specifications for each filament have been determined, and they are stated in the table below.

A humidifier is defined as a piece of equipment that is used to enhance the humidity (moisture) level in a specific room or throughout an entire building. Humidifiers are typically used to enhance the amount of moisture in the air, which is particularly important during the winter months when the air is dry. Accordingly, the aim of employing a humidifier in this study was to expose the PETG and TPU filaments to moisture before 3D printing in order to determine the influence of humidity on the surface topography and porosity of pre-dried 3D printed parts.

Table 3.2: The specification of filaments.

Filaments	Specification
PETG	Filament diameter: 1.75mm Length: 328 meters Weight: 1kg (2.2 lbs) of filament Printer Temperature: 220°C
TPU	Filament diameter: 1.75mm Length: 344 meters Weight: 1kg (2.2 lbs) of filament Printer Temperature: 220°C

3.6 Drying Method

Most filaments used in 3D printing are hygroscopic, which means they absorb moisture from the air surrounding them. During 3D printing, tiny water molecules in the filament boil away, leaving behind pockmarks as they expand when heated from a liquid to a steam state. When the filament melts and creates holes in the material flow, a poor 3D print occurs. Drying the filament can be an excellent solution for enhancing print quality. In this study, a dehydrator, as shown in Figure 3.4, is used. This drying process will remove the moisture-absorbing material from the 3D printed object and improve the surface quality of the part.

A spool is usually put in the dryer, and the right setting is chosen, and then the dryer starts to work. When the spool is dry, it can be taken out after a set amount of time. Table 3.3 shows the temperature and time to bake the 3D filaments.

Figure 3.4: SUNLU FilaDryer S1.

Table 3.3: Drying time and baking temperature for 3D filaments.

Material	Parameter Dehydrator
PETG	Baking temperature: 50˚C Time: 6 hr
TPU	

3.7 FDM 3D Printing

In Fused Deposition Modelling, the computer-aided drawing model makes a real-life object. The process takes in data from the CAD model and deposits each layer on top of each other to create the 3D model. It pushes filament through a nozzle on the working bed, and the first layer is covered. Then, it moves on to the next layer. When the filament comes into contact with the print head, it is heated up and liquidized. The temperature of the heating varies depending on the type of filament. The layer deposition is done very thinly, and the direction of the heat is significant to make sure the material is put where it needs to be. Cooling fans attached to the extrusion head can help to speed up the cooling of the material on the platform in some cases. The nozzle size used is 0.4mm. The bed size is 235x235 mm, and the build volume is 220x220x250 mm. In this study, the FDM printer used is the Ender 3 Pro 3D printer, depicted in Figure 3.5.

Figure 3.5: Ender 3 V2 3D printer machine.

3.7.1 Process Setting Parameters

Some parameters are needed to be set in the 3D printing process, such as printing temperature, build plate temperature, printing speed, filling percentage, and layer thickness. Few setting parameters have been set to follow during the printing process. The process parameters will remain the same for all three conditions of PETG and TPU filaments used. In this study, the PETG and TPU filament is used in the 3D printing process, and its parameters setting are shown in Table 3.4.

Table 3.4: Parameter setting for 3D printing.

Material	Parameter Setting
PETG	Printing temperature: 220°C Build Plate Temperature: 60°C Printing speed: 50 mm/s Filling percentage: 100% Layer thickness: 0.1mm
TPU	

The printing temperature for PETG and TPU filaments has been set to 220°C. Hay (2021) recommended the PETG temperature is set in the range of 220°C to 250°C. On the other hand, TPU is a form of temperature-sensitive polymer; the temperature in the nozzle is likely too high if the temperature is kept constant at 230°C, as stated by Xiao and Gao (2017). This could lead to some instances of TPU thermal degradation and as a result, a slight decrease in tensile strength. Therefore, for TPU, the printing temperature is set to 220°C.

Furthermore, Greenburg (2021) stated that the build plate temperature should be between 50°C and 60°C because PETG melts at a high temperature. This is because PETG has a high melting point. There is a good PETG printing speed that ranges from 30mm/s to 50mm/s, with the ideal printing speed being 50mm/s. It is more efficient to produce better-quality output with a lower speed, which saves money. Sarcevic (2021) suggested that PETG printing should be possible to go 50 mm/s. Therefore, 50 mm/s is set for the printing speed. Other than that, it is recommended to use 100% as the filling percentage for the best mechanical resistance and quickest printing results possible (Alvarez C. *et al.*, 2016).

3.7.2 Number of Specimens

In this study, 120 samples were printed for both PETG and TPU filaments of three different conditions. The description of the type of PETG and TPU filaments and the number of specimens for the printing process is represented in Table 3.5. Three samples were divided into three tests with three different conditions: surface roughness, tensile strength, SEM and porosity tests, respectively. After completing the surface roughness test, the sample will be utilized to perform the tensile test on the material. Three samples were used for surface roughness and tensile testing and then for SEM, while three more samples were used for porosity testing.

Table 3.5: Number of specimens.

Condition		Number of specimens	
		Dried	Un-dried
New PETG and TPU filament roll, which acts as the reference.		6	6
Used PETG and TPU filament roll stored in an open environment, exposed to a humidifier.	48 hours	6	6
	96 hours	6	6
	150 hours	6	6
Used PETG and TPU filament roll stored in the vacuum bag, with the silica gels for.	50 grams	6	6

3.8 Surface Roughness Test

Figure 3.6: Surface roughness tester (Mitutoyo SJ-301).

Figure 3.7: Reference for workpiece.

The surface roughness is assessed using a Mitutoyo Surftest SJ-301 profilometer, as shown in Figure 3.6. The significant configuration in this study is the travel length, which is constrained by the small and limited surface area of the sample. This device must first be calibrated before it may be used to take a measurement. The measuring technique for the calibration test is carried out on a reference workpiece of accuracy roughness specimen, as shown in Figure 3.7. Because the equipment is only capable of producing measurements on a flat surface, the experiment must be repeated several times. The samples used in this study were prepared under three different conditions stated.

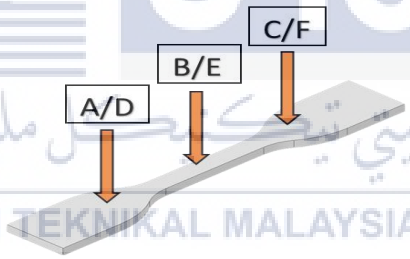

Figure 3.8: Measurement area on each side of the sample.

The surface roughness measuring area for the tensile sample is depicted in Figure 3.8. The six locations were chosen because they have large, flat surfaces that are easy to measure. The sample area is approximately 2mm from each side of the sample area, on average. This is done on both sides (A, B, C,) of the sample (A, B, C,) representing the top sample and (D, E and F), representing the bottom sample, in order to determine consistency and the average value, which is the Ra value, of the sample. The arithmetic means of the absolute values of the deviations from the roughness profile Ra (Zi). The same method will be used at other conditions of surface roughness. All measurements of each sample will be analysed in the analysis of variance or (ANOVA) method in Minitab 16 software.

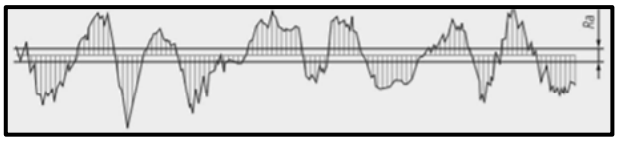

Figure 3.9: The arithmetic means roughness value which Ra.

The average value is calculated between the roughness profile and the mean line, as shown in Figure 3.9. To avoid measurement errors and obtain the average, Ra value, three measurements are made for each chosen point. Regardless, the Ra value is the mean of a set of specific surface valleys and peak measurements. To eliminate measurement error, the chosen points are originally marked to ensure that all Ra measurements are performed on the same side for all samples. The measurement findings could be captured, written down, extracted as SPC data, and then forwarded to a computer. This test was carried out with the chosen samples, which included three samples from each condition.

3.8.1 Machine Set-up

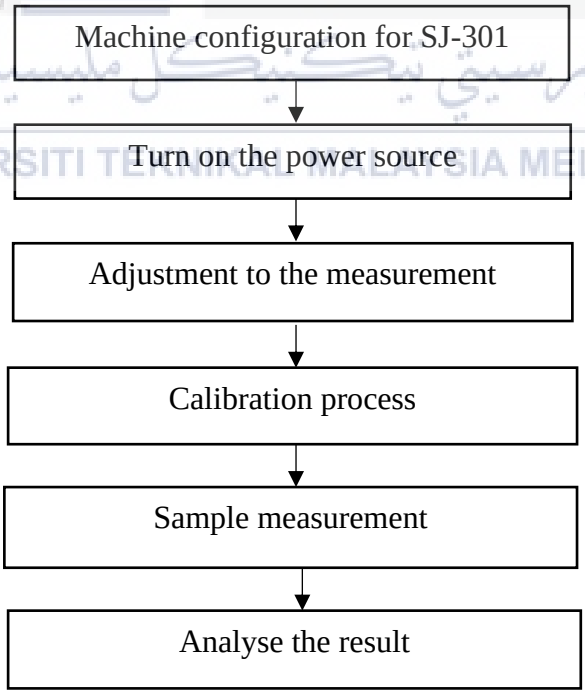

Figure 3.10: Procedures for surface roughness measurement.

This is the first step shown in the flow chart in Figure 3.10 configuration of the Mitutoyo Surftest SJ-301 surface roughness tester that must be provided for the measured sample. Also, turn on the tester's power source. Use an AC adapter or built-in battery to get a power source. The third step is to change the variable being measured to get the result. The fourth step is calibration, which is the most important. Calibration is the process of altering the gain of the SJ-301 detector so that it can take accurate readings. This is done easily by measuring the accuracy of a given sample.

During the calibration process for the sample, the stylus specimen calibration is parallel to the sample, and the state calibration machine is set to a setting corresponding to the value on the sample. The value entered is based on the sample reference and when the start button is pressed, the probe or stylus will move in sequence with that value. On the results screen displayed, two results will be shown. One is for the value that has been entered, and the other is for the calibration that has been performed. If the result shown on the screen is not the same as the sample value. There is no way to measure it as long as it is not the same as the sample. In the next step, measurements are performed. In other words, the roughness of each sample is determined at selected points on both sides, and the results are displayed.

3.8.2 Calibration Procedure

As previously stated, the essential step of calibrating the instrument necessitates the modification of the method. In order to calibrate a workpiece, a sample of accurate roughness is used as a reference, and the difference between the measured and reference values is changed in order to gain adjustment if the measured value falls between the measured and reference values, which is the case specifically for specimens of accuracy. The calibration measurement on the SJ-301 makes it simple to correct for this discrepancy. Calibration should be done regularly, regardless of how the SJ-301 will be used. Furthermore, calibration is required when the instrument is turned on for the first time, as well as when a detector is installed or replaced. Accurate measurements cannot be obtained unless the equipment has been accurately calibrated. The calibration technique is described in greater detail in Table 3.6.

Table 3.6: Procedures for calibration.

Step	Description
1	In the measurement mode, press the [CAL / STD / RANGE] key. In the calibration mode, the current calibration value is displayed. In this condition, the calibration value can be adjusted. 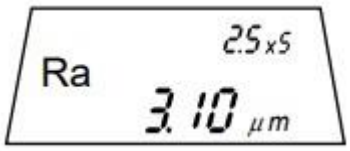
2	Change the calibration value if the values presented differ from the ones stated on the accuracy set. If the calibration value does not need to be changed, move on to the next step. 
3	Confirm the shown value, then press the [n/ENT] key. The value entered has been defined. 
4	The calibration value has now been determined. Press and hold the [START/STOP] key. Calibration measurement with the specimen of accurate ruggedness is performed during the calibration measurement (the detector crosses), and "——" is displayed. 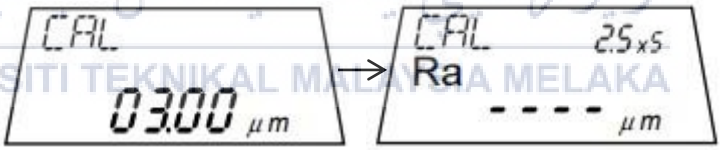
5	When the calibration measurement is done, the calibrated value is presented. After that, press the [n/ENT] key. The calibration factor will be updated, and the calibration process is done. 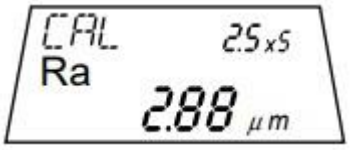

Furthermore, to start the measurement, position the SJ-301 on a workpiece and press the [START/STOP] button. Following the completion of the measurement, the findings are shown on the LCD for confirmation. To obtain the most precise readings possible for surface roughness, a stable base separated from all sources of vibration must be provided. When the measurement is subjected to excessive vibration, the results may be unreliable. Figure 3.11 illustrates example of measurement that the Mituyoto Surftest SJ-301 can perform.

Figure 3.11: Example of measurement on Mituyoto Surftest SJ-301.

3.8.3 Analysis of Variance using ANOVA

Table 3.7: Example result of the ANOVA for surface roughness (K. Durgashym, 2019).

Source	DF	Seq SS	Contribution	Adj SS	Adj MS	F-value	P-value
Layer Thickness	2	207.90	41.87%	207.90%	103.948	13.07	0.000
Feed Rate	2	88.98	17.92%	88.98%	44.490	5.59	0.012
Infill Density	2	40.58	8.17%	40.58%	20.289	2.55	0.103
Error	20	159.11	32.04%	159.11%	7.956		
Total	26	496.57	100.00%				

The experiments aimed to study the influence of humidity on the surface roughness of the pre-dried 3D printed parts. The pre-dried 3D printed surface roughness is analyzed using Analysis of Variance (ANOVA) in Minitab Software as shown in Table 3.7 the example results of the ANOVA method for surface roughness. In this study, the surface roughness depends on several parameters of three conditions like using the new filament as a reference, used filament and exposed to a humidifier, and used filament stored in a vacuum bag with silica gel. Measurements of the surface roughness in terms of Ra is conducted using the surface roughness tester focusing on three conditions that have been stated for this study. There are two materials, PETG and TPU will be measured to examine whether there is a difference in the surface roughness depending on their three different conditions. The

resulting data thus obtained have been treated with statistical techniques according to the conditions applied and analyzed using the ANOVA method. Due to the presence of more than two groups, the ANOVA approach is used to determine whether or not there is a difference between them. It is suspected that the influence of humidity will affect the surface roughness for each condition.

3.9 Porosity Test (Archimedes Principle)

After the PETG and TPU 3D printing process is completed, porosity testing will be conducted on the pre-dried 3D printed PETG and TPU parts. The porosity of the microstructure is related to density, which is a significant physical attribute. The Archimedes principle is employed in this study to examine the porosity of 3D filaments. The water immersion technique will be used with an analytical balance from a density kit and distilled water as the immersion medium to determine the relative density of the PETG and TPU samples using Equation 3.2. Water penetration indicates the presence of porosity in the sample.

$$\rho = \left(\frac{W_a}{W_a - W_w}\right)\rho_W$$

Where ρ is relative density of sample (g/cm³), Equation 3.2

W_a = weight of the sample in the air (g)

W_w = weight of the sample in water (g)

ρ_W = density of distilled water (0.1g/cm^3)

The analytical balancing scale measuring method using distilled water is used to reduce the severity of air bubbles. This instrument can precisely measure the weight of samples in water and air. The process of determining the density of pre-dried PETG and TPU parts starts with determining the dry weight of the sample. Figure 3.12 indicated a densimeter is employed as the measurement equipment for the density test. Following that, the sample must be immersed in water and the weight of the sample in the water measured (Ww). The sample is then removed from the water, and its weight is measured in the air (Wa). Following the measurement, the density of the sample can be calculated using

Equation 3.2. In addition, the porosity on the microstructure will be examined using a Scanning Electron Microscope (SEM).

Figure 3.12: Densimeter

3.9.1 Porosity test set-up

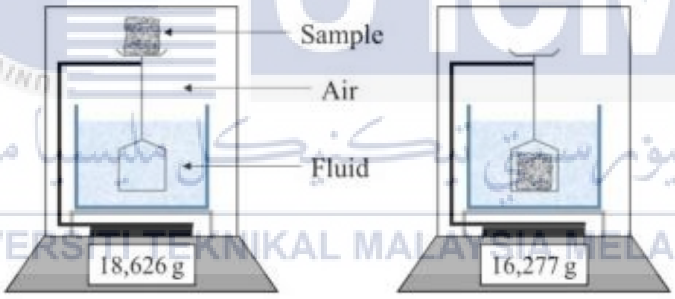

Figure 3.13: Example result of the different weight of the sample (a) weight in air (b) weight in water (de Terris et al., 2019).

In this study, a sample of pre-dried 3D printed PETG and TPU will be measured three times to determine the presence of porosity by calculating the volume of the sample using a densimeter. The weight of the sample will be determined by measuring the weight of the sample in the air and the weight of the sample in water as shown in Figure 3.13. The test sample must have a minimum mass of 5.0 g in order to achieve the best level of precision. In the event where less precision may be accepted, many test samples will be utilised to achieve the minimal mass, provided that each test specimen has a mass of at least 1.0 g (ASTM International, 2017).

First and foremost, the dry weight sample will be determined. The test specimen is initially weighed in the air using a densimeter and the results are recorded. It is important that the test specimen, densimeter, and surrounding air are all at the same temperature when the weighing is performed to ensure a consistent result. It is recommended that the densimeter be calibrated on a regular basis with a standard mass that is nearly equivalent to the mass of the test specimen to ensure better reproducibility.

This is followed by the determination of the measurement weight in water. Figure 3.14 illustrates a suitable bridge for supporting the container of water over the pan of the balance (a). If the scale is equipped with a lower beam hook, it can also be used to support a container of water below the balance for weighing large specimens. Figure 3.14 (b) shows the illustration to ensure that the suspension wire between the container of water and the bottom of the balance is not exposed to air flows, it is necessary to utilise this configuration. Test specimen support should be suspended from a beam hook on the balance. Then place the test specimen on top of it. At least 6 mm of water should cover any wire twists and the specimen support basket so that surface tension forces don't affect the weight. Specimens and their supports should be free to move around freely on the balance beam hook. They should also be completely free of air bubbles when they are submerged in water. Care should also be taken to make sure the surface of the water isn't covered in dust.

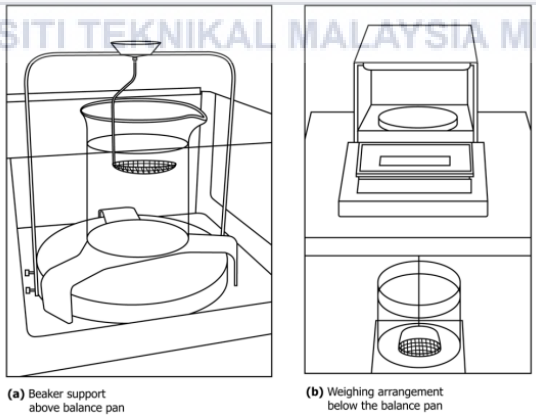

Figure 3.14: Methods for weighing sample in water (ASTM International, 2017).

According to the three different conditions, each sample will be tested three times in the air and in water. After the scale has been re-calibrated, the measuring process begins. Once the scale has attained equilibrium, each measurement result will be recorded. After the scale has been re-calibrated, measurements are taken. Each measurement result will be recorded after the scale has reached equilibrium. With the use of Archimedes' principle, we can calculate the density of a sample to examine the porosity that occurs in the sample. If the sample allows water penetration, then porosity occurs.

3.9.2 ImageJ software analyzer

In order to investigate the fracture surface of each sample, a scanning electron microscope (SEM) is used, and the images will be analysed with the help of ImageJ software. To determine the structure of pre-dried PETG and TPU 3D printed with distinct three conditions specified for this study, this method is utilized. The image will be used to analyse the gap that appears between layers by layers of PETG and TPU materials as they are extruded from an FDM nozzle. The length of the interlayer gaps between each sample will be determined using ImageJ software after the SEM images were captured. The first step in utilising the ImageJ software is to choose a scale to work with. As a result, the length of the interlayer gap was measured using the same scale as that used for the SEM images. Figure 3.15 below shows the example result of ImageJ measured the interlayer gap layer by layer.

Figure 3.15: Example result of ImageJ software.

3.10 Tensile Test

Figure 3.16: Shimadzu Tensile Testing Machine.

Tensile testing is a critical method used to determine the ultimate tensile strength (UTS), yield strength, and ductility of a material. Tensile testing, commonly known as tension testing, is a method for assessing tension as a load for proof tests until it is completely broken. In this study, the purpose of the tensile test is to examine the porosity in the middle of the cross-section of the sample. The Shimazu Universal Tensile Testing Machine as shown in Figure 3.16 is utilized to perform this test. During the process of tensile testing, specimens are held in place between the bottom and upper clamps while the program connects to the computer, and when the test begins, the top clamp gradually goes upward with the set speed and force. The specimen fractured as the clamp moved upward because it could not sustain the stress. This machine employs a 20kN force cell and a testing speed of 5 mm/min for moving the machine's clamps. The shape and dimensions of the tensile test specimens are 3D printed to fulfil the specifications outlined in the American Society for Testing and Materials (ASTM) standard D638 (Standard Test Method for Tensile Properties of Plastics).

3.10.1 Tensile test set-up

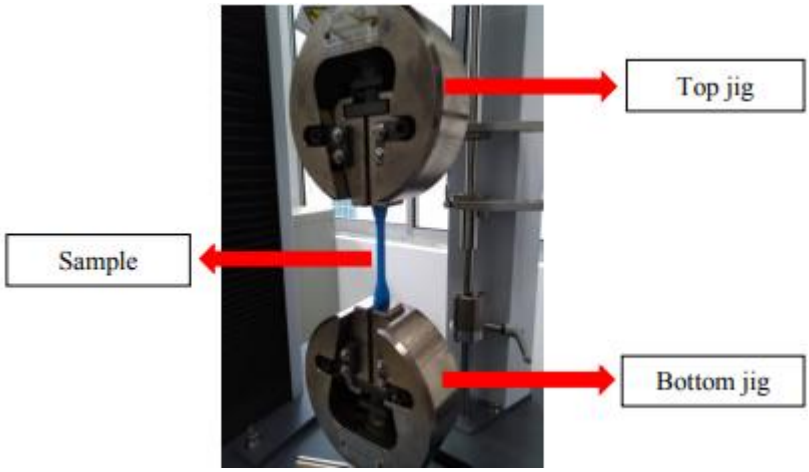

Figure 3.17: Tensile test set-up.

Figure 3.17 shows the tensile test set-up, which will be used in this study. The top jig and bottom jig will hold on to the sample until the sample breaks. The software "Trapezium-X" was used to look at the maximum force, stress, and strain (Shimadzu Corp., Kyoto, Japan). The average tensile strength value for the three replications of each condition is found by using Equation 3.3, which is the same for each condition. The data is used to make a stress-strain diagram to show how stress and strain in a material are linked. Another thing they did was look at the stress and strain curves in each of three conditions to see how humidity affects the 3D printed parts. If the stress-strain curves change when PETG and TPU are exposed to humidity, means that the properties of PETG and TPU have changed because of the humidity.

$$Average = \frac{Sum\ of\ tensile\ strength\ values}{Number\ of\ smples} \tag{3.3}$$

3.10.2 Tensile test result

3.10.2.1 Data from the test

Table 3.8: Data obtained from the result.

Tensile test result for condition (a)		
Humidity Condition	**Maximum Force (Average) (N)**	**Maximum Stress (Average) (N/mm^2)**
New filament roll, which acts as the reference		
Tensile test result for condition (b)		
Humidity Condition	**Maximum Force (Average) (N)**	**Maximum Stress (Average) (N/mm^2)**
50 grams desiccant gel		
Tensile test result for condition (c)		
Humidity Condition	**Maximum Force (Average) (N)**	**Maximum Stress (Average) (N/mm^2)**
Humidified for 48 hours		
Humidified for 96 hours		
Humidified for 150 hours		

Table 3.8 provides the data obtained from the tensile test result that will be produced after the test, because the test will provide us with the maximum force and the greatest stress possible. As a result, it is representative of all of the conditions that will be investigated in this research. Consequently, the stress and strain can be calculated, and a stress and strain graph may be plotted as a result of the tensile test.

3.10.2.2 Stress and strain graph

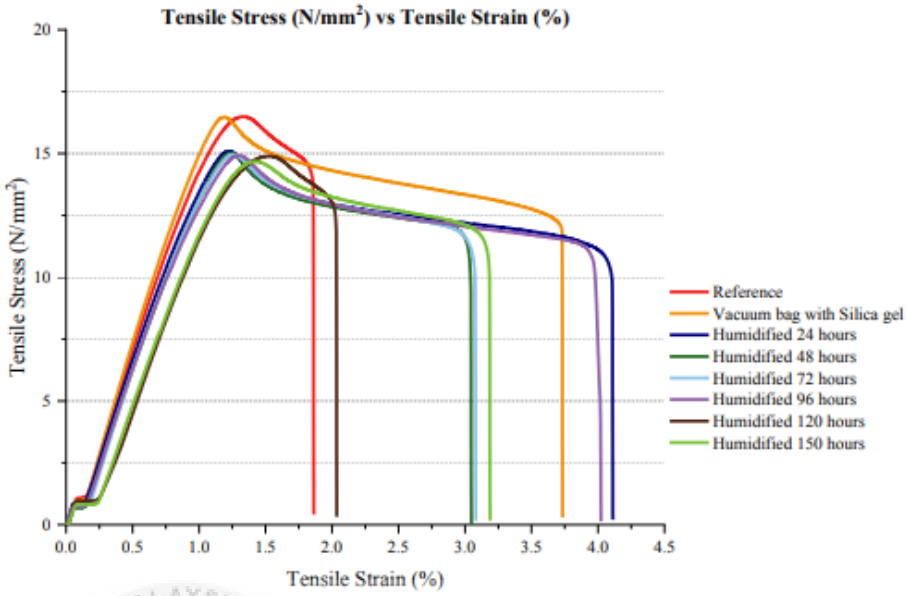

Figure 3.18: Example of the stress and strain graph which is generated from the data obtained.

Figure 3.18 illustrates an example of a stress and strain graph that is derived from the results of a tensile test. The stress-strain curve can be used to determine how stress varies as strain increases. It is determined by gradually applying a load to a test coupon and monitoring the deformation and it is possible to calculate the shear stress and strain. The ultimate tensile strength (UTS) was determined in this research.

3.11 Sputter Coating Process

Figure 3.19: SC 7620 Mini Sputter Coater.

A sputter coat is a physical vapor deposition method used to generate a very thin functional coating on a substrate. Sputtering coatings were used to ensure high-quality SEM pictures from samples. Sputtering samples requires a very thin coating of conducting metals such as chromium, platinum, or gold to be applied to the sample. The 3D printed components fracture (PETG, TPU) were sputter-coated with 10nm of 20% palladium and 80% gold to enhance the SEM picture. Because of its high conductivity and tiny grain size, gold was chosen as a coater for this picture. Figure 3.19 shows the SC 7620 Mini Sputter Coater that will be utilized in this study. Sputtered coating will be applied to the fractured section. The sputter coat, coatings the material with the highest and lowest tensile strength. In this procedure, electrons are attracted to the surfaces of non-conductive materials using a charging mechanism. Figure 3.20 shows the difference in SEM images for (a) before sputter-coating and (b) after sputter-coating.

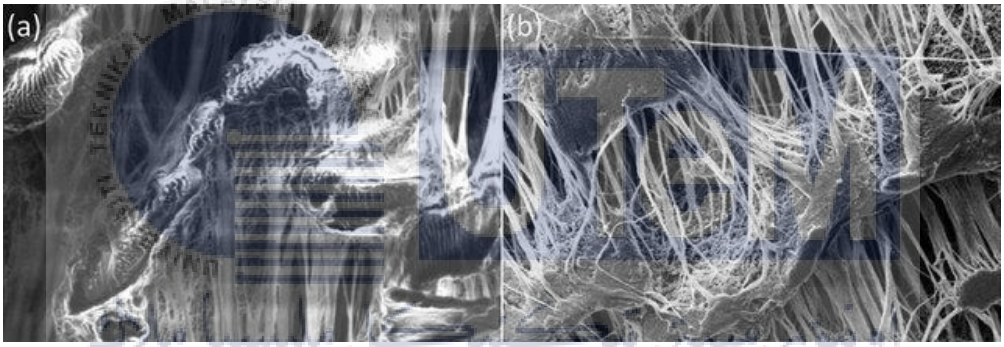

Figure 3.20: The different SEM image for (a) before sputter-coating (b) after sputter-coating (Heu *et al.*, 2019).

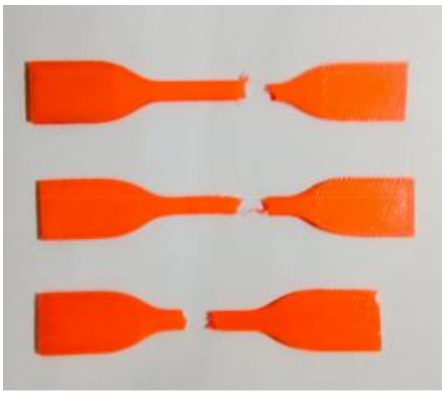

Figure 3.21: Fractured tensile sample (Srinivasan et al., 2020).

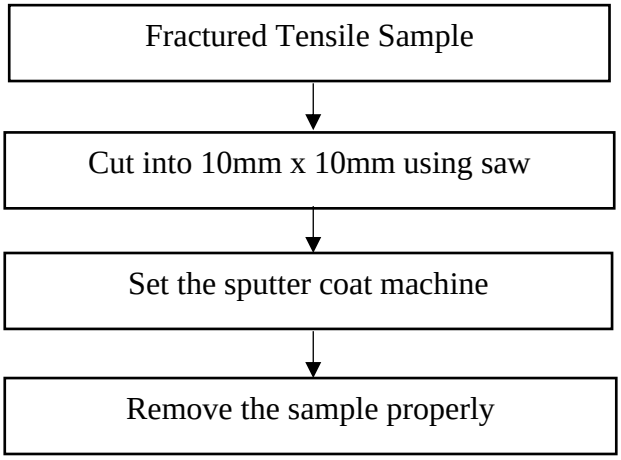

Figure 3.22: Process flow of sputter coat.

The first step which is shown in Figure 3.22 which is the flowchart to configure the fractured tensile samples with the closest maximum force value to the average value is used to conduct the sputter coat process. The fractures tensile sample as shown in Figure 3.21 were cut into 10mm x 10 mm using a saw because the sputter coater machine only allows the small specimen to be added inside it. After that, the machine sputter coat machine will be set with the sample is sputter-coated with 10nm thick of gold-palladium using SC7620 Mini Sputter Coater machine. Gold was chosen as a coater due to its high conductivity and tiny particle size, leading to a high-resolution image. It took three minutes to ensure the sample is thoroughly coated. In addition, remove the sample properly from the machine and the samples were kept in an airtight container after the coating process to prevent contamination.

3.12 Scanning Electron Microscopy (SEM) Process

Figure 3.23: Carl Zeiss Evo 50.

The microstructural analysis is performed in this study to acquire a thorough understanding of the effects of humidity on the pre-dried 3D printed PETG and TPU specimens. After sputter coating, the specimens were examined under a scanning electron microscope to determine their microstructure. Visual inspection of a surface with a scanning electron microscope (SEM) helps reveal contaminates or unknown particles, as well as the cause of failure and material interactions. SEM is a machine that provides nanoscale-level information on a range of materials without the need for sample preparation. The images are produced by scanning a focused electron beam across a surface with SEM equipment. In this study, a Carl Zeiss Evo 50 scanning electron microscope (SEM) with a 15 kV acceleration is used to analyse the microstructure of materials at 50x and 100x magnification power is shown in Figure 3.23. An electron beam is directed towards a target and scanned over the item to generate a two-dimensional (2D) picture in a scanning electron microscope. As electrons in the beam make contact with the sample, several signals are created, providing information on the surface topography, porosity, and composition of the sample. Other than that, the SEM will be analysed using the ImageJ software to observe the structure of the specimens. Kakanuru and Pochiraju (2020) discovered large voids in the SEM picture of the sample, which they believe are caused by the degradation of the materials. Figure 3.24 clearly illustrates the change in geometry of voids between aged and unaged specimens.

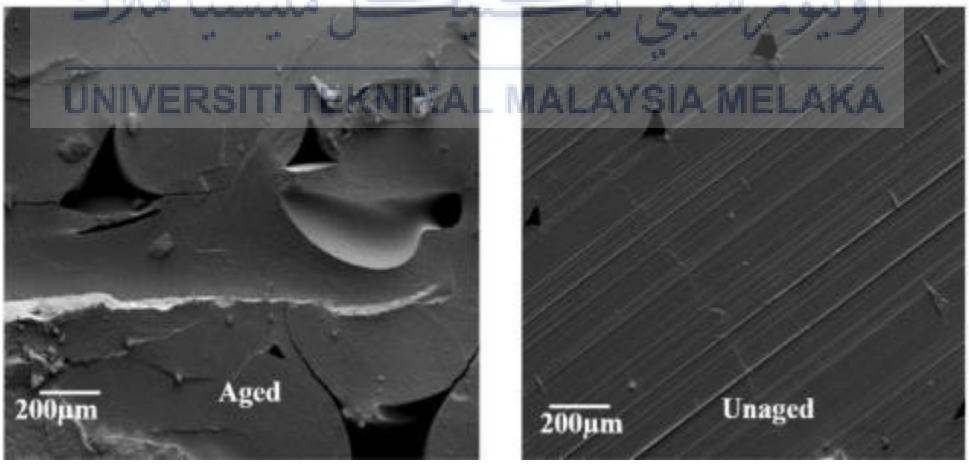

Figure 3.24: The microstructure of 3D printed PLA (Kakanuru and Pochiraju, 2020).

CHAPTER 4
RESULT AND DISCUSSION

4.1 Introduction

This chapter presents the analysis of surface roughness, tensile strength, SEM images, and density test of 3D printed PETG and TPU specimens from three different humidity conditions: (a) new PETG and TPU filament roll, which acts as the reference; (b) used PETG and TPU filament roll stored in the vacuum bag, with the addition of desiccant; (c) used PETG and TPU filament roll stored in an open environment, exposed to a humidifier for a variant of 48, 96, and 150 hours. This chapter discusses the result and compares the un-dried and pre-dried samples for PETG and TPU at three different humidity conditions. A comparison of the un-drying filament with the pre-drying filament using a dryer is presented.

4.2 Surface Roughness Analysis Using ANOVA

The surface roughness analysis is performed using Mituyoto Surftest Roughness Tester and following standard ISO 1997 with traveling length (λc) of 0.8mm. The roughness average (Ra) is measured on specimens with three different humidity conditions; (i) new filament roll that act as a reference, (ii) used filaments roll stored in the vacuum bag with 50 g desiccant; (iii) used filaments roll exposed to a humidifier for 150 hours. The surface roughness test requires six samples from each condition, including for the un-dried and dried group. For this investigation, five measurements were taken at each of the selected measurement points, as described in the methodology section, to minimize the possible measurement errors.

ANOVA has been used to analyze surface roughness results for each of the stated conditions. F-value is calculated for each sample and a comparison was made between the un-dried and dried samples. In addition, a comparison between the thermoplastic polymer (PETG and TPU) was also executed. The results and analyses of the surface roughness of PETG and TPU are presented in Sections 4.2.1 and Section 4.2.2, respectively. The ANOVA analysis determines whether H_0 is rejected or not. H_0 is assuming that all mean is the same. Consequently, the F-value for all samples is more significant than F-critical. Therefore, H_0 is rejected, concluding that there is a difference between the mean in all conditions.

4.2.1 The Roughness Average (Ra) Reading of PETG

This subtopic presents the result of PETG average roughness for all conditions stated. The top of the sample is the measurement for points A, B, and C. Nonetheless, the bottom of the sample is the measurement for points D, E, and F. The analysis of the best point of surface roughness is carried out as a direct result of the data that were averaged over the three samples.

4.2.1.1 New filament rolls of PETG as reference

Table 4.1: The average roughness for the new un-dried PETG (reference)

New filament rolls as a reference (un-dried)								
Reading Point	1(µm)	2(µm)	3(µm)	4(µm)	5(µm)	Sum	Average	Variance
Sample 1								
A	2.98	2.96	2.89	2.91	2.78	14.52	2.904	0.00613
B	4.21	4.95	4.98	2.51	4.28	20.93	4.186	1.00813
C	6.5	5.07	4.78	4.77	7.82	28.94	5.788	1.80097
D	2.07	1.86	2.26	2.97	3.82	12.98	2.60	0.64233
E	2.99	4.12	2.71	2.7	3.14	15.66	3.132	0.34027
F	8.08	5.92	6.85	6.37	7.68	34.9	6.98	0.80315
Sample 2								
A	3.54	5.93	3.57	3.28	3.44	19.76	3.952	1.23547
B	2.85	2.87	2.24	2.68	3.21	13.85	2.77	0.12475
C	4.54	5.12	3.57	4.26	4.22	21.71	4.342	0.31552
D	6.69	5.9	8.67	7.19	6.47	34.92	6.98	1.10268
E	3.31	3.51	3.6	3.04	4.47	17.93	3.586	0.29043
F	2.47	4.51	2.91	2.12	2.14	14.15	2.83	0.98465
Sample 3								
A	5.38	6.66	7.05	8.08	7.9	35.07	7.01	1.17948
B	2.22	2.72	3.54	2.66	1.99	13.13	2.626	0.35368
C	3.14	2.52	2.75	3.75	4.09	16.25	3.25	0.43765
D	6.9	5.71	4.55	5.88	8.35	31.39	6.278	2.03677
E	3.09	3.8	2.98	3.77	2.58	16.22	3.244	0.28003
F	3.13	1.92	2.06	2.65	2.21	11.97	2.39	0.24433

The data presented in Table 4.1 indicates the result of a surface roughness test conducted on a new un-dried PETG filament roll that act as a reference. The reading shows that the lowest reading was found in sample 1 at point D, with an average value of 2.60µm and the highest reading was found in sample 1 at point F, with a value of 6.98µm. Aside from that, the lowest reading for sample 2 is at point B, with a value of 2.77µm. In comparison, the reading that is the highest for sample 2 is 6.98µm at point D. In addition, the reading that is the lowest for sample 3 can be found at point F, where it is 2.39µm, and the reading that is the highest can be found at point A, where it is 7.01µm. The finding shows that the average roughness fluctuates in all measurement points, showing that the 3D printing technology could not guarantee a standard waviness and even surface structure throughout the sample.

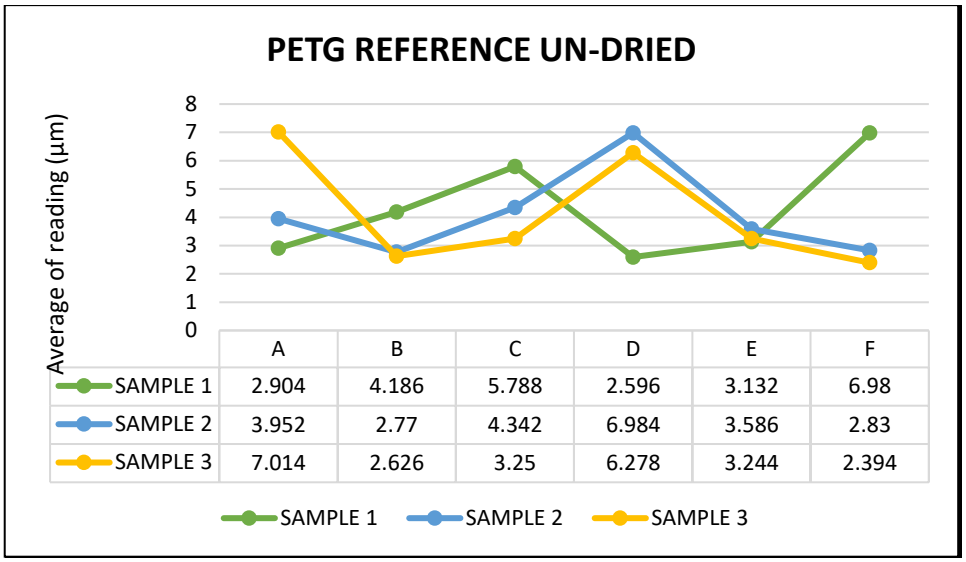

Figure 4.1: The average reading of new un-dried PETG (reference)

The average reading of the new un-dried PETG filament rolls that were used as references for the three samples is presented in Figure 4.1. Based on the results, the top of samples 2 and 3 at point B and the bottom of samples 1 and 3 at point E offer the best interactions when compared to the other points. Therefore, point B, which has a value of 2.77µm for sample 2 and 2.61µm for sample 3 is the best point to have at the top of the sample. In addition, point E, which has a value of 3.13µm for sample 1 and 3.24µm for sample 3 is the best point for the bottom of the sample. A microstructure analyses of the points detected could be further analyzed using the SEM machine in the future work.

Table 4.2: ANOVA result for new un-dried PETG (reference)

Sample 1						
Source of Variation	SS	df	MS	F	P-value	F crit
Between Groups	78.0928167	5	15.6185633	20.3677	6.28E-08	2.620654
Within Groups	18.40392	24	0.76683			
Total	96.4967367	29				
Sample 2						
Source of Variation	SS	df	MS	F	P-value	F crit
Between Groups	60.2041867	5	12.0408373	17.82	2.18E-07	2.620654
Within Groups	16.214	24	0.67558333			
Total	76.4181867	29				
Sample 3						
Source of Variation	SS	df	MS	F	P-value	F crit
Between Groups	98.8317767	5	19.7663553	26.17	5.53E-09	2.620654
Within Groups	18.12776	24	0.75532333			
Total	116.959537	29				

Table 4.2 tabulates the ANOVA result for the new un-dried PETG filament rolls acts as a reference for three samples. The F-value for sample is bigger than the F-critical. So, H_0 is rejected. By comparing the data from three sample, sample 2 shows the lowest reading for F-value with 17.82µm. In contrast, sample 3 indicates the highest reading for surface roughness with a value 26.17µm. Therefore, the ANOVA analysis confirms that the new PETG filament which was un-dried fails to provide a similar surface texture throughout the sample.

Table 4.3: The average roughness of the new pre-dried PETG (reference)

New filament rolls as a reference (pre-dried)								
Reading / Point	1(µm)	2(µm)	3(µm)	4(µm)	5(µm)	Sum	Average	Variance
Sample 1								
A	2.89	2.03	2.22	1.94	2.06	11.14	2.228	0.14717
B	1.88	1.21	2.44	1.49	2.96	9.98	2.00	0.50343
C	3.34	2.1	2.75	2.22	1.81	12.22	2.444	0.36673
D	3.32	2.85	2.97	2.59	3.32	15.05	3.01	0.09895
E	3.65	4.89	3.11	4.41	3.32	19.38	3.876	0.56508
F	3.06	3.93	4.62	4.46	4.46	20.53	4.11	0.40998
Sample 2								
A	4.38	3.08	3.29	3.8	2.8	17.35	3.47	0.3926
B	3.02	1.98	2.44	3	2.4	12.84	2.57	0.19532
C	2.65	3.26	2.71	2.97	2.72	14.31	2.862	0.06457
D	5.25	4.56	4.49	4.12	5.43	23.85	4.77	0.30275
E	4.69	5.15	3.92	3.89	4.07	21.72	4.344	0.30758
F	5.54	5.2	5.02	4.89	5.56	26.21	5.24	0.09122
Sample 3								
A	2.67	2.54	2.58	2.59	3.37	13.75	2.75	0.12235
B	3.03	2.43	2.39	2.56	2.49	12.9	2.58	0.0674
C	2.9	2.87	2.88	3.19	3.74	15.58	3.116	0.13943
D	3.8	3.14	3.88	2.5	3.01	16.33	3.266	0.33258
E	3.51	3.61	4.51	5.61	3.74	20.98	4.196	0.77998
F	5.82	4.92	4.89	5.21	4.3	25.14	5.03	0.30527

Table 4.3 shows the results of surface roughness tests performed on new pre-dried PETG filament rolls which act as reference. The lowest reading is in sample 1 at point B, which has an average value of 2.00µm, and the highest reading is in sample 1 at point F, which has a value of 4.11µm. Aside from that, the lowest reading for sample 2 is at point B, with a value of 2.57µm, and the highest reading for sample 2 is at point C, with a value of 5.24µm. Also, the lowest reading for sample 3 can be found at point B, where it is 2.58µm, and the highest reading can be found at point F, where it is 5.03µm.

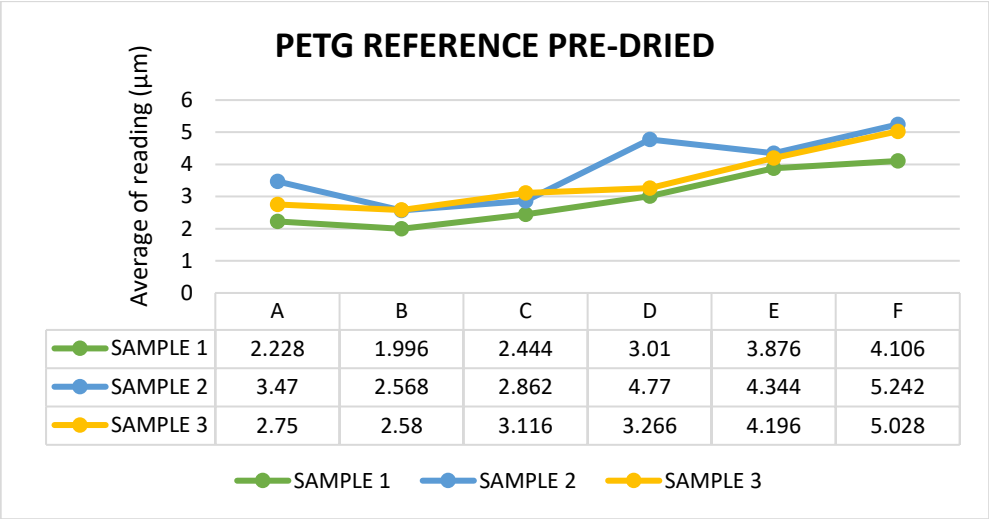

Figure 4.2: The average reading of new pre-dried PETG (reference)

Figure 4.2 depicts the average reading of the new pre-dried PETG filament rolls used as references for the three samples. Based on the data, we can determine that samples 2 and 3 for point B have the best interactions when compared to the other points with value 2.57µm for sample 2 and 2.58µm for sample 3. But, the lowest reading at point B is for sample 1 with a value of 2.00µm.

Table 4.4: The ANOVA result of new pre-dried PETG (reference)

Sample 1						
Source of Variation	SS	df	MS	F	P-value	F crit
Between Groups	19.42291	5	3.884581333	11.14	1.23E-05	2.62065415
Within Groups	8.36536	24	0.348556667			
Total	27.78827	29				
Sample 2						
Source of Variation	SS	df	MS	F	P-value	F crit
Between Groups	28.94056	5	5.788112	25.65	6.75E-09	2.62065415
Within Groups	5.41616	24	0.225673333			
Total	34.35672	29				
Sample 3						
Source of Variation	SS	df	MS	F	P-value	F crit
Between Groups	22.14815	5	4.429629333	15.21329357	9.03E-07	2.62065415
Within Groups	6.98804	24	0.291168333			
Total	29.13619	29				

Table 4.4 shows the ANOVA result of the surface roughness test for new pre-dried PETG filament rolls act as reference for three samples. So, showed that the F-value for all samples is larger than F-critical. So, H_0 is rejected. By comparing the data from the three samples, we can see that sample 1 has the lowest F-value, at 11.14µm. On the other hand, sample 2 has the highest value for surface roughness, which is 25.65µm.

4.2.1.2 Used filament roll stored in the vacuum bag with 50g desiccant

Table 4.5: The average roughness for used un-dried PETG (silica)

Used filament roll stored in the vacuum bag with 50g desiccant (un-dried)								
Reading Point	**1(µm)**	**2(µm)**	**3(µm)**	**4(µm)**	**5(µm)**	Sum	Average	Variance
Sample 1								
A	2.74	3.1	3.06	3.19	3.2	15.29	3.058	0.03512
B	3.19	3.55	2.37	3.18	4.37	16.66	3.33	0.52342
C	2.67	2.8	2.87	2.56	2.01	12.91	2.582	0.11647
D	2.62	3.29	1.71	2.72	2.16	12.5	2.5	0.35665
E	1.59	1.78	2.08	2.18	1.64	9.27	1.854	0.06958
F	1.4	1.99	1.93	1.46	1.19	7.97	1.59	0.12213
Sample 2								
A	2.82	2.24	2.47	2.21	3.45	13.19	2.638	0.26557
B	2.71	1.9	2.89	3.55	2.83	13.88	2.78	0.34668
C	3.76	3.27	2.89	3.55	2.83	16.3	3.26	0.164
D	2.76	3.27	2.39	2.89	2.48	13.79	2.758	0.12307
E	2.13	2.25	1.11	2.75	1.47	9.71	1.942	0.42452
F	1.45	2.45	1.65	1.43	1.68	8.66	1.73	0.17392
Sample 3								
A	3.02	2.85	2.19	2.32	3.92	14.3	2.86	0.47245
B	2.51	2.56	3.2	3.32	2.62	14.21	2.842	0.14892
C	2.54	2.79	2.5	2.33	2.4	12.56	2.512	0.03097
D	1.69	1.58	2.41	2.15	1.68	9.51	1.90	0.12937
E	1.76	1.7	1.9	2.66	1.77	9.79	1.958	0.15932
F	2.11	1.68	1.66	1.85	2.79	10.09	2.018	0.21877

Table 4.5 shows the results of surface roughness tests done on used PETG un-dried filament rolls stored in a vacuum bag with 50g of desiccant. The lowest reading is in sample 1 at point F, which has an average value of 1.59µm. The highest reading is in sample 1 at point B, which has a value of 3.33µm. In addition, the lowest reading for sample 2 is at point F, which has a value of 1.73µm, and the highest reading for sample 2 is at point B, which has a value of 2.78µm. Then, the lowest reading for sample 3 is 1.90µm at point D, and the highest reading is 2.86µm at point A.

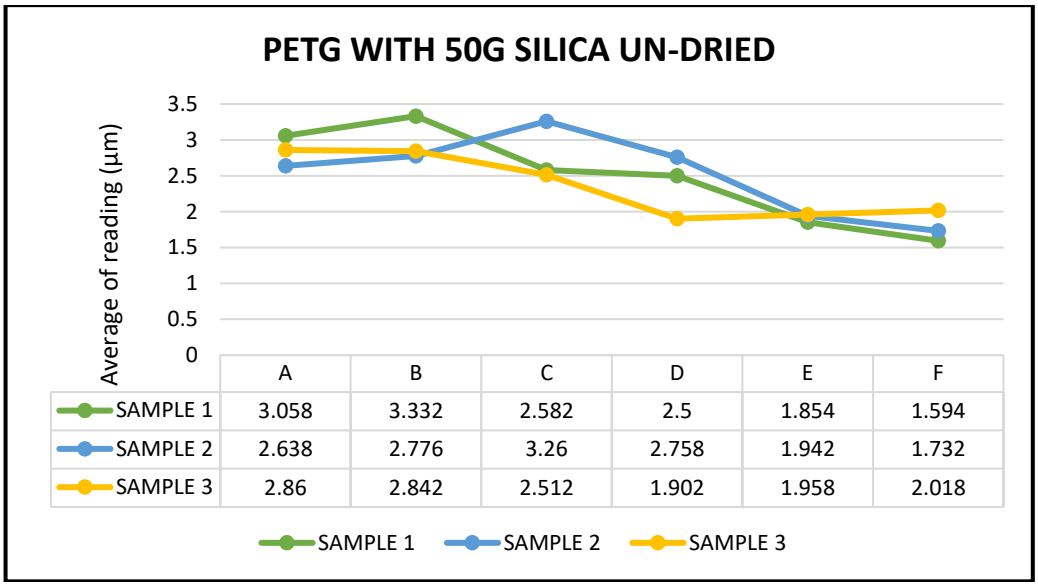

Figure 4.3: The average reading of used un-dried PETG (silica)

Figure 4.3 presented the average reading of used PETG un-dried filament roll stored in the vacuum bag with 50g desiccant for the three samples. Based on the results, samples 2 and 3 for point B and point E offer the best interactions when compared to the other points. Therefore, the best point at the top of the sample at point B with a value 2.78µm for sample 2 and 2.82µm for sample 3. In addition, the best point for the bottom of the sample at point E with a value of 1.94µm for sample 2 and at point E with a value of 1.96µm for sample 3.

Table 4.6: The ANOVA result for used un-dried PETG (silica)

Sample 1						
Source of Variation	SS	df	MS	F	P-value	F crit
Between Groups	11.2369867	5	2.24739733	11.02	1.3467E-05	2.620654148
Within Groups	4.89348	24	0.203895			
Total	16.1304667	29				
Sample 2						
Source of Variation	SS	df	MS	F	P-value	F crit
Between Groups	8.19349667	5	1.63869933	6.56460047	0.00055752	2.620654148
Within Groups	5.99104	24	0.24962667			
Total	14.1845367	29				
Sample 3						
Source of Variation	SS	df	MS	F	P-value	F crit
Between Groups	4.96494667	5	0.99298933	5.14	0.00241727	2.620654148
Within Groups	4.6392	24	0.1933			
Total	9.60414667	29				

Table 4.6 displays the ANOVA results for the surface roughness test for three samples of used PETG un-dried filament stored in a vacuum bag with 50g desiccant. Consequently, the result reveals that the F-value for each sample is greater than F-critical. Therefore, $H_0$is are rejected. Comparing the data from the three samples reveals that sample three has the lowest F-value, at 5.14µm. In contrast, sample 1 has the greatest surface roughness value, which is 11.02µm.

Table 4.7: The average roughness test for used pre-dried PETG (silica)

Used filament roll stored in the vacuum bag with 50g desiccant (pre-dried)								
Reading / Point	**1(µm)**	**2(µm)**	**3(µm)**	**4(µm)**	**5(µm)**	**Sum**	**Average**	**Variance**
Sample 1								
A	4.72	3.53	4.59	3.69	4.21	20.74	4.15	0.27952
B	4.28	4.88	3.62	3.82	3.89	20.49	4.098	0.24842
C	4.38	3.91	4.78	3.43	4.13	20.63	4.126	0.25583
D	3.1	3.67	2.36	3.47	2.27	14.87	2.974	0.40473
E	2.38	2.72	2.35	1.25	2.36	11.06	2.21	0.31317
F	2.48	2.89	2.8	2.83	2.66	13.66	2.732	0.02697
Sample 2								
A	4.61	4.68	4.56	4.22	3.41	21.48	4.296	0.27663
B	3.77	3.44	3.63	3.47	3.84	18.15	3.63	0.03135
C	4.55	4.58	3.95	4.02	4.43	21.53	4.31	0.08963
D	2.06	2.11	2.24	1.81	2.07	10.29	2.058	0.02437
E	1.97	2.01	1.83	2.1	2.72	10.63	2.13	0.11973
F	1.85	2.69	2.5	2.95	2.8	12.79	2.558	0.18357
Sample 3								
A	3.16	3.29	3.64	3.66	3.4	17.15	3.43	0.0476
B	3.38	3.49	3.63	3.68	3.6	17.78	3.556	0.01453
C	3.36	3.41	4.23	3.09	4.18	18.27	3.654	0.26813
D	3.99	2.71	3.47	3.96	3.87	18	3.6	0.2909
E	3.46	3.6	3.59	3.76	4.27	18.68	3.736	0.10043
F	3.85	3.69	4.33	4.56	3.63	20.06	4.01	0.16932

Table 4.7 displays the outcomes of surface roughness tests conducted on used PETG pre-dried filament rolls kept in a vacuum bag with 50g of desiccant. Sample 1, at point E has an average value of 2.21µm which displays the lowest reading and the highest reading of sample 1 at point A which has a value of 4.15µm. The lowest measurement for sample 2 is at point E, which has a value of 2.13µm, while the highest reading for sample 2 is at point C, which has a value of 4.31µm. The minimum value for sample 3 is 3.43µm at point A, and the maximum reading is 4.01µm at point F.

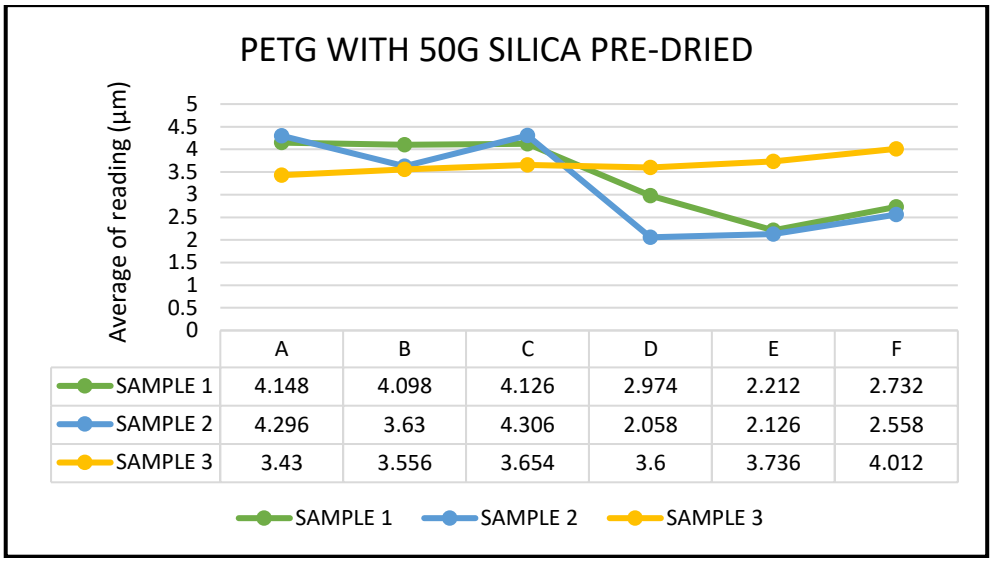

Figure 4.4: The average reading of used pre-dried PETG (silica)

Figure 4.4 presented the average reading of used PETG pre-dried filament roll stored in the vacuum bag with 50g desiccant for the three samples. As a result, when compared to the other points it can find out that the best interactions of points for samples 2 and 3 at point B and point E for sample 1 and 2. Therefore, the best point to have at the top of the sample at point B with a value of 3.63µm for sample 2 and 3.56µm for sample 3. In addition, the best point for the bottom of the sample at point E for sample 1 is 2.21µm and 2.13µm for sample 2.

Table 4.8: The ANOVA result for used pre-dried PETG (silica)

Sample 1						
Source of Variation	SS	df	MS	F	P-value	F crit
Between Groups	18.0540567	5	3.6108113	14.172642	1.67E-06	2.620654
Within Groups	6.11456	24	0.2547733			
Total	24.1686167	29				
Sample 2						
Source of Variation	SS	df	MS	F	P-value	F crit
Between Groups	27.3532167	5	5.4706433	45.26	1.91E-11	2.620654
Within Groups	2.90112	24	0.12088			
Total	30.2543367	29				
Sample 3						
Source of Variation	SS	df	MS	F	P-value	F crit
Between Groups	0.98450667	5	0.1969013	1.33	0.286817	2.620654
Within Groups	3.56364	24	0.148485			
Total	4.54814667	29				

Table 4.8 shows the ANOVA results for the Surface Roughness Test for three samples of used PETG pre-dried filament stored in a vacuum bag with 50g desiccant. As a result, the result shows that the F-value for each sample is larger than F-critical. So, H_0 is rejected. By comparing the data from the three samples, we see that sample 3 has the lowest F-value, at 1.33µm. In contrast, Sample 2 has the highest surface roughness value, which is 45.26µm.

4.2.1.3 Humidified filament for 150 hours

Table 4.9: The average roughness for used un-dried PETG (humidified 150 hours)

Humidified filament for 150 hours (un-dried)								
Reading / Point	1(µm)	2(µm)	3(µm)	4(µm)	5(µm)	Sum	Average	Variance
Sample 1								
A	3.08	3.47	2.5	3.68	2.98	15.71	3.142	0.20982
B	5.77	4.54	3.47	4.64	3.53	21.95	4.39	0.89385
C	5.55	3.49	4.14	4.36	3.35	20.89	4.178	0.76897
D	1.27	1.41	1.55	1.49	1.31	7.03	1.406	0.01388
E	1.33	0.83	1.38	1.92	2.14	7.6	1.52	0.26905
F	1.09	1.69	1.66	1.03	1.29	6.76	1.352	0.09632
Sample 2								
A	3.97	3.26	3.57	3.25	3.08	17.13	3.426	0.12373
B	3.14	5	4.4	4.34	4.38	21.26	4.252	0.46052
C	3.89	4.77	5.09	3.83	3.92	21.5	4.30	0.3446
D	1.24	1.28	1.15	1.32	1.14	6.13	1.23	0.00628
E	1.73	1.56	1.24	1.55	1.25	7.33	1.466	0.04583
F	1.89	2.01	1.47	1.73	2.01	9.11	1.822	0.05192
Sample 3								
A	3.68	3.15	3.54	2.89	3.14	16.4	3.28	0.10405
B	3.03	5.87	3.57	3.34	4.06	19.87	3.97	1.26463
C	4.09	4.14	4.01	3.85	2.96	19.05	3.81	0.23785
D	1.81	2.09	1.46	1.59	1.61	8.56	1.712	0.06032
E	1.56	1.63	1.71	1.88	1.68	8.46	1.692	0.01427
F	0.88	1.24	1.33	1.36	1.32	6.13	1.23	0.03938

Table 4.9 displays the outcomes of surface roughness tests conducted on used PETG un-dried filament exposed to a humidifier for 150 hours. For sample 1, the lowest reading at point F has an average value of 1.35µm and the highest reading of sample 1 at point B has a value of 4.39µm. The lowest reading for sample 2 is at point D, which has a value of 1.23µm, while the highest reading for sample 2 is at point C, which has a value of 4.3µm. The lowest value for sample 3 is 1.23µm at point F, and the highest reading is 3.97µm at point B.

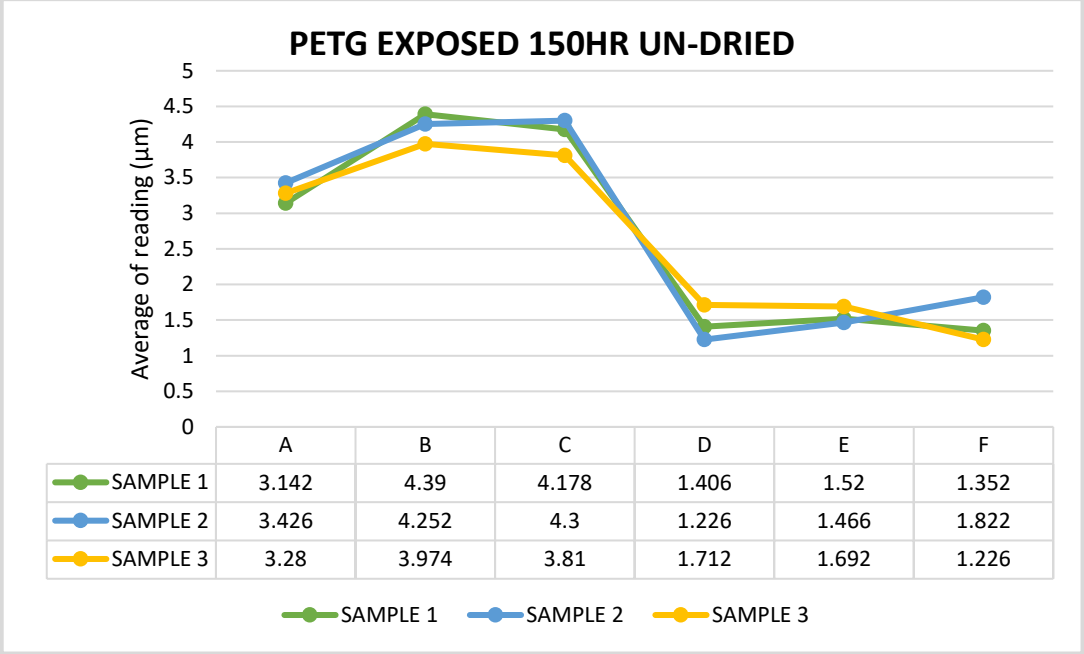

Figure 4.5: The average reading of used un-dried PETG (humidified 150 hours).

Figure 4.5 indicates the average reading of the used PETG un-dried filament that was exposed to humidifiers for 150 hours for three samples. According to the result stated, the best interaction is only at point E sample 1 and 2 which indicates the value of 1.5µm sample 1 and 1.466µm for sample 2.

Table 4.10: The ANOVA result for used un-dried PETG (humidified 150 hours).

Sample 1						
Source of Variation	SS	df	MS	F	P-value	F crit
Between Groups	50.56198667	5	10.11239733	26.94376013	4.136E-09	2.620654148
Within Groups	9.00756	24	0.375315			
Total	59.56954667	29				
Sample 2						
Source of Variation	SS	df	MS	F	P-value	F crit
Between Groups	49.73942667	5	9.947885333	57.78726667	1.345E-12	2.620654148
Within Groups	4.13152	24	0.172146667			
Total	53.87094667	29				
Sample 3						
Source of Variation	SS	df	MS	F	P-value	F crit
Between Groups	36.56893667	5	7.313787333	25.50579715	7.1309E-09	2.620654148
Within Groups	6.882	24	0.28675			
Total	43.45093667	29				

Table 4.10 displays the ANOVA results for the Surface Roughness Test for three samples of used PETG un-dried filament exposed to humidifiers for 150 hours. As a result, the F-value for each sample is larger than F-critical. Hence, the H_0 is rejected. When compared the data from the three samples, it can be observed that sample 3 has the lowest F-value, at 25.51µm. Sample 2 had the highest surface roughness value of 57.79µm.

Table 4.11: The average roughness for used pre-dried PETG (humidified 150 hours).

Humidified filament for 150 hours (pre-dried)								
Reading / Point	**1(µm)**	**2(µm)**	**3(µm)**	**4(µm)**	**5(µm)**	**Sum**	**Average**	**Variance**
Sample 1								
A	4.37	5.51	7.58	5.32	2.48	25.26	5.05	3.43817
B	4.13	3.73	4.7	4.5	2.95	20.01	4.002	0.48307
C	2.63	4.04	5.92	2.52	6.96	22.07	4.414	3.91498
D	2.27	2.18	3.24	2.48	2.35	12.52	2.504	0.18143
E	2.21	1.4	1.82	1.28	1.39	8.1	1.62	0.15125
F	2.61	1.98	2.53	1.48	1.1	9.7	1.94	0.42895
Sample 2								
A	2.6	2.66	2.76	1.89	2.19	12.1	2.42	0.13485
B	2.8	2.18	2.73	2.82	3.18	13.71	2.74	0.12932
C	3.01	3.54	2.91	3.23	2.82	15.51	3.102	0.08327
D	1.13	1.53	2.13	1.24	1.89	7.92	1.584	0.17978
E	1	0.89	1.31	2.13	1.26	6.59	1.32	0.23677
F	3.02	3.61	1.92	3.18	1.56	13.29	2.658	0.76502
Sample 3								
A	2.17	2.46	3.06	1.99	2.07	11.75	2.35	0.18915
B	3.61	2.67	2	3.25	3.21	14.74	2.95	0.39352
C	2.54	2.6	3.15	2.61	3.18	14.08	2.816	0.10233
D	2.05	2.73	2.24	2.37	2.93	12.32	2.464	0.12958
E	2.34	2.69	2.69	2.57	2.48	12.77	2.554	0.02213
F	2.16	2.23	2.92	1.36	1.7	10.37	2.07	0.34928

Table 4.11 shows the result of surface roughness tests of used PETG pre-dried filament exposed to a humidifier for 150 hours. For sample 1, the average value of the lowest reading at point E is 1.62µm, while the average value of the highest reading at point A is 5.05µm. The reading for sample 2 with the lowest value is at point E, where it is 1.32µm, while the reading with the greatest value is at point B, where it is 2.74µm. In sample 3, position F has the lowest measurement of 2.07µm while point B has the highest reading of 2.95µm.

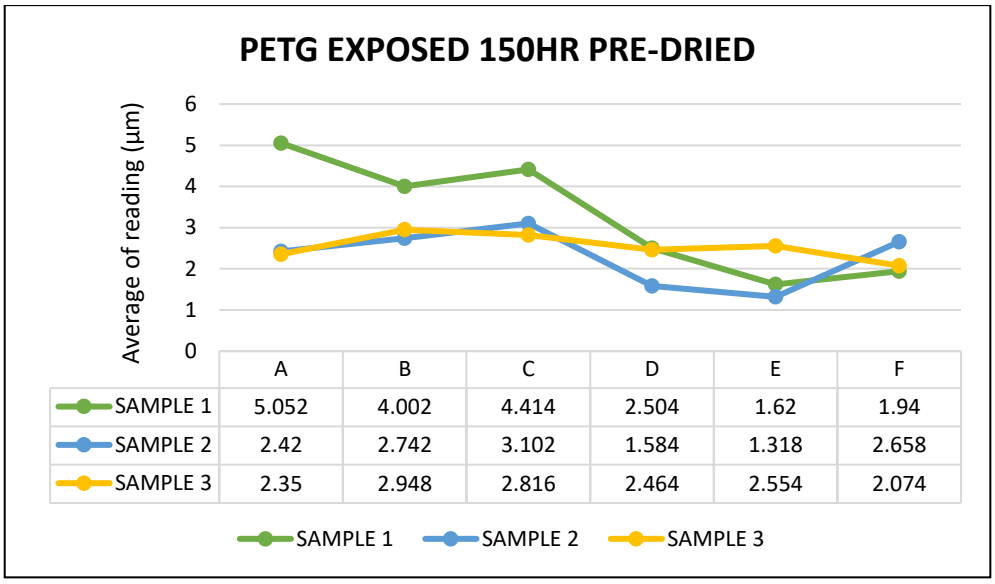

Figure 4.6: The average reading of used pre-dried PETG (humidified 150 hours).

Figure 4.6 indicates the average reading of the used PETG pre-dried filament that was exposed to humidifiers for 150 hours for three samples. According to the result stated, the best interaction at point A for sample 2 and 3 of the top of the sample and at point D for sample 1 and 3 of the bottom of the sample. Besides, the best interaction point at point A is 2.42µm for sample 2 and 2.35µm for sample 3. In addition, the best interaction point at point D is 2.50µm for sample 1 and 2.46µm for sample 3.

Table 4.12: The ANOVA result for used Pre-dried PETG (humidified for 150 hours).

Sample 1						
Source of Variation	SS	df	MS	F	P-value	F crit
Between Groups	50.48474667	5	10.0969493	7.04614479	0.00035208	2.620654148
Within Groups	34.3914	24	1.432975			
Total	84.87614667	29				
Sample 2						
Source of Variation	SS	df	MS	F	P-value	F crit
Between Groups	12.29008	5	2.458016	9.65	3.7944E-05	2.620654148
Within Groups	6.11604	24	0.254835			
Total	18.40612	29				
Sample 3						
Source of Variation	SS	df	MS	F	P-value	F crit
Between Groups	2.508376667	5	0.50167533	2.54	0.05578162	2.620654148
Within Groups	4.74396	24	0.197665			
Total	7.252336667	29				

Table 4.12 shows the ANOVA results for surface roughness test for three samples of used PETG pre-dried filament that were exposed to humidifiers for 150 hours using the ANOVA method. As a result, the F-value for each sample is larger than F-critical. Hence, the H_0 is rejected. The data from the three samples compared, and sample 3 has the lowest F-value of 2.54µm. Also, sample 2 has the highest surface roughness with a value of 9.65µm.

4.2.2 The roughness average (Ra) reading of TPU

This subtopic describes the TPU results for each of the conditions mentioned. The measurements for points A, B, and C were collected at the top of the sample. However, the measurements for points D, E, and F were collected at the bottom of the sample. The data that were averaged over the three samples directly led to the analysis of the best point of surface roughness.

4.2.2.1 New filament rolls of TPU as reference

Table 4.13: The average roughness for the new un-dried TPU (reference).

New filament rolls as a reference (un-dried)								
Reading / Point	1(µm)	2(µm)	3(µm)	4(µm)	5(µm)	Sum	Average	Variance
Sample 1								
A	10.18	10.81	13.56	12.75	10.38	57.68	11.536	2.31813
B	10.25	10.79	10.54	11.57	11.01	54.16	10.832	0.25052
C	10.84	13.02	15.01	14.51	14.08	67.46	13.49	2.73557
D	3.42	3.75	3.76	3.73	4.08	18.74	3.748	0.05457
E	3.76	3.25	3.56	3.9	3.62	18.09	3.62	0.05962
F	3.97	4.06	3.91	3.72	4.16	19.82	3.964	0.02753
Sample 2								
A	12.37	13.77	12.93	11.08	14.47	64.62	12.924	1.70328
B	15.36	16.41	17.16	16.81	15.7	81.44	16.29	0.56367
C	10.6	15.65	16.9	10.93	15.9	69.98	13.996	8.93183
D	5.05	2.94	2.93	3.41	4.52	18.85	3.77	0.93125
E	4.92	5.38	4.7	4.85	4.54	24.39	4.878	0.10012
F	5.37	4.72	4.97	5.92	4.96	25.94	5.188	0.22187
Sample 3								
A	15.29	14.55	11.39	14.88	15.41	71.52	14.304	2.76978
B	14.47	14.89	15.5	13.58	15.82	74.26	14.85	0.78057
C	12.37	12.61	13.59	11.12	12.45	62.14	12.428	0.77452
D	2.11	1.5	1.85	1.88	2.32	9.66	1.93	0.09457
E	1.77	2.83	2.63	3.12	2.5	12.85	2.57	0.25465
F	2.38	1.89	1.94	2.28	2.47	10.96	2.192	0.06877

The data presented in table 4.13 indicates the result of a surface roughness test conducted on new un-dried TPU filament rolls acts as a reference. The reading that is the lowest can be found in sample 1 at point E, with an average value of 3.62µm and the reading that is the highest can be found in sample 1 at point C, with a value of 13.49µm. Aside from that, the reading that is the lowest for sample 2 is at point D, with a value of 3.77µm, while the reading that is the highest for sample 2 is 16.29µm at point B. In addition, the reading that is the lowest for sample 3 can be found at point D, where it is 1.93µm, and the reading that is the highest can be found at point B, where it is 14.85µm.

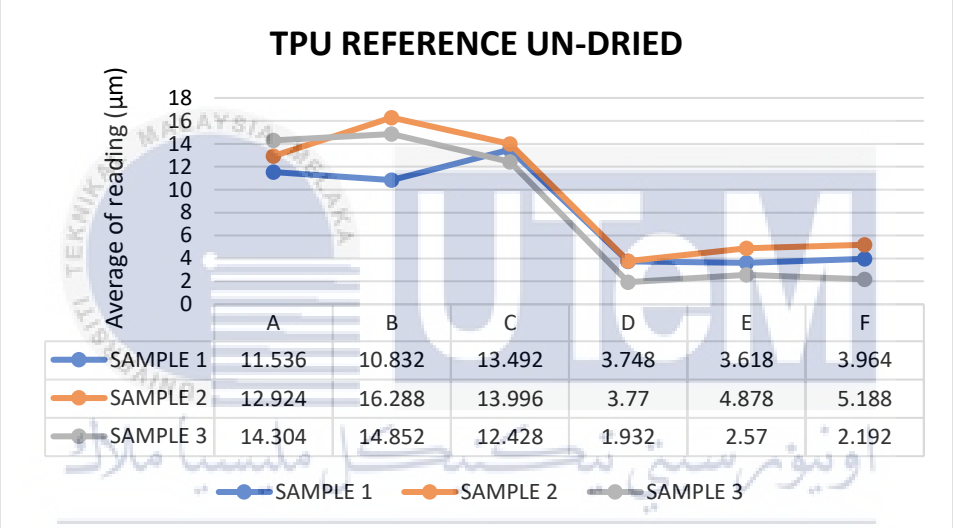

Figure 4.7: The average reading of new un-dried TPU (reference)

Figure 4.6 presented the average reading of the new un-dried TPU filament rolls that were used as references for the three samples. Based on the results, the best interaction points when compared to others is only at point D for sample 1 and sample 2 with the value of 3.75µm and 3.77µm respectively.

Table 4.14: ANOVA result for new un-dried TPU (reference)

Sample 1						
Source of Variation	SS	df	MS	F	P-value	F crit
Between Groups	520.7348	5	104.147	114.7427	6.02E-16	2.620654
Within Groups	21.78376	24	0.907657			
Total	542.5186	29				
Sample 2						
Source of Variation	SS	df	MS	F	P-value	F crit
Between Groups	754.0177	5	150.8035	72.66	1.06E-13	2.620654
Within Groups	49.80808	24	2.075337			
Total	803.8258	29				
Sample 3						
Source of Variation	SS	df	MS	F	P-value	F crit
Between Groups	1031.615	5	206.323	261.01	4.25E-20	2.620654
Within Groups	18.97144	24	0.790477			
Total	1050.586	29				

Table 4.14 state the ANOVA result for new un-dried TPU filament rolls acts as a reference for three sample. So, as the result indicated that the F-value for all sample is bigger than F-critical. Hence, H_0 is rejected. By comparing the data from three sample, sample 2 shows the lowest reading for F-value with 72.66µm. In contrast, sample 3 indicates the highest reading for surface roughness with a value 261.01µm. As a consequence of this, the smoothness of the surface of the sample will correspond directly to the reading of surface roughness.

Table 4.15: The average roughness of the new pre-dried TPU (reference)

New filament rolls as a reference (pre-dried)								
Reading / Point	1(µm)	2(µm)	3(µm)	4(µm)	5(µm)	Sum	Average	Variance
Sample 1								
A	18.9	16.53	19.08	14.91	14.81	84.23	16.85	4.30073
B	16.58	17.5	13.96	13.64	15.94	77.62	15.524	2.79708
C	13.93	12.54	15.21	19.38	18.02	79.08	15.816	8.05403
D	2.11	1.5	1.85	1.88	2.32	9.66	1.93	0.09457
E	1.77	2.83	2.63	3.12	2.5	12.85	2.57	0.25465
F	2.38	1.89	1.94	2.28	2.47	10.96	2.192	0.06877
Sample 2								
A	15.99	15.89	16.25	15.38	12.98	76.49	15.30	1.77887
B	16.46	16.22	16.96	13.14	12.42	75.2	15.04	4.3924
C	13.5	14.2	12.01	12.32	14.26	66.29	13.258	1.09682
D	3.13	2.84	3.25	1.89	1.57	12.68	2.536	0.57638
E	2.51	2.24	3.01	1.64	1.37	10.77	2.154	0.43643
F	1.36	1.92	1.26	1.57	1.81	7.92	1.58	0.07983
Sample 3								
A	10.99	17.32	11.99	10.62	12.01	62.93	12.586	7.37753
B	19.55	11.6	18.24	12.18	15.82	77.39	15.48	12.56062
C	10.66	11.52	12.5	11.15	11.23	57.06	11.412	0.46567
D	1.1	0.89	1.23	1.59	1.75	6.56	1.312	0.12472
E	1.11	1.46	1.53	1.19	1.23	6.52	1.304	0.03288
F	1.78	1.09	1.26	0.96	1.37	6.46	1.29	0.09907

Table 4.15 shows the results of surface roughness tests performed on new pre-dried TPU filament rolls which act as reference. The lowest reading is in sample 1 at point D, which has an average value of 1.93µm, and the highest reading is in sample 1 at point F, which has a value of 16.85µm. Aside from that, the lowest reading for sample 2 is at point F, with a value of 1.58µm, and the highest reading for sample 2 is at point A, with a value of 15.30µm. Other than that, the lowest reading for sample 3 can be found at point F, where it is 1.29µm, and the highest reading can be found at point B, where it is 15.48µm.

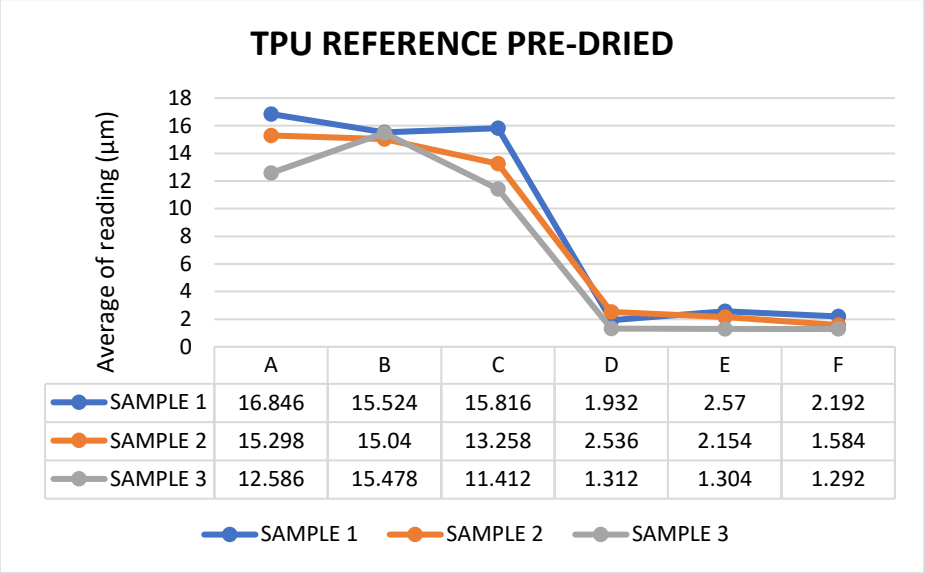

Figure 4.8: The average reading of new pre-dried TPU (reference)

Figure 4.8 depicts the average reading of the new pre-dried TPU filament rolls used as references for the three samples. Based on the data, we can determine that the best interaction is only at point B for samples 1 and 3 with a value 15.52µ for sample 1 and 15.48µm for sample 3. But, the lowest reading at point B is for sample 2 with a value 15.04µm.

Table 4.16: The ANOVA result of new pre-dried TPU (reference)

Sample 1						
Source of Variation	SS	df	MS	F	P-value	F crit
Between Groups	1440.50735	5	288.1014693	111.023	8.78E-16	2.620654
Within Groups	62.27932	24	2.594971667			
Total	1502.78667	29				
Sample 2						
Source of Variation	SS	df	MS	F	P-value	F crit
Between Groups	1175.4111	5	235.0822193	168.70	7.01E-18	2.620654
Within Groups	33.44292	24	1.393455			
Total	1208.85402	29				
Sample 3						
Source of Variation	SS	df	MS	F	P-value	F crit
Between Groups	1098.02703	5	219.6054053	63.78	4.54E-13	2.620654
Within Groups	82.64196	24	3.443415			
Total	1180.66899	29				

Table 4.16 shows the ANOVA result of the surface roughness test for new pre-dried TPU filament act as reference for three samples. Based on the results showed that the F-value for all samples is larger than F-critical. So, H_0 is rejected. By comparing the data from

the three samples, we can see that sample 3 has the lowest F-value, at 63.78µm. Other than that, the highest value for surface roughness is 168.70µm for sample 2.

4.2.2.2 Used filament roll stored in the vacuum bag with 50g desiccant.

Table 4.17: The average roughness for used un-dried PETG (silica)

Used filament roll stored in the vacuum bag with 50g desiccant (un-dried)								
Reading / Point	1(µm)	2(µm)	3(µm)	4(µm)	5(µm)	Sum	Average	Variance
Sample 1								
A	17.48	21.28	22.16	20.65	18.78	100.35	20.07	3.6352
B	18.32	21.75	18.89	17.65	16.15	92.76	18.552	4.24462
C	10.9	17.64	13.64	15.18	10.01	67.37	13.474	9.72958
D	1.85	2.49	2.28	2.63	3.86	13.11	2.622	0.56577
E	1.81	2.79	1.97	2.63	2.89	12.09	2.418	0.24412
F	1.38	2.24	2.05	1.53	1.05	8.25	1.65	0.23885
Sample 2								
A	10.65	8.38	9.33	20.99	11.2	60.55	12.11	25.86385
B	18.2	17.52	16.85	16.78	16.82	86.17	17.23	0.38498
C	11.53	13.52	13.81	20.52	14.27	73.65	14.73	11.57155
D	1.18	1.39	1.05	1.38	1.68	6.68	1.336	0.05733
E	1.02	1.29	1.01	1.05	1.11	5.48	1.10	0.01328
F	1.46	1.56	1.58	1.53	1.64	7.77	1.554	0.00438
Sample 3								
A	15.31	19.62	15.33	16.38	15.28	81.92	16.384	3.48873
B	18.68	16.55	15.7	16.5	21.06	88.49	17.70	4.75312
C	11.42	12.72	9.33	11.38	16.82	61.67	12.334	7.76068
D	1.19	1.16	1.05	0.97	1.28	5.65	1.13	0.01475
E	1.38	1.42	1.75	1.2	0.93	6.68	1.336	0.09093
F	1.22	0.98	1.1	1.52	1.47	6.29	1.258	0.05432

Table 4.17 shows the results of surface roughness tests done on used TPU un-dried filament rolls stored in a vacuum bag with 50g of desiccant. The lowest reading is in sample 1 at point F, which has an average value of 1.65µm and the highest reading is in sample 1 at point A which has a value of 20.07µm. In addition, the lowest reading for sample 2 is at point E which has a value of 1.10µm and the highest reading for sample 2 is at point B which has a value of 17.23µm. Besides that, the lowest reading for sample 3 is 1.13µm at point D, and the highest reading is 17.70µm at point B.

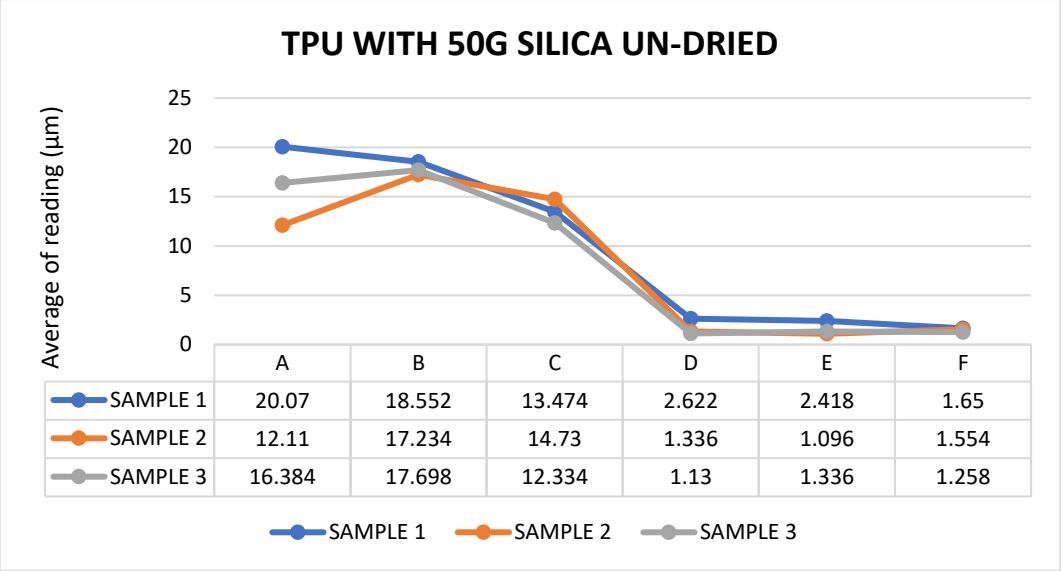

Figure 4.9: The average reading of used un-dried TPU (silica)

Figure 4.9 presented the average reading of used TPU un-dried filament roll stored in the vacuum bag with 50g desiccant for the three samples. Based on the results, the best interaction points only have at the bottom of the sample at point D and E for sample 2 and 3 and then at point F for all sample. The best interaction point at point D is 1.34µm for sample 2 and 1.13µm for sample 3 and then at point E is 1.10µm for sample 2 and 1.34µm for sample 3. Other than that, the best interaction points at point F a with a value 1.65µm for sample 1 and 1.55µm for sample 2 and then 1.26µm for sample 3.

Table 4.18: The ANOVA result for used un-dried TPU (silica)

Sample 1						
Source of Variation	SS	df	MS	F	P-value	F crit
Between Groups	1840.043777	5	368.00876	118.342586	4.22E-16	2.62065415
Within Groups	74.63256	24	3.10969			
Total	1914.676337	29				
Sample 2						
Source of Variation	SS	df	MS	F	P-value	F crit
Between Groups	1405.38092	5	281.07618	44.50	2.28E-11	2.62065415
Within Groups	151.58148	24	6.315895			
Total	1556.9624	29				
Sample 3						
Source of Variation	SS	df	MS	F	P-value	F crit
Between Groups	1597.116547	5	319.42331	118.58	4.13E-16	2.62065415
Within Groups	64.65012	24	2.693755			
Total	1661.766667	29				

Table 4.18 indicates the ANOVA results for the Surface Roughness Test for three samples of used TPU un-dried filament stored in a vacuum bag with 50g desiccant. Consequently, the result reveals that the F-value for each sample is greater than F-critical. Therefore, H_0 is rejected. Comparing the data from the three samples reveals that sample 2 has the lowest F-value at 44.50µm. In contrast, Sample 3 has the greatest surface roughness value which is 118.58µm.

Table 4.19: The average roughness test for used pre-dried TPU (silica)

Used filament roll stored in the vacuum bag with 50g desiccant (pre-dried)								
Reading Point	**1(µm)**	**2(µm)**	**3(µm)**	**4(µm)**	**5(µm)**	**Sum**	**Average**	**Variance**
Sample 1								
A	16.91	8.33	9.25	7.29	16.81	58.59	11.718	22.51552
B	15.86	18.3	19.89	13.85	18.07	85.97	17.19	5.55523
C	8.13	13.12	14.72	7.77	14.88	58.62	11.724	12.35903
D	1.11	1.11	1.54	1.37	1.43	6.56	1.312	0.03772
E	1.3	0.98	1.36	1.25	1.2	6.09	1.218	0.02122
F	1.1	1.15	0.64	1.03	1.33	5.25	1.05	0.06485
Sample 2								
A	17.26	8.27	17.39	17.23	16.05	76.2	15.24	15.475
B	16.17	10.01	7.57	11.91	11.73	57.39	11.478	9.92312
C	17.6	13.34	16.12	14.55	18.04	79.65	15.93	3.9724
D	1.33	1.5	1.28	1.35	1.29	6.75	1.35	0.00785
E	1.27	1.05	1.11	1.28	0.95	5.66	1.13	0.02032
F	1.43	1.27	1.34	1.2	1.3	6.54	1.308	0.00727
Sample 3								
A	15.01	17.71	19.39	16.62	13.93	82.66	16.532	4.66262
B	8.73	22.2	24.35	25.37	21.69	102.34	20.47	45.34332
C	16.6	13.88	16.03	14.73	16.44	77.68	15.536	1.39633
D	1.41	1.23	0.88	1.06	1.22	5.8	1.16	0.03985
E	1.12	1.34	1.25	0.98	1.16	5.85	1.17	0.0185
F	1.14	1.26	0.99	1.63	1.04	6.06	1.212	0.06527

Table 4.19 displays the outcomes of surface roughness tests conducted on used TPU pre-dried filament rolls kept in a vacuum bag with 50g of desiccant. For sample 1, point F has an average value of 1.05µm which displays the lowest reading and the highest reading of sample 1 at point B which has a value of 17.19µm. The lowest measurement for sample 2 is at point E, which has a value of 1.13µm, while the highest reading for sample 2 is at point C, which has a value of 15.93µm. The minimum value for sample 3 is 1.16µm at point D, and the maximum reading is 20.47µm at point B.

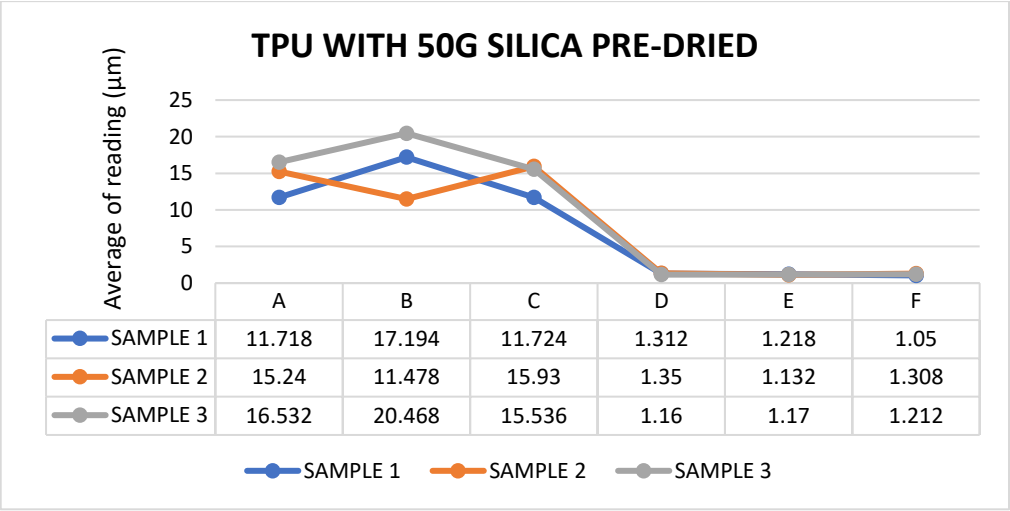

Figure 4.10: The average reading of used pre-dried TPU (silica)

Figure 4.10 presented the average reading of used TPU pre-dried filament roll stored in the vacuum bag with 50g desiccant for the three samples. As a result, the best interactions point for the top of the sample at point C for sample 2 and 3 with the value of 15.93µm and 15.54µm respectively. In addition, the best interaction points for the bottom of the sample at point D, E and F for all three sample. The best interaction point at point D is 1.31µm for sample 1 and 1.35µm for sample 2 and then 1.17 for sample 3. Besides that, the best interaction points at point E are 1.22µm for sample 1 and 1.13µm for sample 2 and then 1.17µm for sample 3. Other than that, the best interaction points at point F with value 1.05µm for sample 1 and 1.31µm for sample 2 and then 1.21µm for sample 3.

Table 4.20: The ANOVA result for used pre-dried PETG (silica)

Sample 1						
Source of Variation	SS	df	MS	F	P-value	F crit
Between Groups	1244.311307	5	248.8623	36.82	1.7E-10	2.620654
Within Groups	162.21428	24	6.758928			
Total	1406.525587	29				
Sample 2						
Source of Variation	SS	df	MS	F	P-value	F crit
Between Groups	1315.835657	5	263.1671	53.70	3E-12	2.620654
Within Groups	117.62384	24	4.900993			
Total	1433.459497	29				
Sample 3						
Source of Variation	SS	df	MS	F	P-value	F crit
Between Groups	2068.365537	5	413.6731	48.17	9.75E-12	2.620654
Within Groups	206.10356	24	8.587648			
Total	2274.469097	29				

Table 4.20 shows the ANOVA results for the Surface Roughness Test for three samples of used TPU pre-dried filament stored in a vacuum bag with 50g desiccant. As a result, the result shows that the F-value for each sample is larger than F-critical. So, H_0 is rejected. By comparing the data from the three samples, we see that sample 1 has the lowest F-value, at 36.82µm. In contrast, Sample 2 has the highest surface roughness value, which is 53.70µm.

4.2.2.3 Humidified Filament for 150 hours

Table 4.21: The average roughness for used un-dried PETG (humidified 150 hours)

Humidified filament for 150 hours (un-dried)								
Reading Point	1(µm)	2(µm)	3(µm)	4(µm)	5(µm)	Sum	Average	Variance
Sample 1								
A	19.05	15.71	13.34	19.64	15.82	83.56	16.712	6.80237
B	20.4	17.19	19.45	20.95	20.73	98.72	19.74	2.36658
C	20.73	18.16	16.24	17.99	20.79	93.91	18.782	3.82567
D	3.89	5.2	3.03	2.88	4.31	19.31	3.862	0.91207
E	2.48	4.45	2.13	2.7	2.55	14.31	2.86	0.83177
F	4.47	5.55	5.81	5.39	4.04	25.26	5.052	0.57492
Sample 2								
A	11.59	19.41	16.08	20.06	18.17	11.59	17.062	11.65897
B	19.99	20.61	21.13	20.02	20.1	19.99	20.37	0.24375
C	20.58	16.54	15.46	18.23	23.5	20.58	18.862	10.45682
D	7.47	4.56	4.02	6.2	6.8	7.47	5.81	2.1636
E	4	5.15	5.97	5.71	5.58	4	5.282	0.60157
F	2.55	4.83	3.82	4.1	3.7	2.55	3.8	0.68095
Sample 3								
A	17.65	16.03	16.23	17.26	20.12	87.29	17.458	2.67737
B	21.06	19.54	21.13	20.3	18.54	100.57	20.11	1.19218
C	13.68	12.91	12.84	13.39	13.61	66.43	13.286	0.15283
D	2.98	4.23	4.09	2.76	3.07	17.13	3.426	0.46413
E	3.04	1.74	1.79	1.72	2.07	10.36	2.07	0.31267
F	2.13	2.77	3.57	2.66	3.39	14.52	2.904	0.33908

Table 4.9 presents the outcomes of surface roughness tests conducted on used TPU un-dried filament exposed to humidifier for 150 hours. For sample 1, the lowest reading at point E has an average value of 2.86µm and the highest reading of sample 1 at point B which has a value of 19.74µm. The lowest reading for sample 2 is at point F, which has a value of 3.80µm, while the highest reading for sample 2 is at point B, which has a value of 19.92µm. The lowest value for sample 3 is 2.07µm at point E, and the highest reading is 20.11µm at point B.

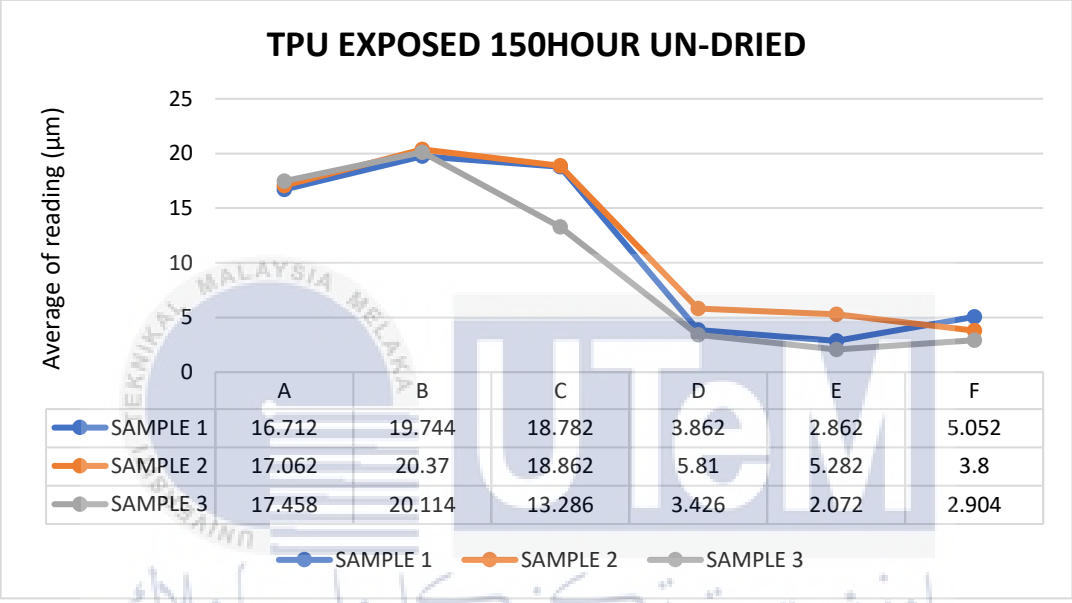

Figure 4.11: The average reading of used un-dried TPU (humidified 150 hours).

Figure 4.11 indicates the average reading of the used TPU un-dried filament that exposed to humidifier for 150 hours for three samples. As a results, the best interactions point for the top of sample at point C for sample 1 and 2 with the value of 18.78µm and 18.86µm respectively. In contrast, there is no the best interaction at the bottom of the sample for the used TPU un-dried filament that exposed to humidifier for 150 hours for three samples

Table 4.22: The ANOVA result for used un-dried PETG (humidified 150 hours).

Sample 1						
Source of Variation	SS	df	MS	F	P-value	F crit
Between Groups	1610.14715	5	322.02943	126.1757	2.02E-16	2.620654
Within Groups	61.25352	24	2.55223			
Total	1671.40067	29				
Sample 2						
Source of Variation	SS	df	MS	F	P-value	F crit
Between Groups	1466.724897	5	293.3449793	68.20	2.15E-13	2.620654
Within Groups	103.22264	24	4.300943333			
Total	1569.947537	29				
Sample 3						
Source of Variation	SS	df	MS	F	P-value	F crit
Between Groups	1625.225827	5	325.0451653	379.56	5.13E-22	2.620654
Within Groups	20.55304	24	0.856376667			
Total	1645.778867	29				

Table 4.22 displays the ANOVA results for the Surface Roughness Test for three samples of used TPU un-dried filament exposed to humidifiers for 150 hours. As a result, the F-value for each sample is larger than F-critical. Hence, H_0 is rejected. When compare the data from the three samples, it can be observed that sample 2 has the lowest F-value, at 68.20µm and sample 3 has the highest surface roughness value of 379.56µm.

Table 4.23: The average roughness for used pre-dried PETG (humidified 150 hours).

Humidified filament for 150 hours (pre-dried)								
Reading / Point	**1(µm)**	**2(µm)**	**3(µm)**	**4(µm)**	**5(µm)**	**Sum**	**Average**	**Variance**
Sample 1								
A	12.51	10.16	12.17	13.22	12.47	60.53	12.106	1.33193
B	14.7	14.69	16.63	15.95	20.55	82.52	16.50	5.80948
C	15.98	16.54	16.02	13.35	14.96	76.85	15.37	1.603
D	1.71	1.73	1.67	1.87	1.67	8.65	1.73	0.0068
E	2.14	2.21	2.17	1.82	1.52	9.86	1.972	0.08787
F	2.11	1.85	1.86	1.88	2.26	9.96	1.992	0.03397
Sample 2								
A	18.74	15.13	13.83	19.21	15.57	82.48	16.50	5.55808
B	16.34	18.01	18.43	15.67	16.71	85.16	17.032	1.33712
C	13.2	14.66	11.42	12.6	11.02	62.9	12.58	2.1226
D	1.42	1.6	1.62	1.8	1.3	7.74	1.548	0.03732
E	1.31	1.12	1.58	1.14	1.13	6.28	1.26	0.03893
F	1.35	2.07	1.9	1.78	1.94	9.04	1.808	0.07627
Sample 3								
A	14.61	14.7	17.53	14.5	16.09	77.43	15.486	1.72503
B	14.56	17.92	20.59	19.34	22.58	94.99	19.00	9.08502
C	17.41	16.33	13.78	15.38	13.61	76.51	15.302	2.67147
D	3.16	2.96	3.86	2.47	3.14	15.59	3.118	0.24942
E	2.88	2.93	3.65	2.74	2.84	15.04	3.01	0.13367
F	4.51	3.32	4.33	4.91	3.98	21.05	4.21	0.35985

Table 4.23 shows the result of surface roughness tests of used TPU pre-dried filament exposed to humidifier for 150 hours. For sample 1, the average value of the lowest reading at point D is 1.73µm, while the average value of the highest reading at point B is 16.50µm. The reading for sample 2 with the lowest value is at point E, where it is 1.26µm, while the reading with the greatest value is at point A, where it is 16.50µm. For sample 3, point E has the lowest reading of 3.01µm while point B has the highest reading of 19.00µm.

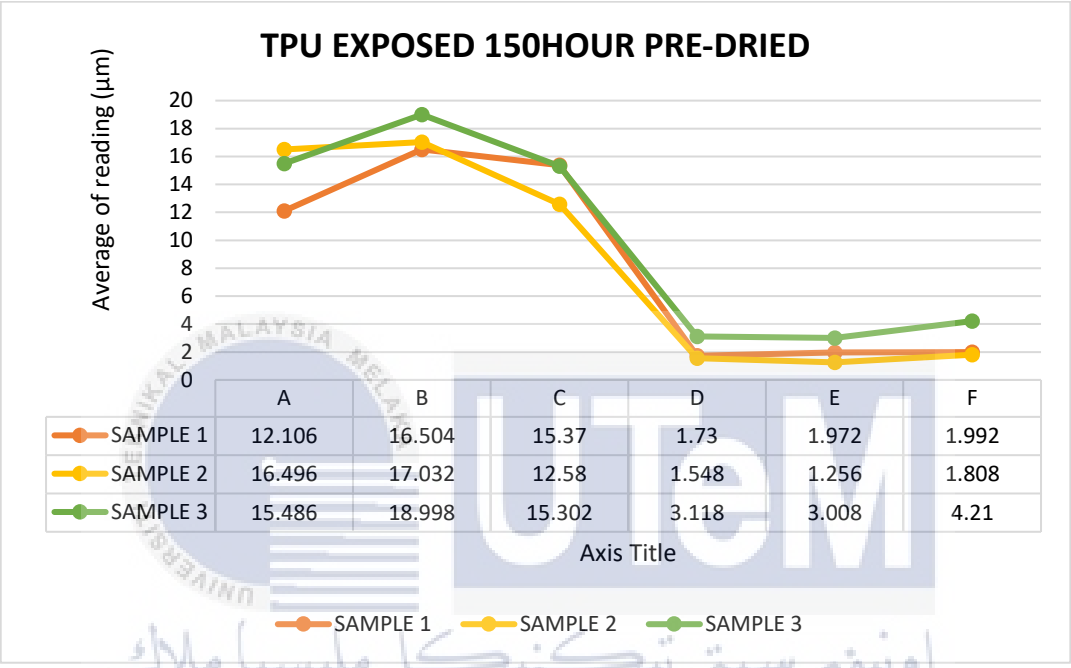

Figure 4. 12: The average reading of used pre-dried PETG (humidified 150 hours).

Figure 4.12 shows the average reading of the used PETG pre-dried filament that was exposed to humidifiers for 150 hours among three samples. Based on the result stated, the best interaction at point C for sample 1 and 3 of the top of sample and at point D for sample 1 and 2 and then at point F for sample 1 and 2 of the bottom of the sample. Besides, the best interaction point at point C is 15.37µm for sample 1 and 15.30µm for sample 3. In addition, the best interaction point at point D is 1.73µm for sample 1 and 1.55µm for sample 2 and then at point F with value 2.00µm for sample 1 and 1.81µm for sample 2.

Table 4.24: The ANOVA result for used Pre-dried PETG (humidified for 150 hours).

Sample 1						
Source of Variation	SS	df	MS	F	P-value	F crit
Between Groups	1273.86427	5	254.7729	172.2787	5.49E-18	2.620654
Within Groups	35.4922	24	1.478842			
Total	1309.35647	29				
Sample 2						
Source of Variation	SS	df	MS	F	P-value	F crit
Between Groups	1494.765387	5	298.9531	195.60	1.25E-18	2.620654
Within Groups	36.68128	24	1.528387			
Total	1531.446667	29				
Sample 3						
Source of Variation	SS	df	MS	F	P-value	F crit
Between Groups	1344.715057	5	268.943	113.44	6.86E-16	2.620654
Within Groups	56.89784	24	2.370743			
Total	1401.612897	29				

Table 4.24 indicates the ANOVA results for the surface roughness test for three samples of used TPU pre-dried filament exposed to humidifiers for 150 hours. As a result, the F-value for each sample is larger than F-critical. Hence, H_0 is rejected. When compare the data from the three samples, it can be observed that sample 3 has the lowest F-value, at 113.44µm and sample 2 has the highest surface roughness value of 195.60µm.

4.2.3 Discussion on Surface Roughness

It is necessary to measure the surface roughness in order to conduct an analysis of the surface roughness of an un-dried and pre-dried sample. The results of the used of filament that exposed to humidifier for 48 hours and 96 hours were not stated because they were almost not affected by the fact that the surface roughness was the same across all conditions but varied depending on whether or not the sample had been un-dried or pre-dried. The surface as a whole is unaffected, but the value differs depending on the point you choose to look at. In this investigation, the technique known as an ANOVA was chosen to carry out a comparison between the three samples used for each of the conditions.

As mentioned in chapter 3, the component of the ANOVA approach is specified to be done at the point range. Additionally, the measurement of surface roughness is done at the point range. The analysis of ANOVA is carried out on each individual sample for each individual condition. In this study, the influence of humidity had a negative impact on the surface quality of 3D printed parts formed of PETG and TPU. This is because it gave a rough surface due to the increasing humidity.

The drying process gives the surface of 3D printed parts produced of PETG and TPU a substantially smoother texture than before because it has the lowest surface roughness measurement. This helps to improve the surface quality. Furthermore, the un-dried sample has a surface roughness that is much higher than that of the pre-dried sample in all conditions. According to Mat (2020), the surface roughness rating that is highest corresponds to the surface finish that is the worst. Therefore, the pre-dried samples exhibit a surface roughness that is superior to that of the un-dried samples.

4.3 Tensile Maximum Force and Maximum Stress Analysis

The average value of maximum force and maximum stress for each sample set was computed once the tensile test results were received. The machine applied the 20kNforce cell with a 5mm/min testing speed. The findings are organized into groups based on the humidity conditions of PETG and TPU filaments used, (a) new filament roll, which acts as the reference, (b) used filament roll stored in the vacuum bag, with the addition of desiccant, (c) used filament roll stored in an open environment and exposed to a humidifier for variant of 48, 96, and 150 hours. The average maximum force and stress for PETG and TPU are presented in sections 4.3.1 and 4.3.2 respectively.

4.3.1 Tensile test analysis for PETG

Table 4.25: The Average Maximum Force and Maximum Stress Results for Tensile Test

Humidity condition		Average Maximum Force (N)		Average Maximum Stress (MPa)		Percentage of Reduction (%)	
		Un-dried	Pre-dried	Un-dried	Pre-dried	Force	Stress
New filament rolls as a reference		677.285	684.3105	40.7381	42.2282	1.03	3.53
Used filament roll stored in the vacuum bag with 50g desiccant		629.924	676.985	38.2336	40.8065	6.95	6.31
Humidified for various hours	48	746.268	763.731	44.714	45.9409	2.29	2.67
	96	731.751	739.282	44.3898	45.8754	1.02	3.24
	150	720.925	730.547	43.6916	44.1878	1.32	1.12

Table 4.25 shows the result of the average maximum force and maximum stress for tensile test of PETG filament stated for all condition. As a result, the average maximum force and stress for the un-dried sample for first condition which is the new filament rolls that act as a reference are 677.285N and 40.738MPa. In contrast, for pre-dried sample are 684.3105N and 42.2282MPa. By comparing the un-dried and pre-dried sample, the average maximum force and maximum stress increased by 1.03% and 3.53%.

In addition, for second condition, the average maximum force and stress for used un-dried filament roll stored in the vacuum bag with 50g desiccant are 629.924N and 38.2336MPa. Other than that, the average maximum force and stress for pre-dried sample are 676.985N and 40.8065MPa. Compared to un-dried samples, the average maximum force and stress increased by 6.95% and 6.31%.

Besides that, for condition three which are used un-dried filament stored in an open environment and exposed to a humidifier for 48 hours, 96 hours, and 150 hours. The average maximum force and stress for un-dried filament of humidified for 48 hours are 746.268N and 44.714MPa. and for the pre-dried sample are 763.731N and 45.9409Pa, respectively. By comparing to un-dried sample, the average maximum force and stress increased by 2.29% and 2.67%. Also, for the un-dried filament of humidified for 96 hours, the average maximum force and stress are 731.751N and 44.3898MPa and then for pre-dried sample are 739.282N and 45.8754MPa. Compared to un-dried sample the average maximum force and stress increased by 1.02% and 3.24%. Furthermore, the average maximum force and stress for the un-dried filament of humidified for 150 hours are 720.925N and 43.6916MPa and then for pre-dried sample are 730.547N and 44.1878MPa. By comparing the un-dried and pre-dried sample, the average maximum force and stress increased by 1.32% and 1.12%. To conclude, all the pre-dried specimens for all conditions exhibit a slightly increase in maximum force, compared to the un-dried specimens.

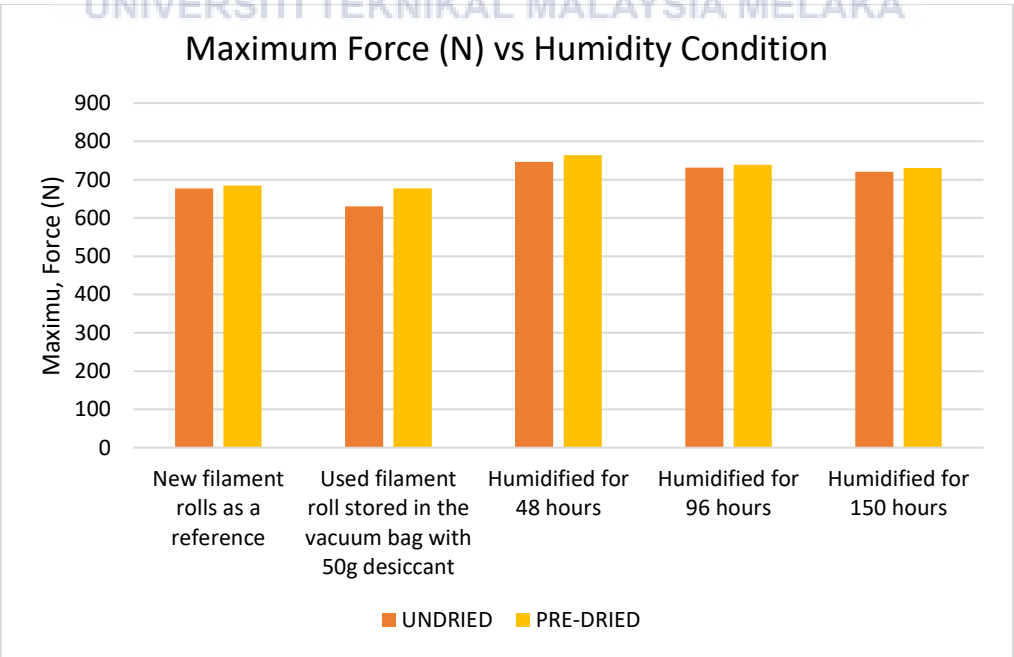

Figure 4.13: Tensile maximum force (N) plot for all conditions of PETG filament

Figure 4.13 shows a summary of the average results from the tensile test that was done to find the maximum force for each sample condition. Figure 4.13 shows that the samples have the most excellent tensile strength when the filament is humidified for 48 hours and then pre-dried by using SUNLU dryer with the average maximum force value 763.731N. The sample with the lowest strength 629.924N is the un-dried filament stored in a vacuum bag with desiccant. Compared to the un-dried sample, the pre-dried sample has always had the highest tensile strength for this PETG material.

4.3.2 Tensile test analysis of TPU

Table 4.26: The Average Maximum Force and Maximum Stress Results for Tensile Test

Humidity condition		Average Maximum force (N)		Average Maximum Stress (MPa)		Percentage of Reduction (%)	
		Un-dried	Pre-dried	Un-dried	Pre-dried	Force	Stress
New filament rolls as a reference		238.082	266.921	14.480	16.837	10.80	14.50
Used filament roll stored in the vacuum bag with 50g desiccant		232.3725	247.617	15.1802	14.8484	6.16	2.24
Humidified for various hours	48	230.972	237.864	14.1452	14.561	2.90	2.86
	96	262.098	276.769	16.2251	16.978	5.30	4.43
	150	239.7855	253.455	14.7350	16.630	5.39	11.4

Table 4.26 shows the result of the average maximum force and maximum stress for tensile test of TPU filament stated for all condition. As a result, the average maximum force and stress for the un-dried sample for first condition which is the new filament rolls that act as a reference are 238.082N and 14.480MPa. In contrast, for pre-dried sample are 266.921N and 16.837MPa. By comparing the un-dried and pre-dried sample, the average maximum force and maximum stress increased by 10.80% and 14.50%.

In addition, for the second condition, the average maximum force and stress for used un-dried filament roll stored in the vacuum bag with 50g desiccant are 232.373N and 15.1802MPa. Other than that, the average maximum force and stress for pre-dried sample are 247.617N and 14.848MPa. Compared to un-dried samples, the average maximum force and stress increased by 6.16% and 2.24%.

Besides that, for condition three which are used un-dried filament stored in an open environment and exposed to a humidifier for 48 hours, 96 hours, and 150 hours. The average maximum force and stress for un-dried filament of humidified for 48 hours are 230.972N and 14.1452MPa and for the pre-dried sample are 237.864N and 14.561MPa. By comparing to un-dried sample, the average maximum force and stress increased by 2.90% and 2.86%. Also, for the un-dried filament of humidified for 96 hours, the average maximum force and stress are 262.098N and 16.2251MPa and then for pre-dried sample are 276.769N and 16.978MPa. Compared to un-dried sample the average maximum force and stress increased by 5.30% and 4.43%. Furthermore, the average maximum force and stress for the un-dried filament of humidified for 150 hours are 239.7855N and 14.735MPa and then for pre-dried sample are 253.455N and 16.630MPa. By comparing the un-dried and pre-dried sample, the average maximum force and stress increased by 5.39% and 11.4%.

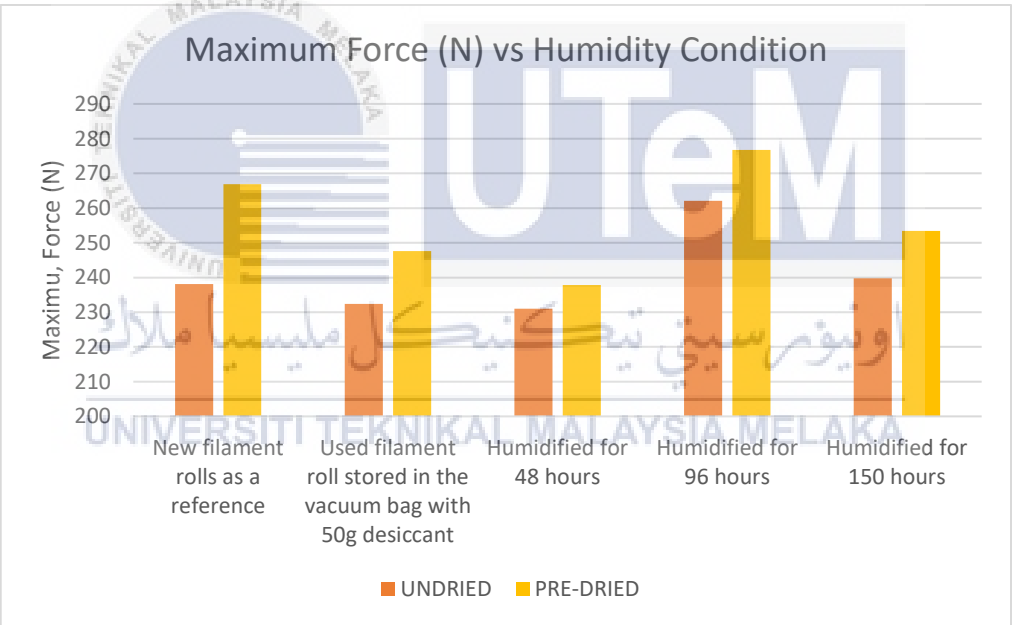

Figure 4.14: Tensile Maximum Force (N) Plot for All Conditions of TPU Filament

Figure 4.14 illustrates summary of the average results from the tensile tests, which were used to determine the maximum force of each sample. Using filament that has been humidified for 96 hours and then pre-dried, the tensile strength of the sample is at its highest force value 276.769N. The un-dried samples that have been humidified for 48 hours the lowest maximum force value 230.972N. The sample that has already been pre-dried has always had the highest tensile strength compared to the un-dried sample. In addition, the un-dried sample for all condition had the lowest tensile strength due to the use of filament from

different spool but the same color that were made by different companies. Khabia and Jain (2019) found that a different brand of filament can give a printed parts different mechanical property.

4.4 Tensile-Stress-Strain Analysis

After the tensile test is done, the tensile-stress-strain analysis can be done by collecting the raw experimental data from Trapezium X software to draw a stress-strain curve. For this study, the data is collected with the Trapezium X software, and the curve is made with the OriginPro software. The graph known as the stress-strain curve illustrates the change in stress that occurs in response to an increase in strain. The tensile-stress-strain analysis for material PETG and TPU will present in section 4.41 and 4.42, respectively.

4.4.1 Tensile-stress-strain analysis of PETG

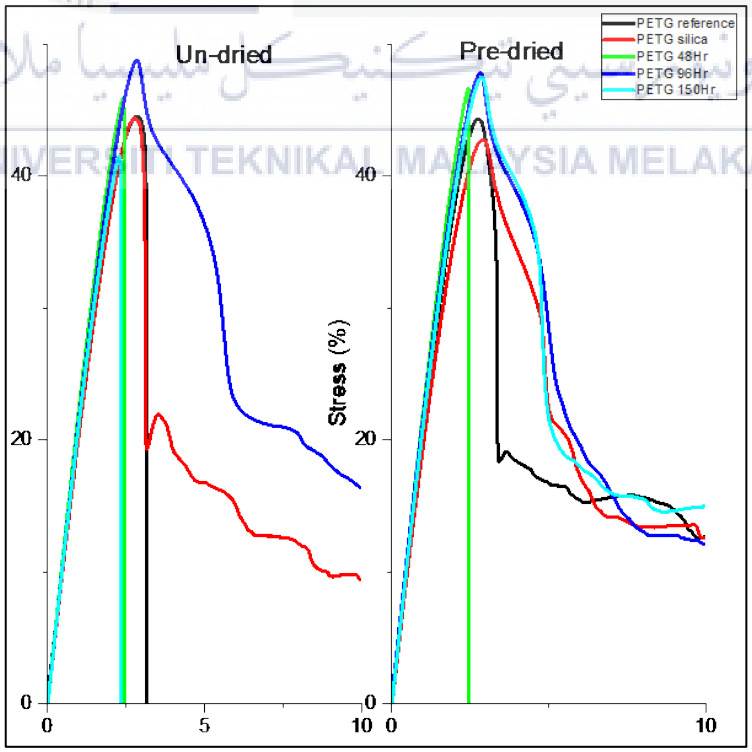

Figure 4.15: Tensile-stress-strain curve for PETG specimen.

Figure 4.15 illustrates the stress-strain curve for all condition stated of un-dried and pre-dried sample. Based on the stress-strain curve, it is divided into 2 part which is for un-dried and pre-dried sample. The peak stress for an un-dried curve is represented by the highest stress value on the stress-strain graph for the filament that was exposed to a humidifier for 96 hours. Similarly for pre-dried sample, the filament that exposed to humidifier for 96 has the highest stress. Also, the result of the stress-strain curve depends on the maximum force for the tensile test. If the force is higher, the stress is higher.

4.4.2 Tensile-stress-strain of TPU

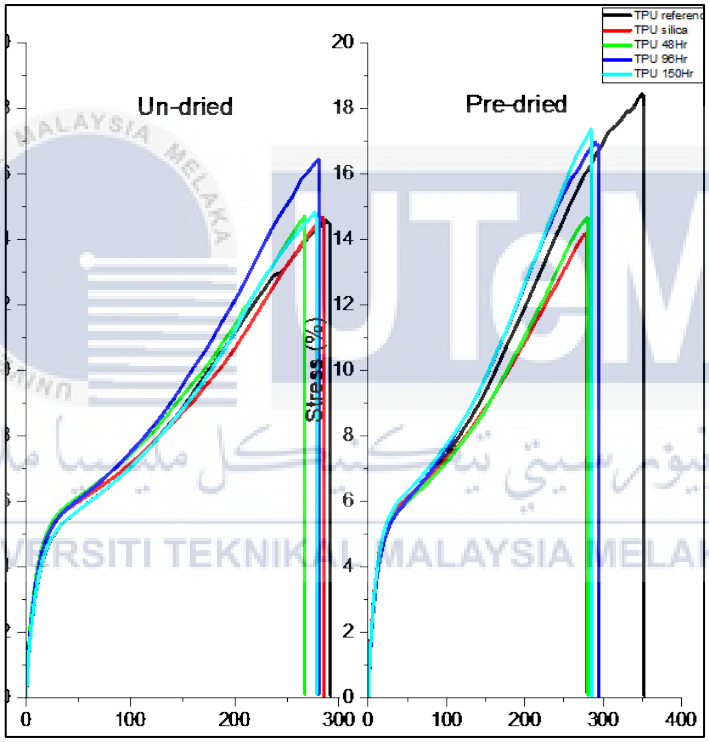

Figure 4. 16: Tensile-stress-strain curve for TPU sample

Figure 4.16 illustrates the stress-strain curve for all condition of the un-dried and pre-dried sample. Based on the stress-strain curve, it is divided into 2 part which is for un-dried and pre-dried sample. For un-dried curve, the highest value of the stress shown in the graph of the stress-strain filament that exposed to humidifier for 96 hours is the highest stress. In contrast, for pre-dried sample of the new filament that act reference is the highest stress. Also, the result of the stress-strain curve depends on the maximum force for the tensile test. If the force is higher, the stress is higher. Meanwhile, for the lowest value of tensile stress on the un-dried filament sample.

4.4.3 Discussion on tensile strength

The tensile test is carried out with the intention of obtaining the fractured cross-sectional sample in order to carry out the SEM analysis on the sample. The data for average maximum force as well as the stress-strain curve can be obtained by tensile testing. The result of the highest maximum force is chosen to be done for SEM. Because PETG has a higher maximum force than TPU does, materials made of PETG tend to be more brittle than those made of TPU. Because it is made of TPU, which is an elastic material, it is not easily scratched. According to this research, the sample after drying has the highest tensile strength. The fact that the drying process will result in an improvement in the characteristics of the material is quite crucial. According to the findings of a study conducted by Zapciu (2021), which investigated the effect of heat treatment on tensile strength, the samples that were heat treated showed a considerable increase in tensile strength when compared to the control group. According to the results of this study, it is possible to observe a reduction in tensile strength and an increase in strain as a result of an increase in humidity, as demonstrated by the stress-strain curve of the material.

4.5 Microstructure Analysis

The fractured surface of tensile test for each sample was observed using a scanning electron microscope (SEM) with a 5.00kV voltage and magnification settings of 30x, 100x, and 150x. Examining the SEM pictures of the fractured surface of the PETG and TPU samples reveals many processes that occurred during printing and led to the performance of destructive testing. The result consists of humidity condition: (a) a new PETG and TPU filament roll, which serves as a reference; (b) a used PETG and TPU filament roll stored in a vacuum bag with the addition of desiccant; (c) a used PETG and TPU filament roll stored in an open environment and exposed to a humidifier for 150 hours. This condition divided into two parts for un-dried and pre-dried sample.

4.5.1 Microstructure Analysis of PETG

In this part, the microstructure result for PETG material will explained in detail. Figure 4.17 depicts the SEM picture of PETG sample fracture under various humidity condition for un-dried and pre-dried sample.

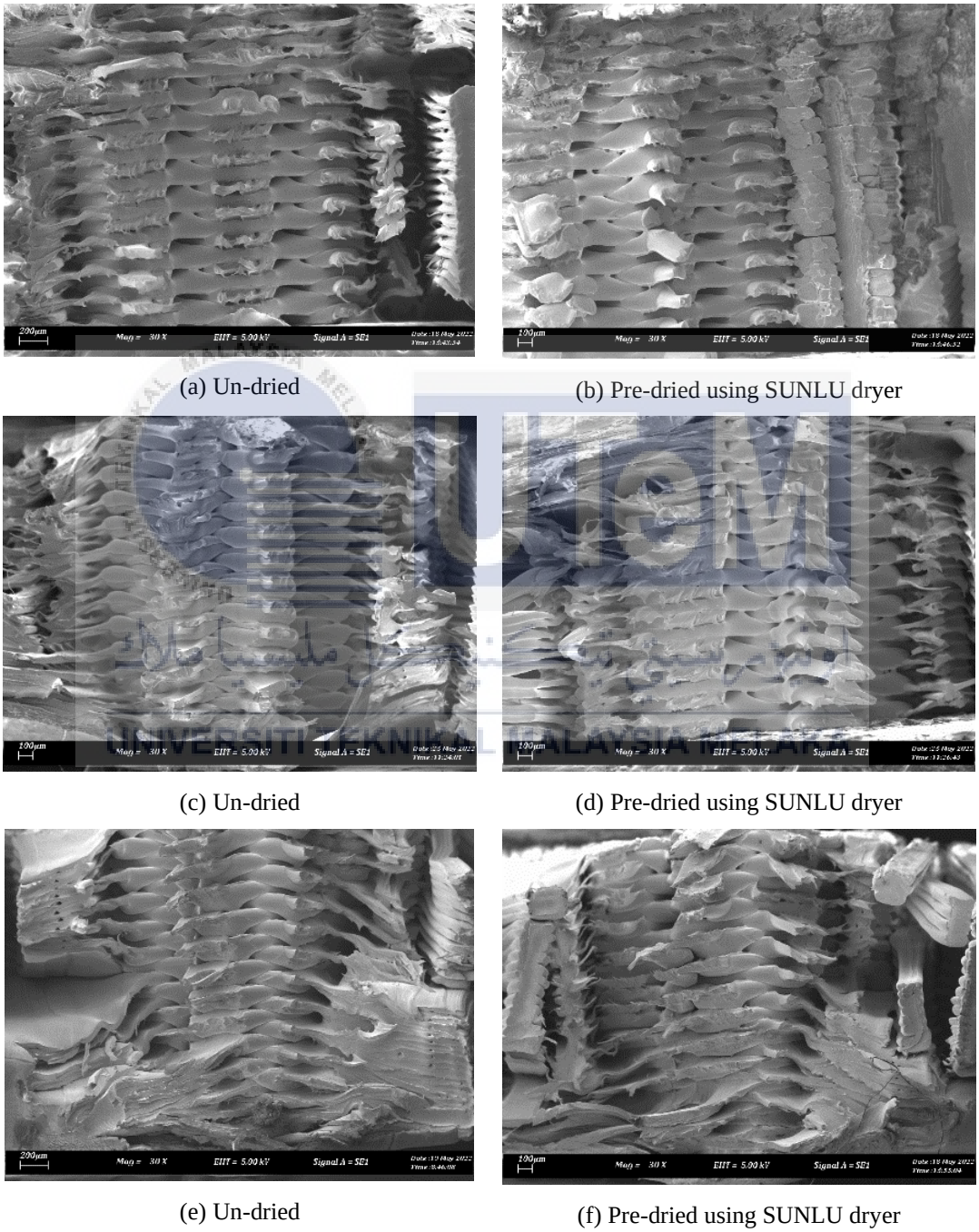

(a) Un-dried (b) Pre-dried using SUNLU dryer

(c) Un-dried (d) Pre-dried using SUNLU dryer

(e) Un-dried (f) Pre-dried using SUNLU dryer

Figure 4.17: SEM image for PETG sample fracture interface of tensile specimen, (a) and (b) for PETG reference, (c) and (d) for PETG stored in vacuum bag with 50g silica, and (e) and (f) for PETG humidified 150 hours.

Figure 4.17 shows the SEM image of the cross-sectional surface fractured of the PETG sample. The surface fractured of a PETG sample that has been humidified for 150 hours better as compared to that of new filament and used filament stored in a vacuum bag containing silica (Figure 4.17 - f) due to the measurement of interlayer gap that discuss later. This reveals that the sample that has been humidified for 150 hours has a stronger tensile strength than the other samples. As a result, the middle layer of the printed sections displays insufficient interlayer adhesion and incomplete diffusion for all PETG specimens. It is also possible to view the inter-bead porosity between the PETG layers. As depicted in the Figure 4.17, the sample has a lacks adhesion between layers. The length of the interlayer gaps between each sample is displayed in Table 4.27.

Table 4. 27: Interlayer Gap Length of PETG sample

Sample	**Average length of interlayer gap (µm)**		**Angle**
	Un-dried	**Pre-dried**	
New filament rolls	65.44	51.98	-90
Vacuum bag with silica gel	147.97	102.17	-90
Humidified for 150 hours	62.21	44.77	-90

Table 4.27 appropriate the average length of the interlayer gap in the SEM picture of the 3D-printed parts of PETG filament for un-dried and pre-dried sample. Based on the result stated, the PETG filament rolls that stored in a vacuum bag containing silica gel is the greatest interlayer gaps. The length of an un-dried sample is 147.97µm, but the length of a pre-dried sample is 102.17µm. Aside from that, the used filament exposed to humidifier for 150 hours has the shortest interlayer gap. In comparison, the pre-dried sample measures 44.77µm and the un-dried sample measures 62.21µm. In addition, the new filament rolls for un-dried sample has the interlayer gaps value 65.44µm and for pre-dried sample is 51.98µm. Moreover, the results indicate that un-dried samples exhibited a larger length interlayers gap than pre-dried samples.

4.5.2 Microstructure Analysis of TPU

In this part, the microstructure result for TPU material will explained in detail. Figure 4.18 depicts the SEM picture of TPU sample fracture under various humidity condition for un-dried and pre-dried sample.

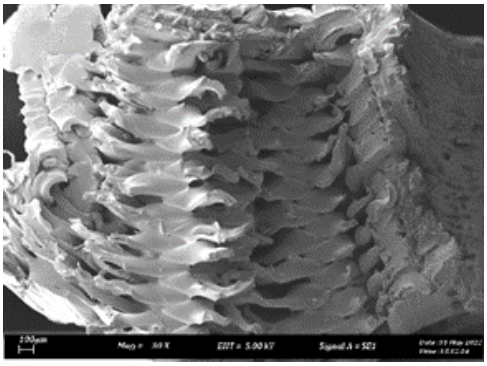

(a) Un-dried

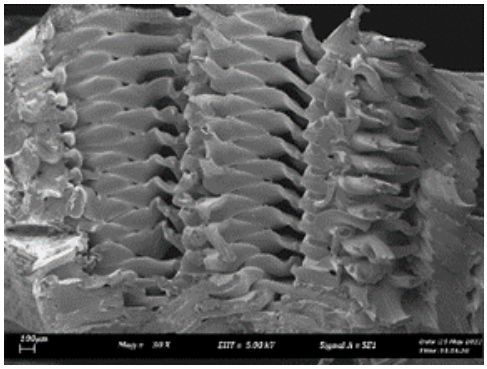

(b) Pre-dried using SUNLU dryer

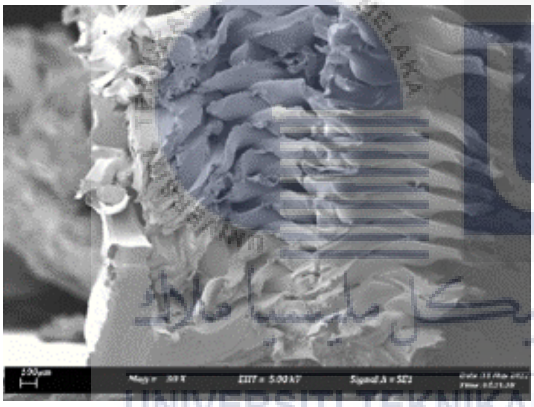

(c) Un-dried

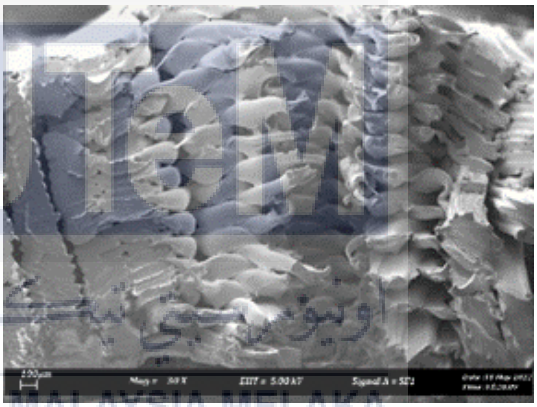

(d) Pre-dried using SUNLU dryer

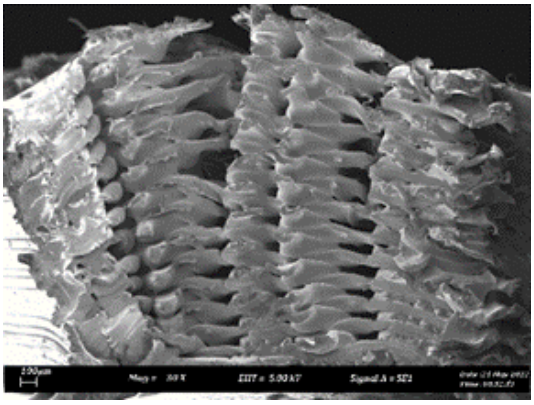

(e) Un-dried

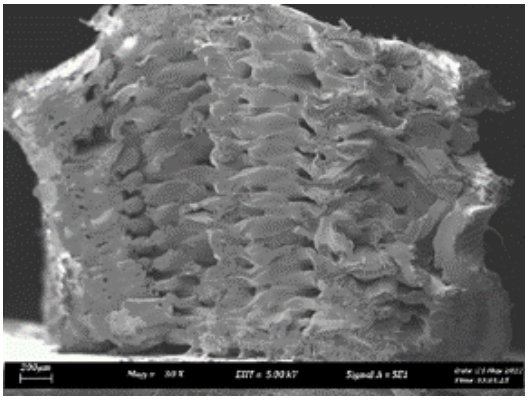

(f) Pre-dried using SUNLU dryer

Figure 4.18: SEM image for TPU sample fracture interface of tensile specimen, (a) and (b) for TPU reference, (c) and (d) for TPU stored in vacuum bag with 50g silica, and (e) and (f) for TPU humidified 150 hours.

Figure 4.18 depicts the SEM picture of the cross-sectional of the fractured surface of TPU. As a result, the sample illustrate that it is poor interlayer adhesion and it is affects to the thickness and interlayer gaps is expanding. In Table 4.28, the length of the interlayer gaps between each sample is presented. It is also possible to view the inter-bead porosity between the TPU layers.

Table 4.28: Interlayer Gap Length of TPU Sample.

Sample	**Average length of interlayer gap (µm)**		**Angle**
	Un-dried	**Pre-dried**	
New filament rolls	84.77	67.17	-90
Vacuum bag with silica gel	88.30	68.25	-90
Humidified for 150 hours	96.30	90.41	-90

Table 4.28 describes the average length of the interlayer gap in the SEM image of 3D-printed TPU filament that have been un-dried and pre-dried. Based on the result, the un-dried sample has a largest of the average length of the interlayer gaps compared to pre-dried sample. The new filament rolls stated the shortest of the average length of interlayer gaps with 84.77µm for un-dried sample and 67.17µm for pre-dried sample. In addition, the filament that exposed to humidifier for 150 hours has a greatest average of interlayer gaps with 96.30µm for un-dried sample and 90.41µm for pre-dried sample. Other than that, the used filament rolls that stored in vacuum bag with addition of silica gel has the average of interlayer gaps value 88.30µm for un-dried sample and 68.25µm for pre-dried sample. It can be stated, the filament that is pre-dried using SUNLU dryer can decreased the average length of the interlayer gaps.

4.5.3 Discussion on Microstructure Analysis

SEM is performed in accordance with the results of tensile testing, in which case a sample with a high force value will be chosen to perform SEM. The results of the tensile test, the tensile strength of the sample after drying is the greatest it can be under all of the conditions mentioned. In addition, the failure of the filament to diffuse completely is the main causes of the interlayer gaps seen in all of the samples.

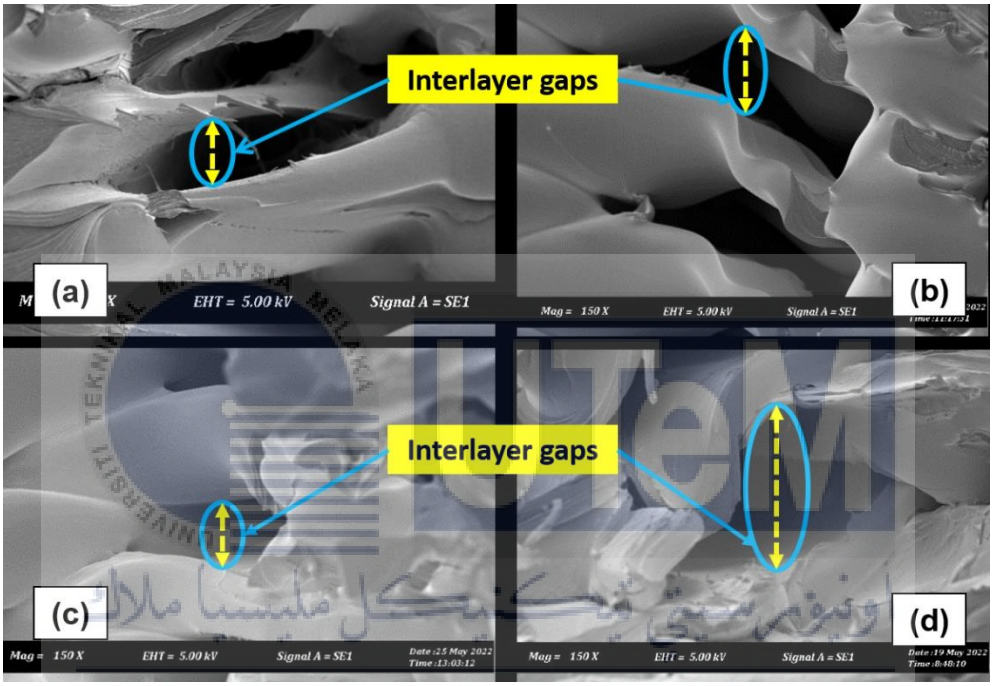

Figure 4.19: Interlayer Gaps for SEM image: (a) Used Pre-dried PETG exposed to humidifier for 150 hours; (b) Used un-dried PETG stored in vacuum bag with silica gels; (c) New TPU filament rolls; (d) Used Un-dried TPU exposed to humidifier for 150 hours.

The interlayer gaps that were measured for the PETG and TPU samples are depicted in Figure 4.19. During this phase of the microstructure analysis, the only thing that is being looked into is the interlayer adhesion and the interlayer gap length. When the filament was exposed to humidity, moisture also had an effect on the interlayer adhesion as well as the interlayer gap (Ayrilmis et al., 2019). If the interlayer bonding is insufficient, then the space between the layers will become larger. When the filament is humidified, tensile strength decreases due to the propagation of a crack in the filament. In addition, when the filament is pre-dried, the interlayer gap decreases and the interlayer bonding improves.

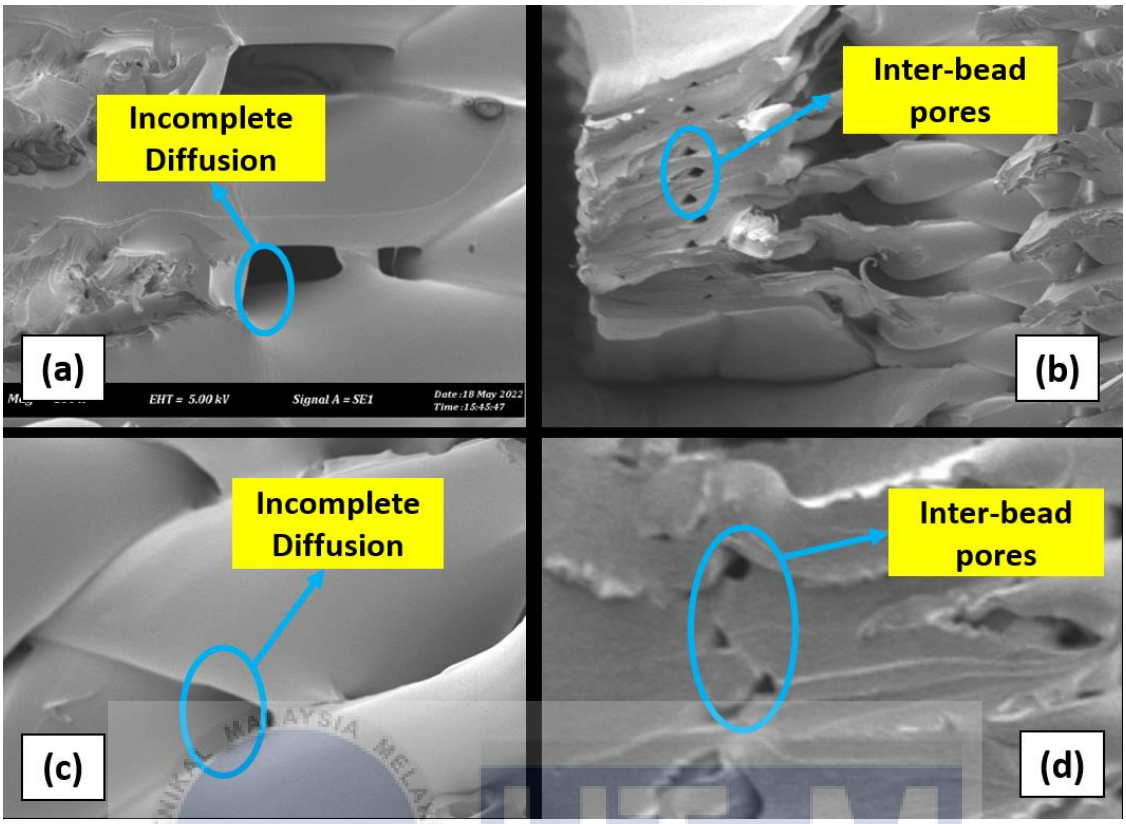

Figure 4.20: Fractured surface; (a) Un-dried PETG New Filament; (b) Un-dried PETG humidified for 150 hours; (c) Un-dried TPU New Filament; (d) Un-dried TPU humidified for 150 hours

Figure 4.20 shows that the fractured surface of PETG and TPU have incomplete diffusion and inter-bead pores. The tensile strength of the sample will decrease as the inter-bead pores and interlayer gaps rise. The un-dried sample has lower tensile strength than pre-dried sample, so the microstructure of the un-dried sample illustrates more defects.

4.6 Density Test Analysis (Archimedes Principle)

A densimeter is used to conduct density tests of the un-dried and pre-dried sample. In this particular test, known as the water immersion method, the Archimedes principle is utilized. The result consists of humidity condition: (a) a new PETG and TPU filament roll, which serves as a reference; (b) a used PETG and TPU filament roll stored in a vacuum bag with the addition of desiccant; (c) a used PETG and TPU filament roll stored in an open environment and exposed to a humidifier for 150 hours. This condition divided into two parts for un-dried and pre-dried sample. The average of density is stated in Table 4.29 and 4.30 for PETG and TPU, respectively. In addition, Figure 4.19 - 4.20 illustrate the relation that exists between the humidity condition and the average density of PETG and TPU respectively.

4.6.1 Density analysis of PETG

Table 4.29: The Result of the Average Density

Humidity condition		Average density (g/cm^3)	
		Un-dried	Pre-dried
New filament rolls as a reference		0.979	1.024
Used filament roll stored in the vacuum bag with 50g desiccant		0.977	0.984
Humidified for various hours	48	1.012	1.038
	96	0.999	1.033
	150	0.992	1.027

Table 4.29 shows the average density of PETG samples for all condition stated. The average density for the new filament rolls is 0.979g/cm^3 for un-dried sample and 1.024g/cm^3 for pre-dried sample. Based on the stated result, the filament that exposed to humidifier for 48 hours has the highest average density weight 1.012 g/cm^3 for un-dried sample and 1.038g/cm^3 for pre-dried sample. Other than that, the lowest average density is stated for the used filament rolls stored in vacuum bag with addition 50 g silica gels with value 0.977g/cm^3 for un-dried sample and 0.984g/cm^3 for pre-dried sample.

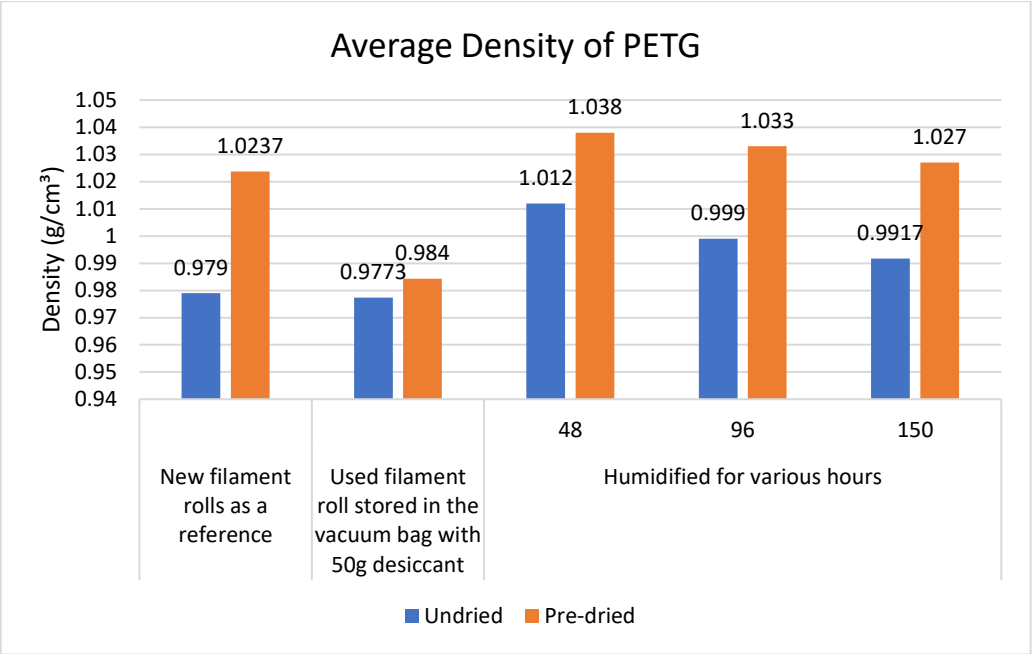

Figure 4.21: Average Density of PETG

Figure 4.21 illustrate the average density of PETG that is performed for each sample condition. As a result, the pre-dried sample has the highest average density compared to un-dried sample. The un-dried used filament rolls that exposed to humidifier for 48 hours stated the highest average density. In contrast, the lowest average density is stated for the used un-dried filament roll stored in vacuum bag with 50g silica gels.

4.6.2 Density Analysis of TPU

Table 4.30: The Result of the Average Density

Humidity condition		Average density	
		Un-dried	Pre-dried
New filament rolls as a reference		0.836	0.843
Used filament roll stored in the vacuum bag with 50g desiccant		0.827	0.832
Humidified for various hours	48	0.822	0.830
	96	0.816	0.818
	150	0.801	0.814

Table 4.30 indicates the average density of the TPU samples for each of the conditions proposed. The result that was stated indicates the un-dried sample has the highest average density weight of 0.836 for un-dried sample, whereas the pre-dried sample 0.843. Aside from that, the used filament that exposed to humidifier for 150 hours has the smallest average density with a value 0.801 for un-dried sample and 0.814 for pre-dried sample.

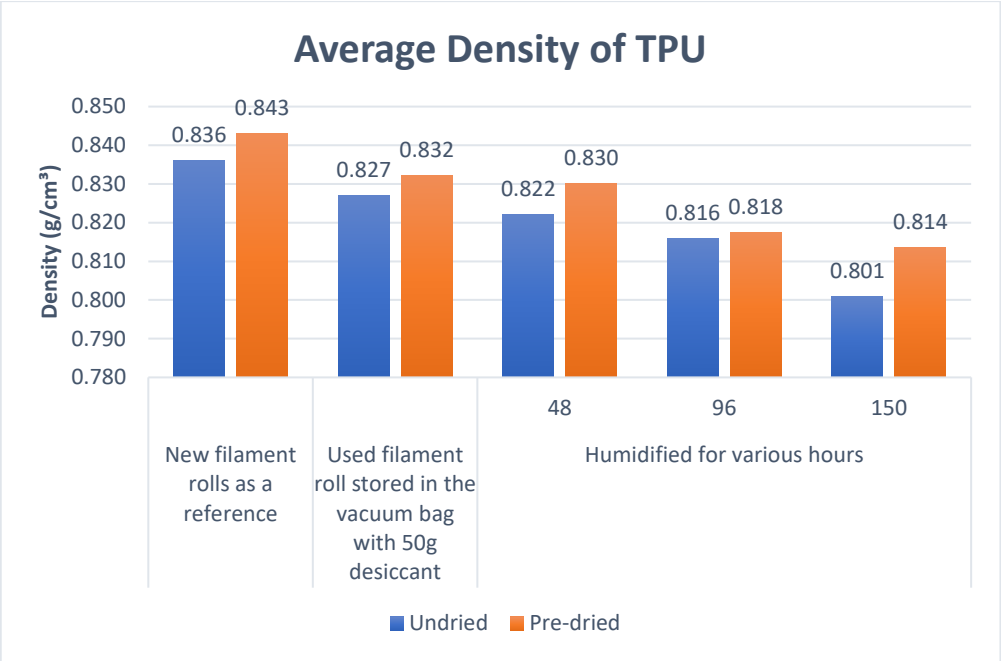

Figure 4. 22: Average Density of TPU

Figure 4.22 illustrate the average density of PETG that is performed for each sample condition. As a result, the pre-dried sample has the highest average density compared to un-dried sample. The un-dried used filament rolls that exposed to humidifier for 48 hours stated the highest average density. In contrast, the lowest average density is stated for the used un-dried filament roll stored in vacuum bag with 50g silica gels.

4.6.3 Discussion on Density Test

Based on the result of density test, the influence of humidity for PETG and TPU filament can decreased the density of the sample. When the filament exposed to the humidifier increased, the density of the of the specimen become decrease and the pores or gaps becomes bigger. Ayrilmis et al (2019) stated in their study that the density of the specimen decreases, whereas porosity of the specimens increases as a result of the experiment. When compared to the density of the pre-dried filament samples, the un-dried PETG and TPU filament samples have a lower density. It can describe that the filament has lower density is absorb water. So, the drying process will decrease the amount of water absorption in the filament. Hence, the porosity increased as the amount of water increased. Windheim (2021) stated the heat treatment process will improve the interface bonding and leads the increasing of the density. Wang et al (2019) suggested that the heat treatment

process can improve the tensile strength and reducing the amount of porosity. In this study, the porosity can be focused at based on the length of the gaps between the layers and the tensile strength. As the tensile strength increases, the amount of porosity gradually decreases.

4.6.3.1 The Comparison between PETG and TPU

According to the density test results, the PETG sample has a higher density value than the TPU sample. Lower density values imply a porous sample. As a result of the average density, the TPU sample is more porous than the PETG sample. It can be demonstrated by calculating the % of porosity using the equation;

$$\% \text{ porosity} = 100 \times [1 - (\frac{\rho measured}{\rho theoritical})] \qquad \text{equation (4.1)}$$

Pmeasured is the value that is derived from taking the average density of the PETG and TPU materials. Ptheoritical is represents the constant density value, which in the case of PETG is 1.27 and in the case of TPU is 1.21.

Table 4.31: Percentage of Average Porosity

Humidity condition		Average Porosity (%)			
		PETG		TPU	
		Un-dried	Pre-dried	Un-dried	Pre-dried
New filament rolls as a reference		22.91	19.39	30.91	30.33
Used filament roll stored in the vacuum bag with 50g desiccant		23.05	22.50	31.65	31.22
Humidified for various hours	48	20.31	18.27	32.07	31.40
	96	21.34	18.66	32.56	32.44
	150	21.91	19.13	33.8	32.77

According to Table 4.31, the un-dried sample displayed a higher porosity than the pre-dried sample. Aside from that, the percentage of porosity in PETG is smaller than TPU. Because of this, it is able to demonstrate that TPU is more porous than PETG. The value of the used pre-dried PETG that was exposed to the humidifier for 48 hours resulted in the

lowest percentage of porosity, which was 18.27%. In contrast, the un-dried TPU that was utilized and then exposed to a humidifier for 150 hours had the highest level of porosity with 33.8%. The findings demonstrate that TPU has a higher porosity than PETG.

4.7 Discussion on The Fabrication of The Specimen

In this study, all sample of PETG and TPU 3D printed parts was printed by using the Ender V2 3D printer. This study computes the study of humidity condition for un-dried and pre-dried sample that will be exposed to the different condition which are the new filament that act as reference, used filament stored in vacuum bag with silica and used filament that humidified for 48, 96 and 150 hours. For second condition, the filament was put in the humidifier in an open environment with a room temperature of 27°C and an average relative humidity of 78–90%. In the time of fabrication, the specimen, the filament comes out of the nozzle, it makes a sound like a bubble or a pop. This shows that the filament was absorb water. When the un-dried sample is exposed to high humidity, the sound comes more often. Also, when the samples are printed there is problems like belt tension, warping, and the filament not stick to the printing bed. When the bed tension goes down, the quality of the printed surface goes down, and the space between layers gets bigger and it also easy for the nozzle to get out of shape. A few times this has happened because the printing has been used for too long. The problem was fixed by making sure the belt tensioner was tighter.

During the printing process, PETG samples does not stick to the printing bed. This could have something with the setting parameter of printer like printing bed and printing temperature. In this study, the temperature of the print is 220°C, while the temperature of the bed is 60°C. This parameter is kept the same in all materials so that it is easier to compare them. Since the temperature of printing has dropped significantly, the PETG filament does not stick to the bed. According to Guessasma et al. (2019), PETG material must be printed over 230 for printing temperature. If not do so, the PETG filament cannot be pasted to the bed for FDM process.

CHAPTER 5
CONCLUSION AND RECOMMENDATION

5.1 Concluding Remark

This purpose of this study to determine the effect of humidity on the surface quality, tensile strength, microstructure, and porosity of PETG and TPU filaments that have been un-dried and pre-dried using the dehydrator. Moisture degrades the tensile strength and increases the porosity of 3D printed items, resulting in their poor surface quality. The effectiveness of drying the filament before printing was evaluated by compared a 3D printed item that was un-dried with one that was pre-dried. A well-known illustration of the drying process is the pre-dried filament produced by a filament dehydrator; for the purposes of this study, the SUNLU drier was utilised. Most of the time, the filament is pre-dried before 3D printing begins, but less research has been done on how this affects the 3D printed part. So, a proposed drying method, the SUNLU dryer, is tested on 3D-printed parts that were made with different amounts of moisture absorption. The proposed drying methods before printing are then analysed, and it is shown that drying could increase the tensile strength, improve the surface quality, and reduce the porosity. Experiments were done on un-dried filaments using a SUNLU Dryer, and the results were discussed in Chapter 4.

The drying method was evaluated based on four performance measures: surface roughness, tensile strength, fracture surface microstructure, and density. It was found that pre-dried filament samples produced better 3D printer parts with the best tensile strength, a high density (low porosity), and good interlayer bonding in the microstructure. The effect of drying the filament on PETG and TPU thermoplastic polymer surface roughness, tensile strength, microstructure, and porosity in additive manufacturing is successfully achieved in this study. The following are the conclusion that can be drawn from this study:

1) The first objective is to analyse the surface roughness of the pre-dried 3D printed PETG and TPU parts using ANOVA. As consequent to the result of surface roughness, pre-dried samples have a smoother surface than un-dried samples because the reading for surface roughness is lower in pre-dried samples than it is in un-dried samples. PETG is more consistent in its smoothness than TPU is due to the fact that it has a surface that is less rough than TPU.

2) The second objective is to measure the tensile strength of the pre-dried 3D printed PETG and TPU parts using a Universal Testing Machine. As an outcome of this, the tensile strength of the sample that was pre-dried was consequently higher than un-dried samples. The tensile strength is thus increased as a result of the drying process.

3) The third objective is to evaluate the cross-sectional microstructure of the fractured tensile specimen of the pre-dried 3D printed parts using the SEM machine. Since humidity has an effect on the microstructure of the un-dried sample, the highest interlayer gaps and larger pores are evident, as well as an incomplete diffusion pattern. In contrast, a smaller number of pores and reduced interlayer gap were observed on pre-dried sample. Interlayer gaps in PETG are smaller compared to TPU.

4) Lastly, to examine the porosity of the pre-dried 3D printed PETG and TPU parts using the Archimedes Principle. Because of the difference in density between PETG and TPU, the results show that the un-dried samples have a greater porosity than the pre-dried samples. The un-dried sample has a lower density value, which results in an increase in porosity. TPU has a lower density than PETG, which results in it having a more porous structure than PETG.

5.2 Recommendation

For future work, the water absorption or humidity of the filament needs to be measured before and after being exposed to the humidity condition for a un-dried sample, and the mass of the pre-dried filament needs to be measured after the drying process. To control the humidity factor, it is best to set up a device that measures humidity in real time during the 3D printing process. The humidity oven can also be used to add moisture to the humidity filament. By measuring the mass of the filament before and after drying, you can get a much better comparison and more accurate data. Also, the humidity could be changed by how much water the filament absorbs. So, FTIR analysis can be used to find out how humidity affects the polymeric chemical chain bonding of the 3D-printed filament that has already been pre-dried and if the drying method can be improved to get rid of the water.

5.3 Sustainability Element

Recent years have seen a rise in the use of additive manufacturing as an alternative to traditional manufacturing because it is better for the environment. So, the materials that were used in this study are good for the environment. The material used in this research is the most common material used in the industry. So, these parts or scraps of materials can be recycled in the right way to make sure they will last. Also, in this study, used filament that has been exposed to the environment and humidity is reused to reduce the amount of waste material.

5.4 Complexity Element

The complexity element clarifies as a difficulty undergoing during this study. It is difficult to control the humidity level and the amount of humidity in the filament but failed to register any measurements. In addition, the humidifier is only lasting for two to three hours, so, humidifier water needs to be replaced frequently. In order to prevent extra humidity after being exposed to the humidifier, the sample filament must be appropriately stored in vacuum bags. Due to restricted resources, microstructure analysis of fracture samples was confined to the high force of samples of tensile test. During sample fabrication, PETG does not stick to bed and must be checked often for proper printing.

5.5 Lifelong Learning Element

The term "lifelong learning" is described as a sort of self-initiated education that focuses on personal growth. Lifelong learning can also be defined as the development of human potential through a supportive process that encourages and enables an individual to acquire all of the knowledge, value, skills, and understanding they'll need over the course of their lives and to put that knowledge to use in any role. Analyzing the surface topography of 3D-printed parts gave us insight into additive manufacturing. There are two ways to observe the surface topography: by contacting it with a profilometer to measure the surface roughness and by not contacting it with a SEM to observe the surface microstructure. Humidity can have a negative impact on the tensile strength and surface quality of 3D printed parts, and this needs to be taken into consideration when improving the quality of 3D printed parts. In this study, the drying process has increased the tensile strength and surface quality of 3D printed parts and reduce the amount of porosity.

REFERENCES

Algarni, M. (2021). *The Influence of Raster Angle and Moisture Content on the Mechanical Properties of PLA Parts Produced by Fused Deposition Modeling*. https://doi.org/10.3390/polym

Al-Maharma, A. Y., Patil, S. P., & Markert, B. (2020). Effects of porosity on the mechanical properties of additively manufactured components: a critical review. In *Materials Research Express* (Vol. 7, Issue 12). IOP Publishing Ltd. https://doi.org/10.1088/2053-1591/abcc5d

Alvarez C., K. L., Lagos C., R. F., & Aizpun, M. (2016). Investigating the influence of infill percentage on the mechanical properties of fused deposition modelled ABS parts. *Ingenieria e Investigacion*, *36*(3), 110–116. https://doi.org/10.15446/ing.investig.v36n3.56610

Asesar. (2015). How To Dehydrate PLA Filament. Retrieved from Asesar: https://www.asensar.com/article/3dprinting/how-to-dehydrate-pla-filament.html

ASTM International. (2017). *Standard Test Method for Density of Powder Metallurgy (PM) Materials Containing Less Than Two Percent Porosity 1*. https://doi.org/10.1520/B0311-17

Ayrilmis, N., Kariz, M., Kwon, J. H., & Kitek Kuzman, M. (2019). Effect of printing layer thickness on water absorption and mechanical properties of 3D-printed wood/PLA composite materials. The International Journal of Advanced Manufacturing Technology, 102(5), 2195-2200.

Bekathwia. (2017). 3D Printer Filament Dry Box. Retrieved from Instructables Workshops: https://www.instructables.com/3D-Printer-Filament-Dry-Box/

Carolo, H. R. (2021). 3D Printer Filament Storage: 12 Ways to Store Filament. Retrieved from All3DP: https://all3dp.com/2/filament-storage-3d-printer/

Corporation, P. A. (2019). Why Is This the Best 3D Printing Filament Storage Solution? Retrieved from PAC: https://blog.gotopac.com/2018/03/07/best-3d-printing-filament-storage-cabinets-2018/

de Terris, T., Andreau, O., Peyre, P., Adamski, F., Koutiri, I., Gorny, C., & Dupuy, C. (2019). *Optimization and comparison of porosity rate measurement methods of Selective Laser Melted metallic parts*. https://www.elsevier.com/open-access/userlicense/1.0/

Dwamena, M. (2020). How to Fix Bubbles and Popping on Your 3D Printer Filament. Retrieved from 3D Printerly: https://3dprinterly.com/how-to-fix-a-popping-noise-sound-on-your-3d-printer/

Eureka. (2021). ADL-3D77 - DRY BOX STORAGE FOR 3D PRINTING FILAMENT. Retrieved from Eureka Dry Tech: https://www.eurekadrytech.com/blog/3d-printing-filament-dry-box

Ghasemi, S., Tajvidi, M., Bousfield, D. W., Gardner, D. J., & Gramlich, W. M. (2017). Dry-spun neat cellulose nanofibril filaments: Influence of drying temperature and nanofibril structure on filament properties. *Polymers*, *9*(9). https://doi.org/10.3390/polym9090392

Heu, R., Shahbazmohamadi, S., Yorston, J., & Capeder, P. (2019). Target Material Selection for Sputter Coating of SEM Samples. *Microscopy Today*, *27*(4), 32–36. https://doi.org/10.1017/s1551929519000610

Hossain, M. A., Zhumabekova, A., Paul, S. C., & Kim, J. R. (2020). A review of 3D printing in construction and its impact on the labor market. In *Sustainability (Switzerland)* (Vol. 12, Issue 20, pp. 1–21). MDPI AG. https://doi.org/10.3390/su12208492

Hsueh, M. H., Lai, C. J., Wang, S. H., Zeng, Y. S., Hsieh, C. H., Pan, C. Y., & Huang, W. C. (2021). Effect of printing parameters on the thermal and mechanical properties of

3d-printed pla and petg, using fused deposition modeling. *Polymers*, *13*(11). https://doi.org/10.3390/polym13111758

Instinct, M. (2019). Identification of PETG Chemical Compound. Retrieved from Structure of PETG (C14H20O5S): https://www.molinstincts.com/structure/PETG-cstr-CT1103556678.html

Jo, W., Kwon, O. C., & Moon, M. W. (2018). Investigation of influence of heat treatment on mechanical strength of FDM printed 3D objects. *Rapid Prototyping Journal*, *24*(3), 637–644. https://doi.org/10.1108/RPJ-06-2017-0131

K. Durgashym, M. I. R. A. B. K. S. (2019). *Experimental investigation on mechanical properties of PETG material processed by fused deposition modeling method _ Elsevier Enhanced Reader*.

Kakanuru, P., & Pochiraju, K. (2020). Moisture Ingress and Degradation of Additively Manufactured PLA, ABS and PLA/SiC Composite Parts. *Additive Manufacturing*, *36*. https://doi.org/10.1016/j.addma.2020.101529

Kovan V, Tezel T, Topal ES, & Camurlu HE. (2018). *PRINTING PARAMETERS EFFECT ON SURFACE CHARACTERISTICS OF 3D PRINTED PLA MATERIALS*.

Kwon, S. W., Lee, S. W., Kim, Y. R., Oh, Y. C., Lee, S. K., Kim, J. H., & Kwon, J. W. (2020). A Filament Supply System Capable of Remote Monitoring and Automatic Humidity Control for 3D Printer. *Journal of Sensors*, *2020*. https://doi.org/10.1155/2020/8846466

Larson, M. G. (2008). Analysis of variance. In *Circulation* (Vol. 117, Issue 1, pp. 115–121). https://doi.org/10.1161/CIRCULATIONAHA.107.654335

Leite, M. (2016). *Water Absorption And Mechanical Properties Evaluation Of Surface Modified Abs Printing Parts*. Vaz.

Liao, Y., Liu, C., Coppola, B., Barra, G., di Maio, L., Incarnato, L., & Lafdi, K. (2019). Effect of porosity and crystallinity on 3D printed PLA properties. *Polymers*, *11*(9). https://doi.org/10.3390/polym11091487

Liu, Z., Zhang, M., Bhandari, B., & Wang, Y. (2017). 3D printing: Printing precision and application in food sector. In *Trends in Food Science and Technology* (Vol. 69, pp. 83–94). Elsevier Ltd. https://doi.org/10.1016/j.tifs.2017.08.018

Lubrizol Life Sciences. (2017). *TPU Drying Guide*.

Mat, M. C., Ramli, F. R., Alkahari, M. R., Sudin, M. N., Abdollah, M. F. B., & Mat, S. (2020). Influence of layer thickness and infill design on the surface roughness of PLA, PETG and metal copper materials. *Proceedings of Mechanical Engineering Research Day*, *2020*, 64-66.

Mohamed, O. A., Masood, S. H., & Bhowmik, J. L. (2015). Optimization of fused deposition modeling process parameters: a review of current research and future prospects. *Advances in Manufacturing*, *3*(1), 42–53. https://doi.org/10.1007/s40436-014-0097-7

Pac, Z. (2021). SILICA GEL DESICCANT. Retrieved from Zetta Pac: https://zettapac.com/products/silica-gel-desiccant/?gclid=CjwKCAiAz--OBhBIEiwAG1rIOibKxNi40V_bTI3mKfyUsmrFHp1DvUprNCimzFbbgMnZxuUgatBpahoCkPIQAvD_BwE

R. Srinivasan, W. R. A. D. R. B. T. B. (2020). *Effect on infill density on mechanical properties of PETG part fabricated by fused deposition modelling _ Elsevier Enhanced Reader*.

Ribeiro, F., Oliveira de Miranda, M. F., dos Santos Saad, N., & Zuquete Guarato, A. (2019, December 4). *EXPERIMENTAL ANALYSIS ON THE MECHANICAL PROPERTIES OF PETG PARTS MADE WITH FUSED DEPOSITION MODELING MANUFACTURING*. https://doi.org/10.26678/abcm.cobem2019.cob2019-1931

Sow, M. T. (2014). Using ANOVA to Examine the Relationship between Safety & Security and Human Development. *Journal of International Business and Economics*, *2*(4). https://doi.org/10.15640/jibe.v2n4a6

Srinivasan, R., Nirmal Kumar, K., Jenish Ibrahim, A., Anandu, K. v., & Gurudhevan, R. (2020). Impact of fused deposition process parameter (infill pattern) on the strength of PETG part. *Materials Today: Proceedings*, *27*, 1801–1805. https://doi.org/10.1016/j.matpr.2020.03.777

Tuan D. Ngo, A. K. G. I. K. T. Q. N. D. H. (2018). *Additive manufacturing (3D printing)_ A review of materials, methods, applications and challenges _ Elsevier Enhanced Reader*.

Tyson, M. (2018). 3D Printing Solution. Retrieved from Starters Guide To Moisture, Drying And Filament Storage: https://www.3dprintingsolutions.com.au/News/Australia/starters-guide-to-moisture-drying-and-filament-storage

Valerga, A. P., Batista, M., Salguero, J., & Girot, F. (2018). Influence of PLA filament conditions on characteristics of FDM parts. *Materials*, *11*(8). https://doi.org/10.3390/ma11081322

von Windheim, N., Collinson, D. W., Lau, T., Brinson, L. C., & Gall, K. (2021). The influence of Porosity, crystallinity and interlayer adhesion on the tensile strength of 3D printed polylactic acid (PLA). *Rapid Prototyping Journal*.

Wang, P., Zou, B., Ding, S., Huang, C., Shi, Z., Ma, Y., & Yao, P. (2020). Preparation of short CF/GF reinforced PEEK composite filaments and their comprehensive properties evaluation for FDM-3D printing. *Composites Part B: Engineering*, *198*. https://doi.org/10.1016/j.compositesb.2020.108175

Wang, X., Zhao, L., Fuh, J. Y. H., & Lee, H. P. (2019). Effect of Porosity on mechanical properties of 3D printed polymers: Experiments and micromechanical modeling based on X-ray computed tomography analysis. *Polymers*, *11*(7), 1154.

Xiao, J., & Gao, Y. (2017). The manufacture of 3D printing of medical grade TPU. *Progress in Additive Manufacturing*, *2*(3), 117–123. https://doi.org/10.1007/s40964-017-0023-1

Zaldivar, R. J., Mclouth, T. D., Ferrelli, G. L., Patel, D. N., Hopkins, A. R., & Witkin, D. (2018). Effect of initial filament moisture content on the microstructure and mechanical performance of ULTEM ® 9085 3D printed parts. *Additive Manufacturing*, *24*, 457–466. https://doi.org/10.1016/j.addma.2018.10.022

Zapciu, A., Amza, C. G., Baciu, F., & Vasile, M. I. (2021, October). Heat treatment of 3D printed polyethylene terephthalate glycol in a supporting powder bed. In *IOP Conference Series: Materials Science and Engineering* (Vol. 1182, No. 1, p. 012083). IOP Publishing.

APPENDICES

A. Gantt Chart of PSM I

No	Task	Semester I (Week)														
		1	2	3	4	5	6	7	8	9	10	11	12	13	14	15	16
1	PSM Title Registration								Mid-Semester Break							Study Week	Final Exam
2	Briefing of Title Selection																
3	Find Journals and Reference Materials on the PSM Title																
4	Define Objectives and Problem Statement																
5	Identify Background and Scope of Study																
6	Carry Out for Literature Review																
7	Conduct on Findings Methodology of Overall Process, Methods, and Instruments																
8	Submission of Log Book to Supervisor																
9	Preparation of Presentation PSM																
10	Presentation for PSM on Online Video																
11	Final Report PSM Checked by Supervisor																
12	Submission of PSM Report to Supervisor and Examiner																

	Plan
	Mid-Semester Break, Study Week, and Final Exam

B. Gantt Chart of PSM II

No	Task	Semester II (Week)														
		1	2	3	4	5	6	7	8	9	10	11	12	13	14	15	16
1	PSM Planning								Mid-Semester Break							Study Week	Final Exam
2	Purchase the Material																
3	Discussion with Supervisor for Project Operation																
4	Preparation for Laboratory																
5	Humidified Filament and Printing Process																
6	Surface Roughness Test, Tensile Test, SEM analysis																
7	Analyze Data from Testing Result																
8	Submission of Logbook to Supervisor																
9	Preparation of Presentation PSM																
10	Presentation for PSM on Online Video																
11	Final Report PSM Checked by Supervisor																
12	Submission of PSM Report to Supervisor and Examiner																

	Plan
	Mid-Semester Break, Study Week, and Final Exam